AD-A012 813

AN INVESTIGATION OF DISPLAYED GROUND REFERENCED POSITION, VELOCITY, AND ACCELERATION FOR PRECISION HOVER

C. N. Tsoubancs

Army Electronics Command
Fort Monmouth, New Jersey

July 1975

218026

Research and Development Technical Report

ECOM-4334

AN INVESTIGATION OF DISPLAYED GROUND REFERENCED POSITION, VELOCITY, AND ACCELERATION FOR PRECISION HOVER

C. M. Tsoubanos

Avionics Laboratory

July 1975

ECOM

US ARMY ELECTRONICS COMMAND FORT MONMOUTH. NEW JERSEY 07703

REPORT DOCUMENTATION PAGE		READ INSTRUCTIONS BEFORE COMPLETING FORM
1. REPORT NUMBER ECOM-4380	2. GOVT ACCESSION NO.	3. RECIPIENT'S CATALOG NUMBER
4. TITLE (and Subtitle) An Investigation of Displayed Ground Referenced Position, Velocity, and Acceleration for Precision Hover		5. TYPE OF REPORT & PERIOD COVERED Technical Report
		6. PERFORMING ORG. REPORT NUMBER
7. AUTHOR(s) D. M. Tscubanos		8. CONTRACT OR GRANT NUMBER(s)
9. PERFORMING ORGANIZATION NAME AND ADDRESS AVIONICS LABORATORY ATTN: AMSEL-Vl-F Fort Monmouth, N.J. 07703		10. PROGRAM ELEMENT, PROJECT, TASK AREA & WORK UNIT NUMBERS 1F2.62202.AH85.11.60
11. CONTROLLING OFFICE NAME AND ADDRESS CG, USAECOM ATTN: AMSEL-VL-F Fort Monmouth, N.J. 07703		12. REPORT DATE JULY 1975
		13. NUMBER OF PAGES 78
14. MONITORING AGENCY NAME & ADDRESS(if different from Controlling Office)		15. SECURITY CLASS. (of this report) UNCLASSIFIED
		15a. DECLASSIFICATION/DOWNGRADING SCHEDULE

16. DISTRIBUTION STATEMENT (of this Report)

Approved for public release; distribution unlimited

17. DISTRIBUTION STATEMENT (of the abstract entered in Block 20, if different from Report)

18. SUPPLEMENTARY NOTES

19. KEY WORDS (Continue on reverse side if necessary and identify by block number)

Hover Symbology	Helicopters
Displays	Manual Hover
Display Gains	
Flight Control	

20. ABSTRACT (Continue on reverse side if necessary and identify by block number)

This report presents a man-machine simulation investigation of displayed ground referenced acceleration, velocity, and position for a manual precision hover task. The study determined the appropriate display gains for the above parameters as a function of three different control systems: the Automatic Stabilization Equipment (ASE), the Stability Augmentation System (SAS) and the Hover Augmentation System (HAS).

(over)

DD FORM 1473 EDITION OF 1 NOV 65 IS OBSOLETE   1

The results of the investigation, optimum display gains, were to be incorporated into the Research Aircraft for Visual Environment (RAVE), project, manual precision hover flight test.

TABLE OF CONTENTS

INTRODUCTION

a. Background. Prior precision hover studies[1,2] have shown that the integration of quantitative flight information with a pictorial terrain presentation of the flight situation into a single display is useful for approach and hover in unattended areas. The difficulty of holding position in a manual precision hover task required that ground position and rate be displayed to the pilot. In these same studies, it was also shown that the positioning errors were on the order of 5 feet rms and less. Although such a figure might satisfy requirements for Medevac and Advanced Helicopter (AAH) hover missions, it would not satisfy the Heavy Lift Helicopter (HLH) mission. To increase the hover accuracies, and perhaps decrease pilot workload, acceleration information was added to the integrated Trajectory Error Display (ITED). This new symbol in preliminary testing reduced the positioning errors by 50 percent and pilot comment was very favorable to its implementations in the display. As a result, a man/machine simulation using the Tactical Avionics System Simulator (TASS) was conducted to investigate the merits of the acceleration symbol.

b. Objective. The objective of this study was to determine the appropriate display gains for the acceleration, velocity, and position symbology as a function of three different control systems, the Automatic Stabilization Equipment (ASE), the Stability Augmentation System (SAS), and the Hover Augmentation System (HAS). The results of the study, optimized display gains for precision hover, would be incorporated into the Research Aircraft in Visual Environment (RAVE) project precision hover flight tests.

SUMMARY OF RESULTS

The results of the experiment have demonstrated that superimposed symbology of ground referenced acceleration along with velocity and position on a video image is required to obtain minimal hover position errors. Also, for certain combinations of displayed gains, the hover position errors appeared to be independent of the flight control augmentation.

Several levels of displayed gains were investigated and some of the results reached are summarized as follows:

a. Acceleration, velocity, and position gains of $2 ft/s^2$: 2.5 ft/s: 12.5 feet, respectively, per inch of symbol travel was found to be optimum.

b. The acceleration vector with the ITED display washed out the effect of the different control augmentation systems.

c. Mean position accuracies in the order of 1 foot and less can be obtained with manual control and the addition of an acceleration vector to the Integrated Trajectory Error Display (TED).

[1] Tsoubanos, C.; Covington, R., "Preflight Test Simulation of Superimposed Integrated Trajectory Error Displays," Technical Report ECOM 4184, January 1974.
[2] Dukes, T. A.; Keane, W. P.; Tsoubanos, C. M.; "Image and Superimposed Symbology - An Integrated Display for Helicopters," AHS Conference, Washington, DC, May 1973.

d. Displayed acceleration was useful in stabilizing the helicopter when equipped with a Stability Augmentation System (SAS) rate feedback flight control system.

e. Approach velocity had to be restricted to less than 5 knots in both axes before switching into the hover mode to avoid overshooting the target.

f. The average time required by the pilots to minimize the positional errors before data collection was initiated was 25 seconds.

g. All subject pilots were in favor of having the acceleration information displayed, although they felt it made them "work" harder.

3. SYSTEM DISCUSSION

a. Aircraft Model. The aircraft dynamics used in the man/machine simulation represented a CH-53A linear perturbation model. The helicopter model including a full Automatic Flight Control System (AFCS) with both heading and altitude hold were programmed on analog computers in the Tactical Avionics System Simulator (TASS).

The model was "flown" by the pilot by use of the standard flight controls, cyclic, collective, and pedals. The aircraft state outputs were used to drive the basic cockpit instruments; the four degree of freedom (roll, pitch, yaw, heave) motion system for pilot motion cues and also a visual system. Random gust disturbances were also injected into the model in the longitudinal and lateral axes to achieve a more realistic simulation. These gust disturbances were passed through a first order filter with a 0.3 rad cutoff frequency and were adjusted to provide approximately 6 ft/s rms levels. Although they are much higher than previous experiment[1], it was felt that since acceleration would be sensitive to these gusts more severe valued disturbances were required. A complete system integration with the pilot in the loop is shown in block diagram as Figure 1.

b. Control Systems.

(1) Stability Augmentation System (SAS). In order to simulate the SAS control system, the attitude loops of the AFCS in pitch and roll were disengaged leaving a basic SAS. This control system tended to be oscillatory in both axes and almost impossible to stabilize under instrument flight. The altitude-hold and heading-hold loops were engaged.

(2) Automatic Stabilization Equipment (ASE). This control system is the full AFCS as provided by Sikorsky Aircraft Company.

(3) Hover Augmentation System (HAS). The third control system used in the experiment was the HAS. The additional control augmentation was used only in the longitudinal-lateral axis. The altitude and heading-hold was derived from the standard AFCS. The gains for the HAS velocity, rate and attitude feedback loops and those of the forward paths were selected by the manufacturer and experimenter, respectively.
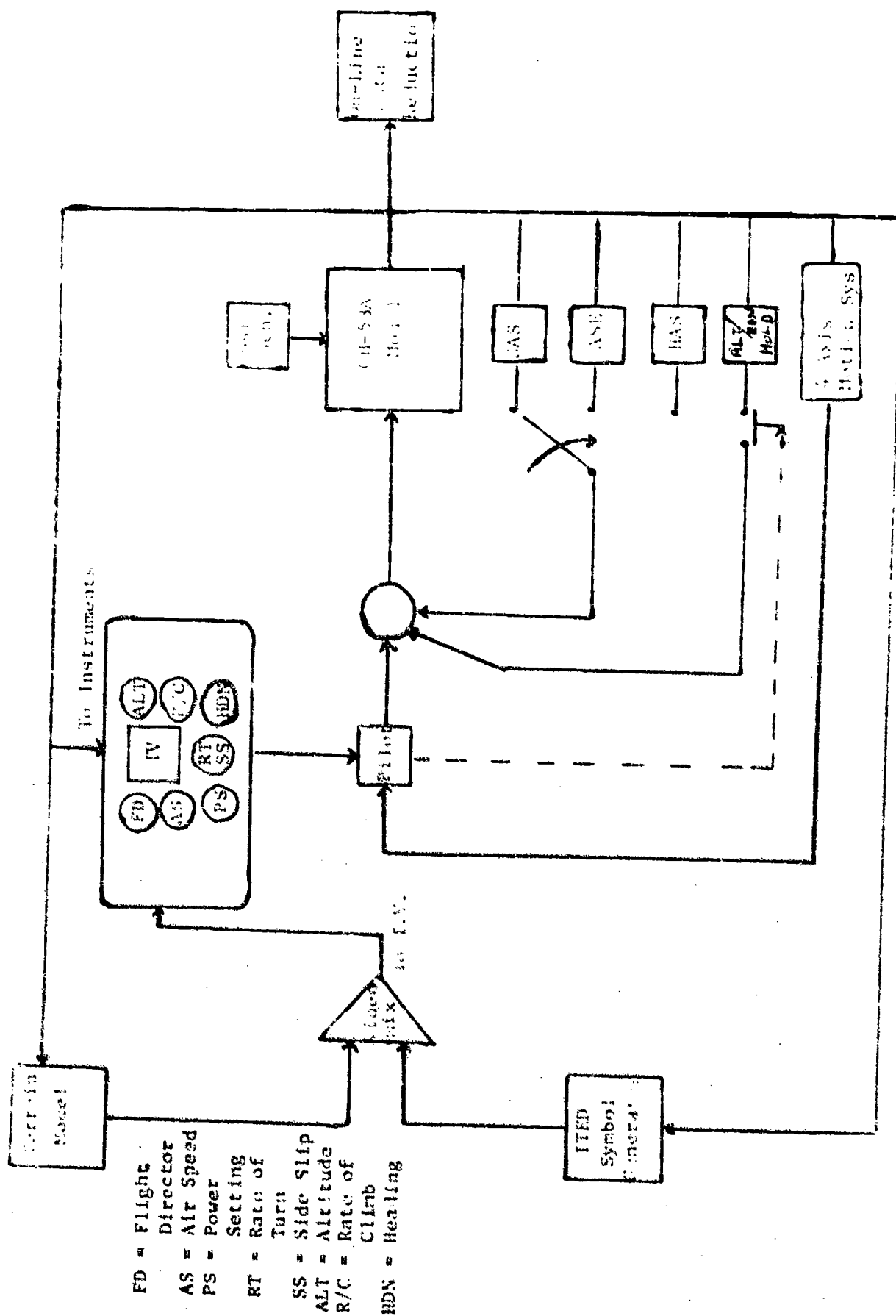
2

FD = Flight
Director
AS = Air Speed
PS = Power
Setting
RT = Rate of
Turn
SS = Side Slip
ALT = Altitude
R/C = Rate of
Climb
HDN = Heading

Figure 1. Mac/man interaction block diagram.

c. **Displays.** Since the pilot was an active controller in the experiment, his environment in the cockpit was kept as near as possible to familiar surroundings. The instrument panel contained the basic instruments found in most helicopters. These included radar altimeter, airspeed, flight director, rate of climb, heading, turn and bank. Power setting was provided, but no other engine instruments were presented. These instruments were placed around a 14-inch TV monitor (Figure 2) on which both a terrain video image representing a 38 by 48 degree field-of-view (FOV) and the Integrated Trajectory Error Display (ITED),[1] shown in Figure 3, were superimposed. Although the simulation study goal was determination of the acceleration, velocity, and position gain combinations for minimum hover position errors, the complete ITED[1] symbology was used in the approach to a hover maneuver to eliminate the scanning for attitude, altitude, and rate of climb information since the approach mode was an integral part of the experiment.

d. **Sensors.**

(1) **Electronic Location Finder (ELF).** The ELF system operates on the principle that the phase shift of a radio wave propagated through space is proportional to the wavelength and the distance traveled. The system measures the phase difference at each of two pairs of accurately spaced receiving antennas to determine the angle of the signal from the ground beacon.[3] This technique is more commonly known as a phase-comparison interferometer.

The basic signals received by the body mounted antennas for angle measurements are with respect to the nominal situation when the helicopter is hovering perfectly over the radiation source. These signals are compensated for roll and pitch attitudes. The resultant characteristic is such that saturation occurs near $+45°$ angle of the beacon with respect to the antennas both longitudinally and laterally.[4] The sketch in Figure 4 shows the ELF block diagram.

In the most straightforward homing procedure, the helicopter is flown toward the ground beacon by keeping the lateral deviation centered while the longitudinal indication, depending at the altitude, would be at full scale. The longitudinal indicator moves off full scale only when the distance is about the same as the altitude. In other words, once the helicopter is inside the so-called $+45°$ ELF cone, both longitudinal and lateral deviations will occur. In order to simplify the calculations of the displayed deviations, considering the saturation near $+45°$, the following small angle approximations are made for the measured angles:

$$\text{Fore, aft} = \frac{x}{\sqrt{x^2 + y^2 + h^2}}$$

$$\text{Left, Right} = \frac{y}{\sqrt{x^2 + y^2 + h^2}}$$

[3]Preliminary Technical Manual, "*Operation and Maintenance Electronic Location Finder System (ELF)*," PHB/536-1, Cubic Corporation.

[4]Contract DAAB06-72-C0161 Phase III. Final Report. "*Integrated Display*," T. A. Dukes, September 1973.
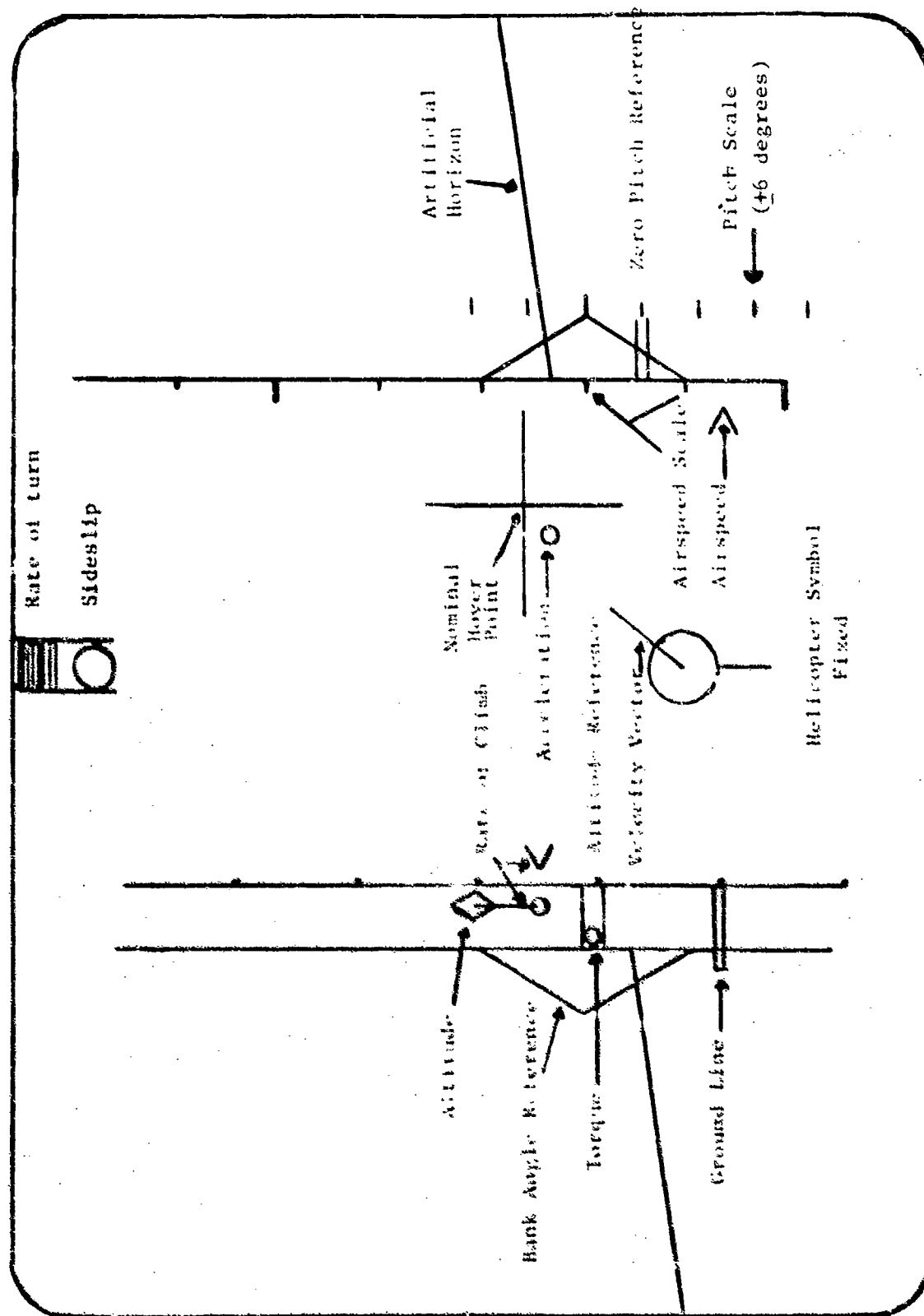
Figure 2. Instrument panel

5

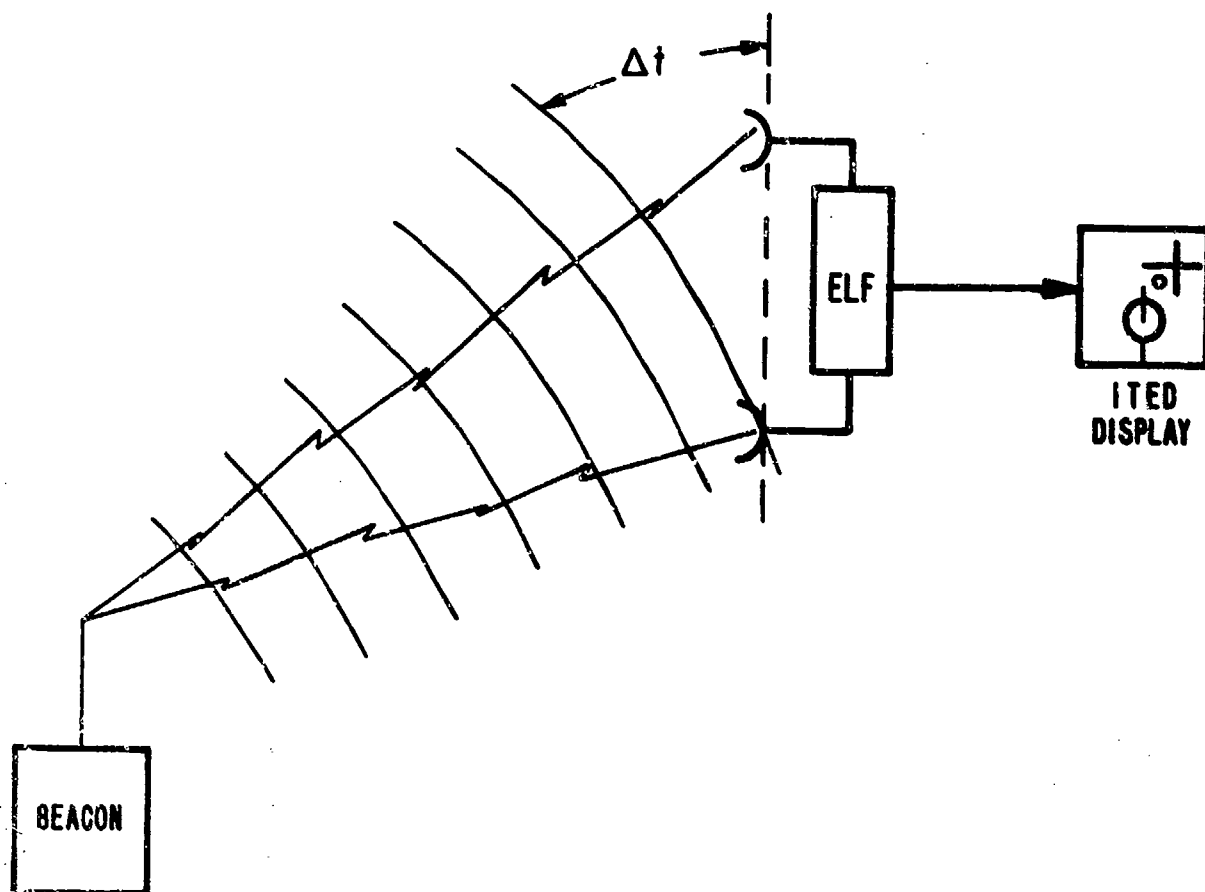Figure 3. Integrated trajected error display (ITED).

Figure 4.   ELF block diagram

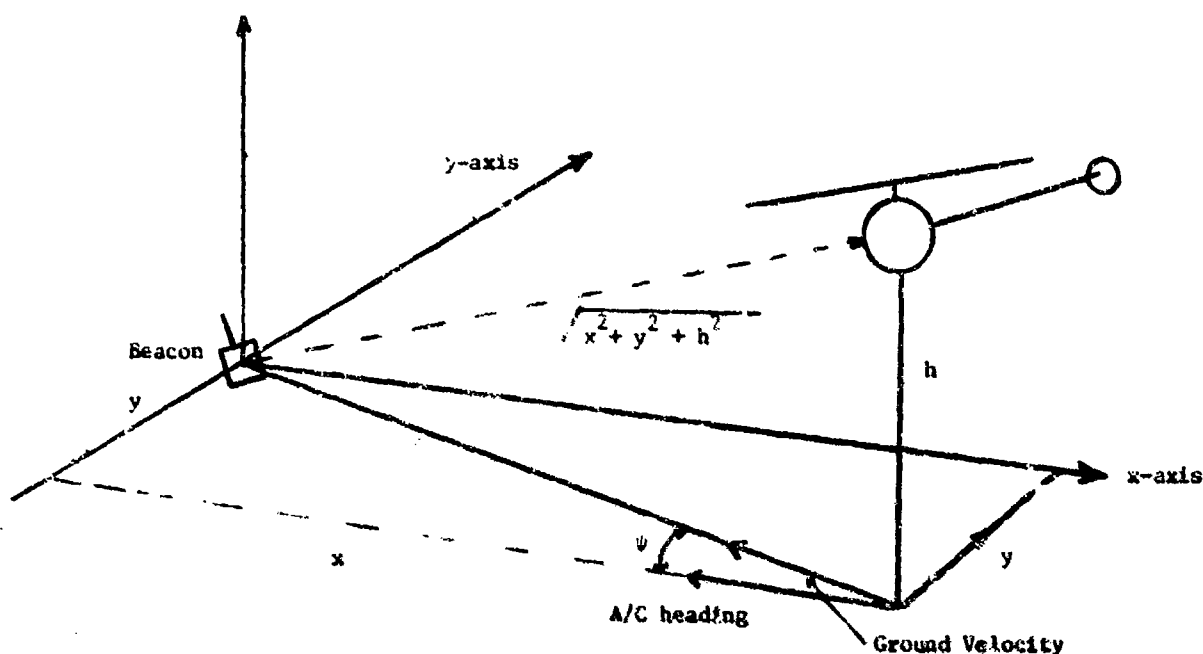The sketch shown in Figure 5 indicates this simple geometry.

Figure 5.   Approach geometry

The saturation is approximated by limits when the above approximations reach values of $\pm 1/\sqrt{2}$.   The general nature of the relationships is still retained with these simplifications.

However, for low level flight, the distance represented by the cone is not sufficient for deceleration to a hover. Therefore, overshoots are generally unavoidable.   A technique has been devised by T. A. Dukes to overcome this problem.[4]

(2) Acceleration Sensor (VG-341).[5] The derivation of acceleration was simulated to be pure acceleration as would be derived from the vertical gyro VG-341. Although the gyro was not simulated, its limits were incorporated. Basically, the VG-341 is a vertical gyro with accelerometers mounted on the pitch and roll gimbals. The gyro angles within $\pm 5°$, the accelerometer is linear and provides the appropriate acceleration in the horizontal plane. Since acceleration is gust sensitive and noisy, attitude which is not sensitive to the high frequencies, was also used in the experiment. Only one cell was included using attitude and this cell had approximately the same gains as pure acceleration.

[5]VG-341 - Vertical Gyroscope - Sales Specification, Sperry Flight Systems Division, Phoenix, Arizona.

e. Experimental Design Plan.

(1) Background. This experiment was based on the results obtained in a previous simulation[1] and a preliminary study investigation of the acceleration vector. In this preliminary acceleration vector investigation, subject pilot performance and comments indicated the acceleration vector a necessary and required symbol for the precision hover task.

In the above mentioned simulation[1] the results of one cell, I_9, indicated that when the position and velocity displayed gains were changed from 25 ft: 5 ft/s per inch to12.5 ft: 5.0ft/s per inch pilot performance improved. However, the increased "quickening" forced the pilot to "work" or concentrate more at the given task. The increased workload was not readily accepted by the subject pilots. Their general comment was to return to the "other case" or 25 ft:5 ft/s per inch displayed.

It was then felt that something should be added with enough lead time to drive the pilot to increase his performance and yet not complain about the workload. An additional result from pilot comment, which unfortunately was overlooked, provided the answer as to what might be needed to drive the pilot and also increase his performance. These subject pilots felt that while they were in the hover mode, the attitude information could have been of more use if it was closer or even on top of the nominal hover point (Figure 6). What the pilots were asking for was for something to give them lead information higher than that provided by the velocity vector, or simply, acceleration.

A preliminary experiment was set up with pure acceleration driving the velocity vector tip (Figure 3). In addition to the acceleration symbol, velocity and position were also displayed. In this preliminary experiment, the pilots were enthusiastic about the acceleration vector concept; however, additional experimentation was required to provide the information as to its usefulness. It was then determined that acceleration should be displayed with respect to the tip of the velocity vector. With this display configurations, the pilot positions the acceleration symbol on the position symbol and as long as he keeps the acceleration symbol on the position symbol, the vector sum of acceleration, velocity, and position will become superimposed on each other as the aircraft position errors are zeroed (Figure 7).

(2) Experimental Design. The experiment was designed to answer two questions:

(a) What combination of displayed acceleration, velocity, and position vector gains provided best hover position performance without sacrificing pilot acceptance?

(b) Can the display of acceleration information improve pilot's hover performance when the flight control systems are varied?

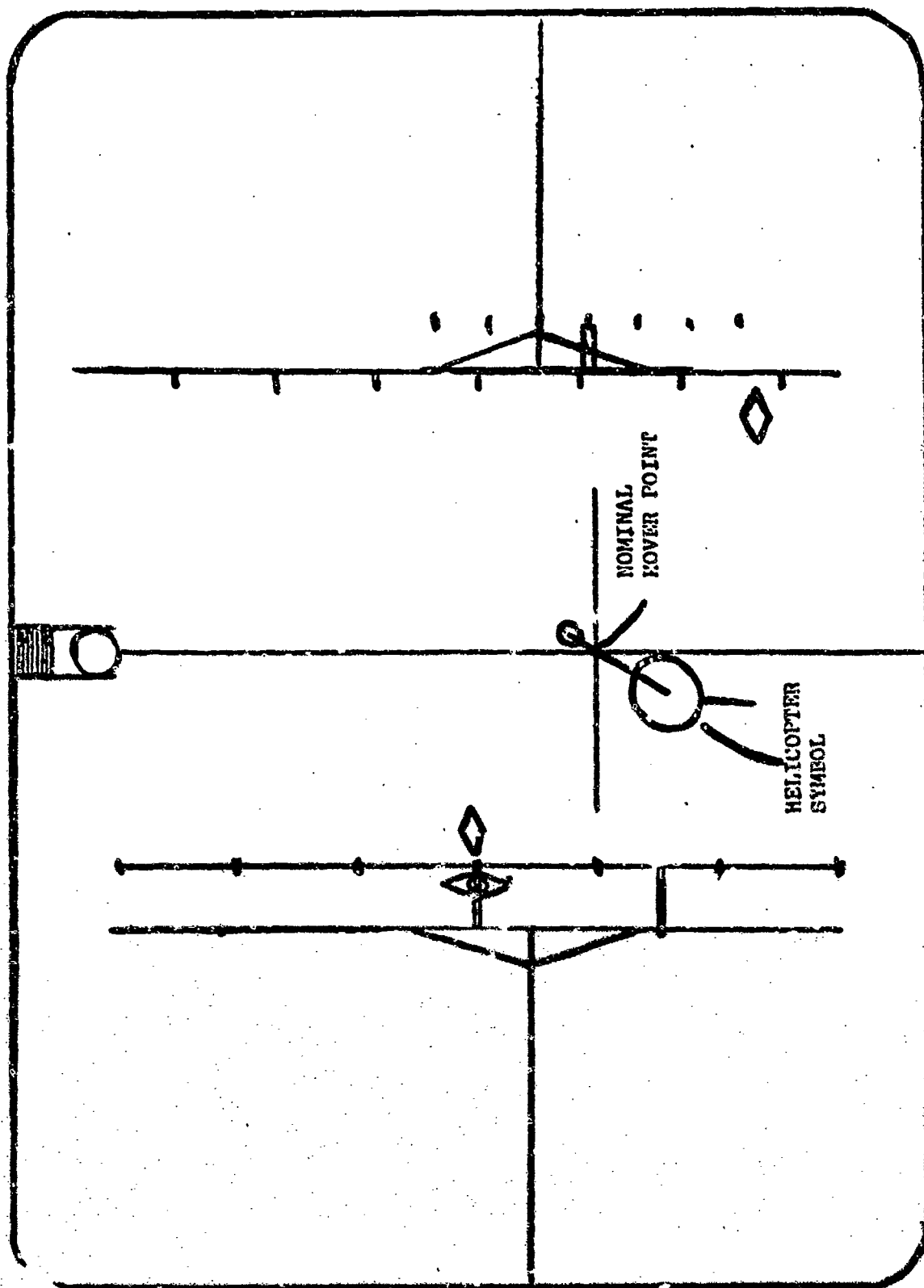With these two questions in mind, the design plan was formulated.

Figure 6. ITED symbology without acceleration

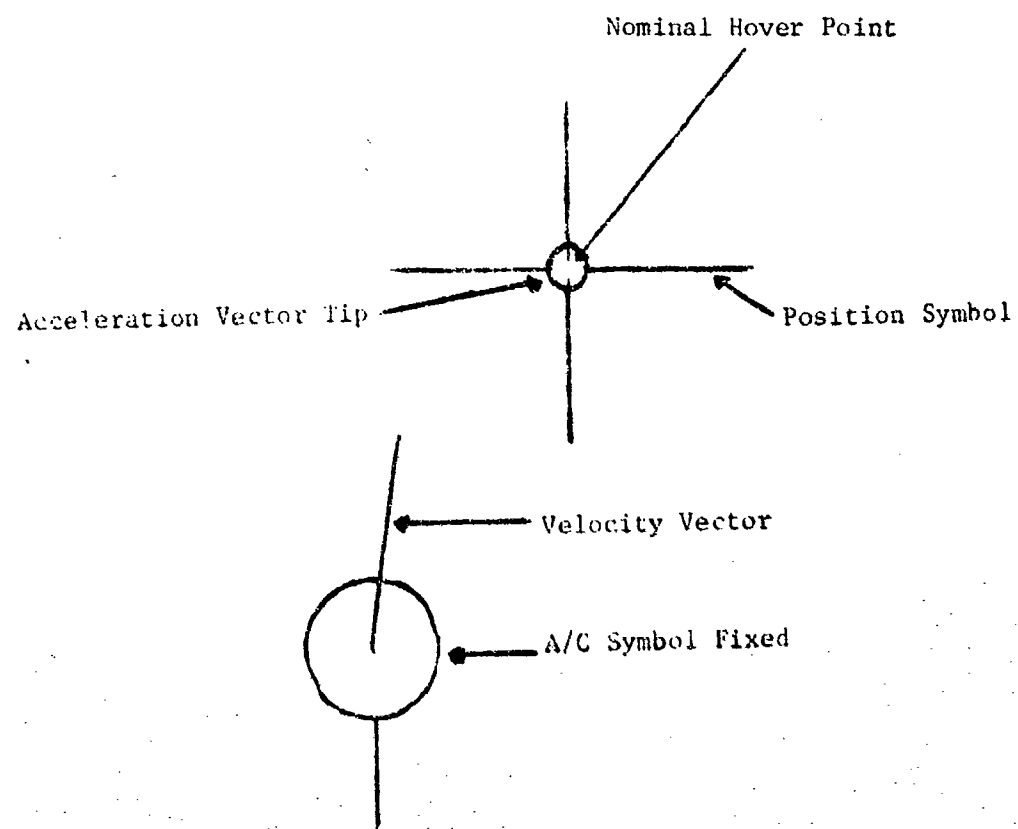NOMINAL
HOVER POINT

HELICOPTER
SYMBOL

10

Figure 7. Acceleration, velocity, and position diagram

Four helicopter aviators were selected as subjects for this study; two military and two civilians. Their experience ranged from combat to project and test pilots. Although all were not qualified to fly a CH-53A, their experience included other military aircraft similar to the CH-53A and for the study in question it was decided that the aircraft model should not become a factor in selecting the pilots. The control systems were selected on the basis of what systems are presently available and future designs were not considered. They included the full AFCS of the CH-53A, the HAS system, and a SAS system.

Two positions and two velocity gains were selected, 25 and 12 ft/inch and 5 and 2.5 ft/s inch, respectively, on the basis of past studies.[1] During the preliminary tests, the acceleration vector gain (2.0 ft/s^2/inch displayed) was selected empirically such that it made the transition to the nominal hover point critically damped. Using this acceleration gain as a base, three others were selected. In all, the acceleration vector gains were 0, 1.33, 2.0, and 3.0 ft/s^2 inch on the display.

The question of the high frequency gusts driving the acceleration vector to a level that the pilot might object was throughly considered. Since pure acceleration is sensitive to the high frequency components of the gusts, an alternative method of using attitude was used for the acceleration vector since attitude would filter out the high frequency gusts components. It was decided to use one level of attitude gain that closely approximated one of the pure acceleration vector gains in the final selection of the cells. This attitude gain was 4 deg/inch or 2.25 ft/s^2 inch.

(3) **Disturbances.** One level of random winds were selected with a magnitude severe enough to be reflected on the pure acceleration display vector. The random winds were digitally derived with a gaussian distribution and filtered through a low pass filter with a 0.30 radian break frequency and adjusted to give an rms value of 6 ft/s. Two independent generations were derived and were recorded on tape. The gusts were introduced in the longitudinal and lateral equations of motion of the simulated helicopter model. An analog recoding and filter is shown in Appendix B.)

(4) **Mission.** The mission was designed as one that might have to be performed within a landing zone, or at a depot, in moving containers from point A to point B.

The aircraft was trimmed at 100-foot altitude and approximately 300 feet from the target. The pilot was instructed to make an approach to the target or landing zone and terminate in a hover altitude. After performing a 2-minute hover, the pilot was presented with a new position signal on his display, again approximately 300 feet away. Once again the pilot had to go from hover to approach by throwing a toggle switch on the collective. This switch controlled the scale factors in velocity from 20 knots per inch in approach to either 5 or 2.5 ft/s inch in hover, and position from 25 ft/inch in approach to 12.5 ft/inch in hover. By having the pilot fly to two different areas, only one replication of each cell was used in the experiment.

(3) Data Collection Control. The pilot controlled data collection since he ultimately decides success or abortion of a mission. It was the intention to let the pilot decide when his position errors were minimized to an acceptable level to initiate data collection. Therefore, at his discretion, he depressed a momentary switch on the cyclic to initiate data collection.

Since it was expected that the time for initializing the hover mode to data collection would vary between control systems, this time was also recorded as another variable. The pilots were unaware that a timing measuring device was being used until the end of the experiment. Pilot comments were also recorded by an observer.

(6) Pilot Training. All four subject pilots were used in the TASS simulator in prior simulation studies. Three of the four had flown the panel mounted display with the superimposed symbology, the fourth pilot had flown the symbology without terrain and an earlier version of the ITED.[6] However, the acceleration symbol was new to all of them.

They all received a briefing of the mission or task involved and an explanation of the display with and without acceleration. They were later individually placed in the flight simulator cockpit for additional familiarization with the total system.

Because the pilots had flown similar superimposed symbology on terrain video and were familiar with the moving base simulator, very little training was required. The most difficult and most time consuming aspect of the training was spent in the approach to the hover. During this maneuver the pilot switched the displayed information to ground referenced and changed the scale factors by a factor of ten they found themselves experimenting on how to make the transition from approach into hover. It was during these training runs that one of the subject pilots devised the following technique:

With the aircraft approximately 300 feet to the rear of the simulated ELF position and at 100-foot altitude, the displayed position symbol was saturated against the limit of the display. This subject suggested that a slow descent rate as well as a forward speed of some small value be initiated and at the instant the displayed position symbol came off its limits, the subject would go into the hover mode. Having done this, he would then use the acceleration vector symbol and follow it to the nominal hover point.

The above technique was tried and after many trials it was discovered that as long as the pilot kept the forward speed below 5 knots[7] and the rate of descent about 100 ft/min he had sufficient time to transition from approach into hover without overshooting the target.

The method described above was then used to help train the pilots on the transition phase from approach to hover. It worked well for the HAS and ASE control systems, but when the SAS system was selected, the pilots had more difficulty and required additional training. The major part of the training time was used to train the pilots in flying with the SAS.

---
[6]Keane, W. P.; Milelli, R. J., "Precise IFR Hovering - An Operational Need and a Feasible Solution," AGARD Conference, May 1971.

[7]Madison, J.; Park, CPT, USAF: fe, Paul J. MAJ, USAF, PAVE Low II Evaluation of an Electronic Locating Finder Coupler System in the HH-52 Helicopter," Technical Report No. 73-47, November 1973.

Once again, it should be noted that the major pilot objection was only in the transition phase from approach to hover but as soon as hover was established, pilots quickly damped the aircraft oscillations and performed the required tasks well. Training data was collected and when the results began to correspond with those of past studies, formal data collection was initiated.

(7) Cell Breakdown. Thirty one (31) cells were selected for the experiment. They consisted of a baseline cell used in a previous experiment[1] without acceleration; four pure acceleration gains, two velocity gains, two position gains, three control systems, and one attitude displayed acceleration gains.

The attitude acceleration was not used with all combinations of position and velocity, because another group was to investigate it. A breakdown of the cells is shown in Figure 8.

4. DATA REDUCTION

An on-line digital data reduction program was used. The variables considered important for this study were the radial ground position, altitude, aircraft flight variables (attitudes and rates), and pilot control movements.

These variables were sampled at 5 samples per second. The digital program calculated the mean, standard deviation, rms, variance, and maximum-minimum values for each variable for the 2-minute hover, and the results were output on the line printer (Figure 9). In addition to the above, the observer also recorded the time required by the pilot to minimize the positional errors to his (pilot) acceptable level before data collection was initiated.

a. Presentations. The results obtained from the four subject pilots during the experiment were simplified as to the number of variables (see Computer Printout, Figure 9) analyzed and the most significant and interesting cells of the experiment are shown with mean, standard deviation, root mean square (rms) and range in bar graph form as a function of radial ground position performance and control systems (See Appendix C, Figures C-1 through C-10). From these bar graphs a selection was made of the cells that gave the best results in mean, rms radial ground position and mean altitude.

b. Analysis. As stated previously, this study was primarily designed to determine the optimum acceleration and velocity vector gains that reduced the horizontal position errors to a minimum level independent of control systems and without pilot objection with respect to "work-load." Because the experiment consisted of two different velocity vector gains with three combinations of acceleration vector gains, the results for minimal radial rms and mean ground position for each velocity vector gain and its combination of three accelerations were compared, and the optimum acceleration-velocity vector was selected. Also, the results obtained using the acceleration was included in the selection.

The above selection of acceleration-velocity gains are shown with the baseline data as functions of radial rms and radial mean ground and control system (Figures 10 and 11).

14

Run No.	Cell No.	Control	Position ft/in.	Velocity fps/in.	Accel frs/in.	Attitude 0/in.	Repl	Gust fps/in.
1	1	ASE	25	5	0	0	1	6.0
2	2	SAS	25	5	0	0	1	6.0
3	3	HAS	25	5	0	0	1	6.0
4	4	HAS	25	5	2.0	0	1	6.0
5	5	SAS	25	5	2.0	0	1	6.0
6	6	ASE	25	5	2.0	0	1	6.0
7	7	ASE	12.5	5.0	3.0	0	1	6.0
8	8	HAS	12.5	5.0	3.0	0	1	6.0
9	9	SAS	12.5	5.0	3.0	0	1	6.0
10	10	SAS	12.5	2.5	1.33	0	1	6.0
11	11	HAS	12.5	2.5	1.33	0	1	6.0
12	12	ASE	12.5	2.5	1.33	0	1	6.0
13	13	SAS	12.5	2.5	2.0	0	1	6.0
14	14	HAS	12.5	2.5	2.0	0	1	6.0
15	15	ASE	12.5	2.5	2.0	0	1	6.0
16	16	HAS	12.5	2.5	3.0	0	1	6.0
17	17	SAS	12.5	2.5	3.0	0	1	6.0
18	18	ASE	12.5	2.5	3.0	0	1	6.0
19	19	HAS	12.5	5	1.33	0	1	6.0
20	20	SAS	12.5	5	1.33	0	1	6.0
21	21	ASE	12.5	5	1.33	0	1	6.0
22	22	ASE	12.5	5	2.0	0	1	6.0
23	23	SAS	12.5	5	2.0	0	1	6.0
24	24	HAS	12.5	5	2.0	0	1	6.0
25	25	HAS	12.5	5	0	0	1	6.0
26	26	ASE	12.5	5	0	0	1	6.0
27	27	ASE	25	5	3	0	1	6.0
28	28	ASE	25	5	1.33	0	1	6.0
29	29	HAS	12.5	2.5	0	4^0/in.	1	6.0
30	30	ASE	12.5	2.5	0	4^0/in.	1	6.0
31	31	SAS	12.5	2.5	0	4^0/in.	1	6.0

Figure 8. Cell breakdown

TABC DATA REDUCTION -- PHASE II

SUBJECT 6   RUN 8   CELL 15   NO 367   TIME 1.63 MIN   22 MAR 74

VARIABLE	MEAN	STANDARD DEVIATION	RMS	MAXIMUM VALUE	MINIMUM VALUE	VARIANCE	RANGE	INITIAL VALUE	FINAL VALUE

NORTH (FT)
EAST (FT)
ALTITUDE (FT)
ROLL (DEG)
PITCH(DEG)
PSI-REF (DEG)
DELTA PSI (DEG)
LONG CYC (IN)
LAT CYC (IN)
COLLECT (IN)
PEDALS (IN)
P (DEG/SEC)
Q (DEG/SEC)
R (DEG/SEC)
N?DOT (FT/SEC)
E?DOT (FT/SEC)
Z?DOT (FT/MIN)
G-LAT (FT/SEC)
G-LONG (FT/SEC)
NE RADIUS (FT)
NE SP RAD (FT)
X (FT)
Y (FT)
XY RADIUS (FT)
XY SP RAD (FT)
PHI-M (DEG)
THETA-M
N?DOT-M(FT/SCC)E
X-M (FT)
Y-M (FT)
XY RAD-M (FT)

	NUMBER OF SIGN REVERSALS	FREQUENCY
N?DOT	35	0.14
E?DOT	44	0.2
LAT CYCLIC	76	0.21
LONG CYCLIC	97	0.26

Figure 9.   Computer printout sample

16
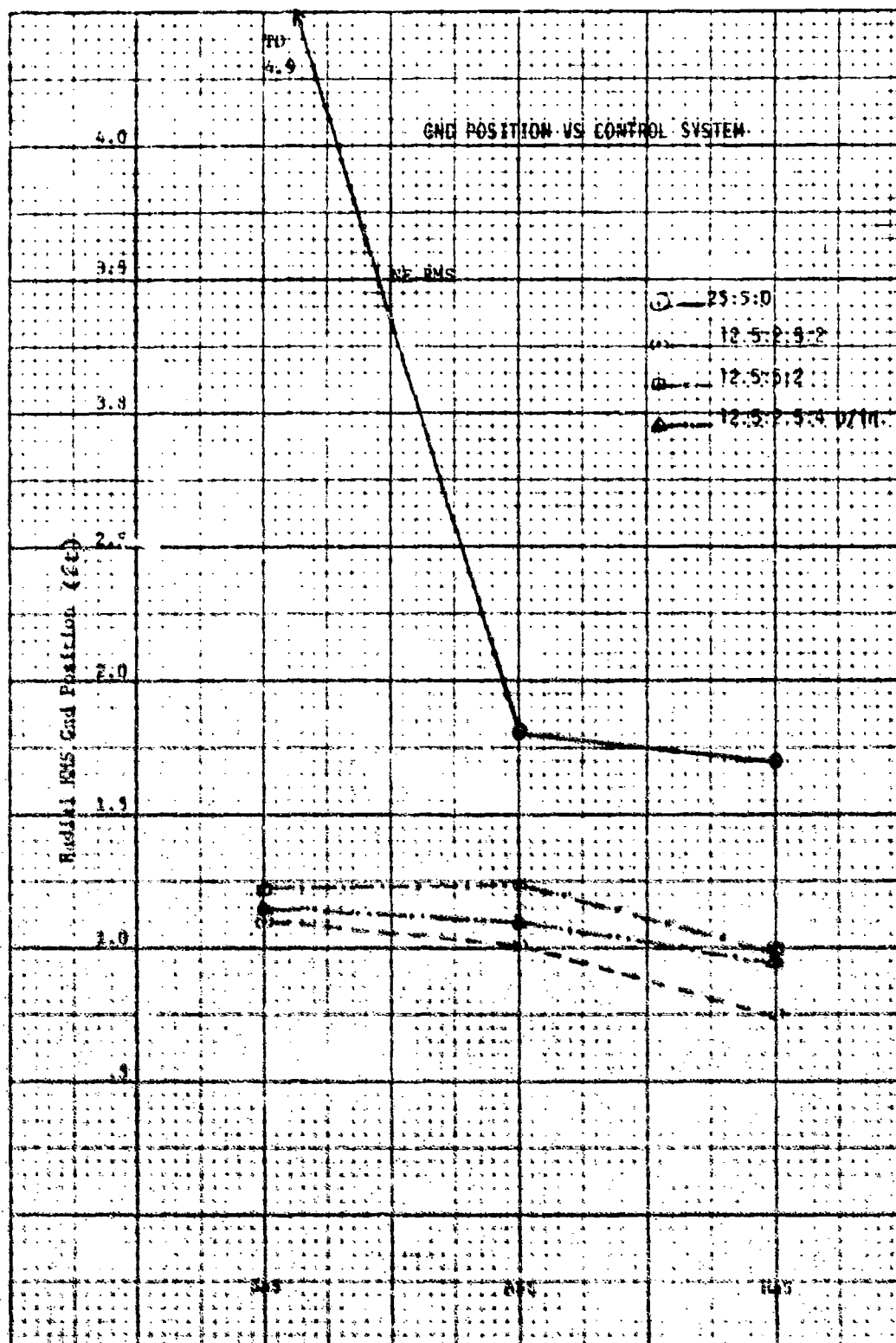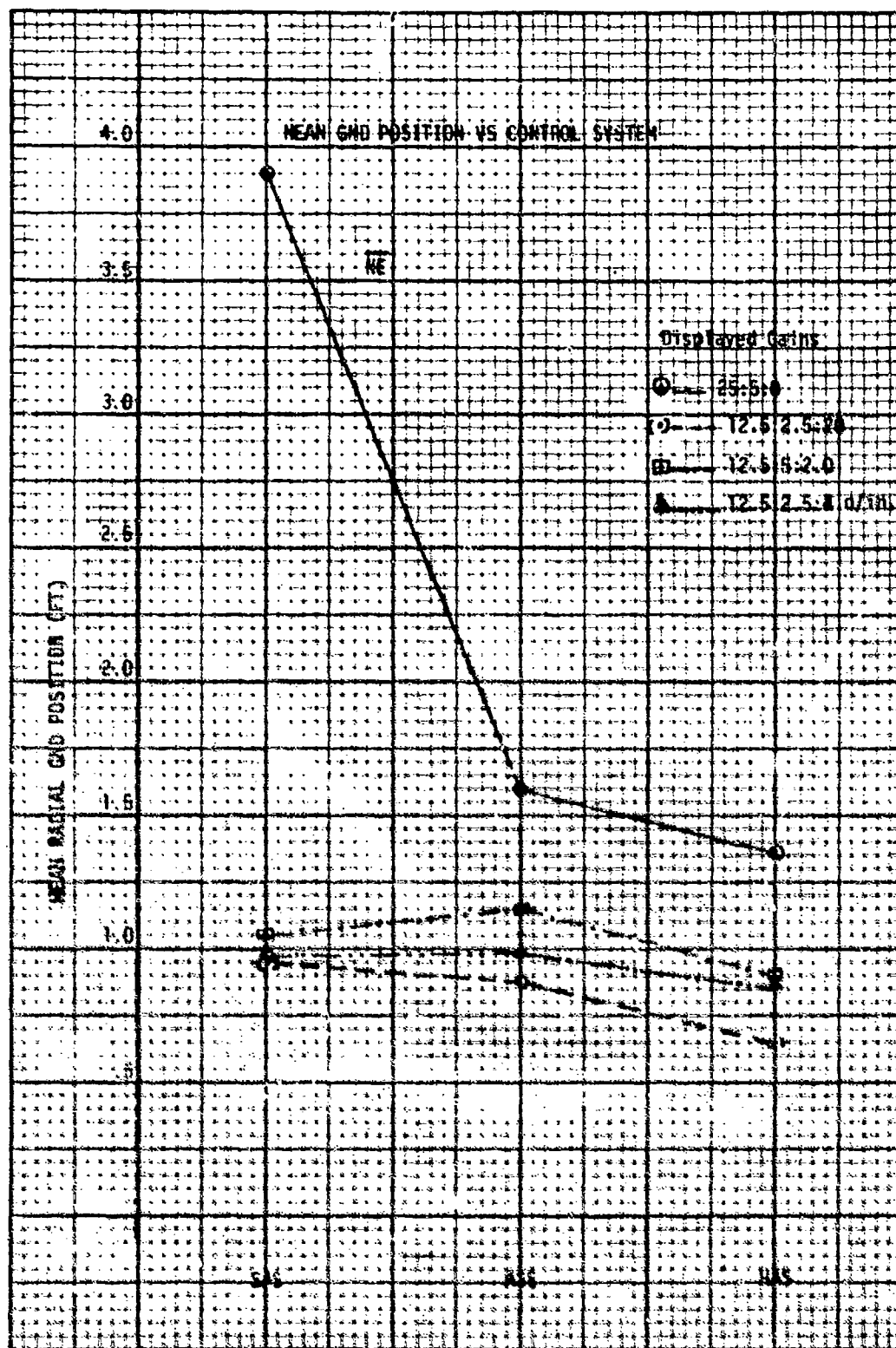
Figure 10. Ground position versus control system

Figure 11. Mean ground position versus control system

18

Another performance parameter that was analyzed is altitude. Since the [pilot] was asked to be near a [reference] altitude before he initiated the data [collec]tion, it was felt that the deviations about the reference altitude should [be pre]sented.

Once again, the combination of acceleration-velocity gain that gave [mini]mum ground position errors was used to show the altitude deviation about the [referen]ce condition as a function of control systems. These altitude deviations [are sh]own in Figure 13.

One other parameter that was recorded was the time required by the pilot [from] the time he changed to the targets for hover until he initiated the [data colle]ction. During the experimental design, it was expected that the time required to minimize the positional errors to his acceptable level [depending] on the mission, whether it was a Medevac, ZAH or HLH would be a valuable [fact]or to record, since a minimization of positional errors results in a [higher cost].

If the three control systems work, one was hoped to offer a optimum [value] of minimum time required from data collection. The results of the time [us]ed for data collection [are shown in] Figure 14 as a function of the [control syste]ms. The calls presented [in this figure] are those with the acceleration-veloc-ity vector gains that gave minimum horizontal positional errors. Two [othe]r variables were analyzed: the pilot workload and the aircraft attitude. [Althou]gh pilot workload was not measured by some "elaborate" technique, the [contr]ol stick rms signals were recorded. These are shown in Figure 14 as [func]tions of rms ground position errors for the cases of acceleration-veloc[ity gai]ns mentioned above. This technique, although not a true indication of [pilot work]load, still gives an indication of pilot stick movement as a function [of cont]rol as well as position accuracy.

Finally, the aircraft attitude and attitude rate rms and range values are [sh]own in Figures 15 through 18 as functions of control. The selection of the [fligh]t variables was to evaluate the aircraft responses with the three control [syste]ms.

SUBJECT PILOT COMMENTS

Before the actual experiment was conducted, a training period was re-[quir]ed. During this training period, the subject pilots flew the three con[trol] systems, ASE, SAS, and HAS with the velocity vector and position, but [witho]ut the acceleration vector.

The pilots were required to make an approach to a hover, and at his dis-[cret]ion begin the data collection. The subjects seemed to have no difficulty [with] the ASE and HAS system. However, they complained strongly about the hand-[li]ng qualities of the helicopter with the SAS system. They felt that the sys-[te]m was "unnatural" to fly. It was purposely intended to have such large de-[vi]ations in control systems in order to determine the usefulness of the ac-[c]eleration vector.
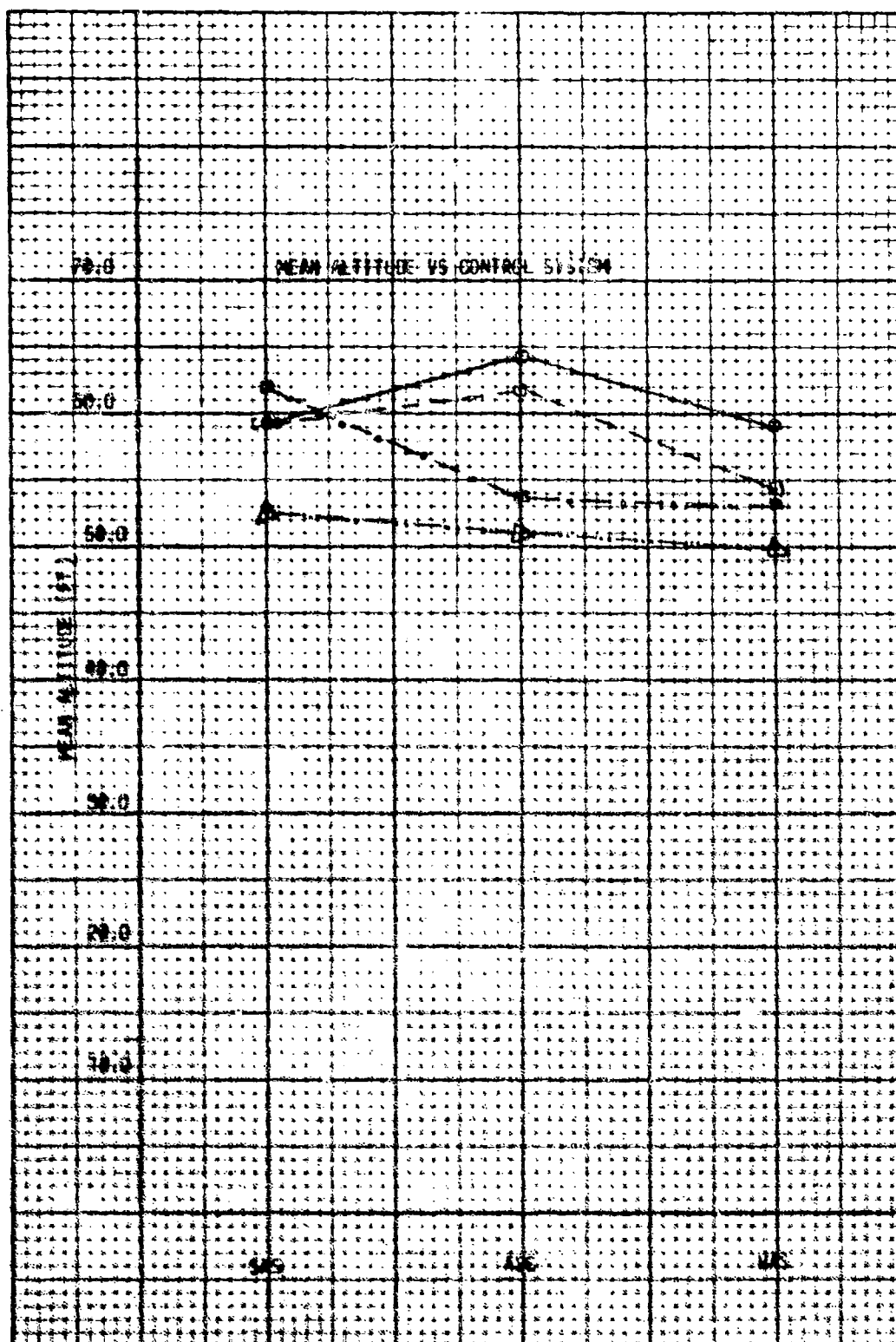
10
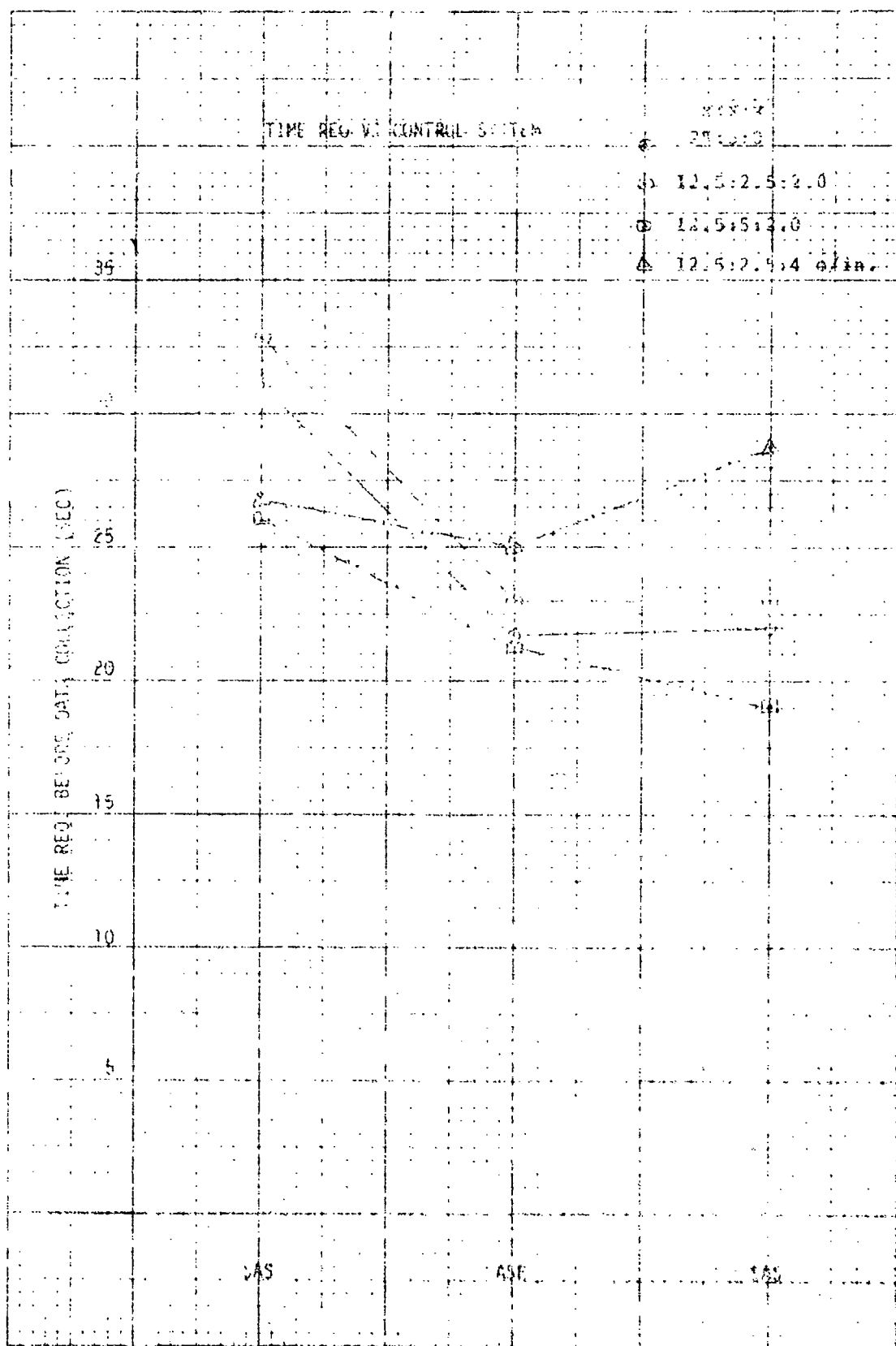
Figure 12. Mean altitude versus control system

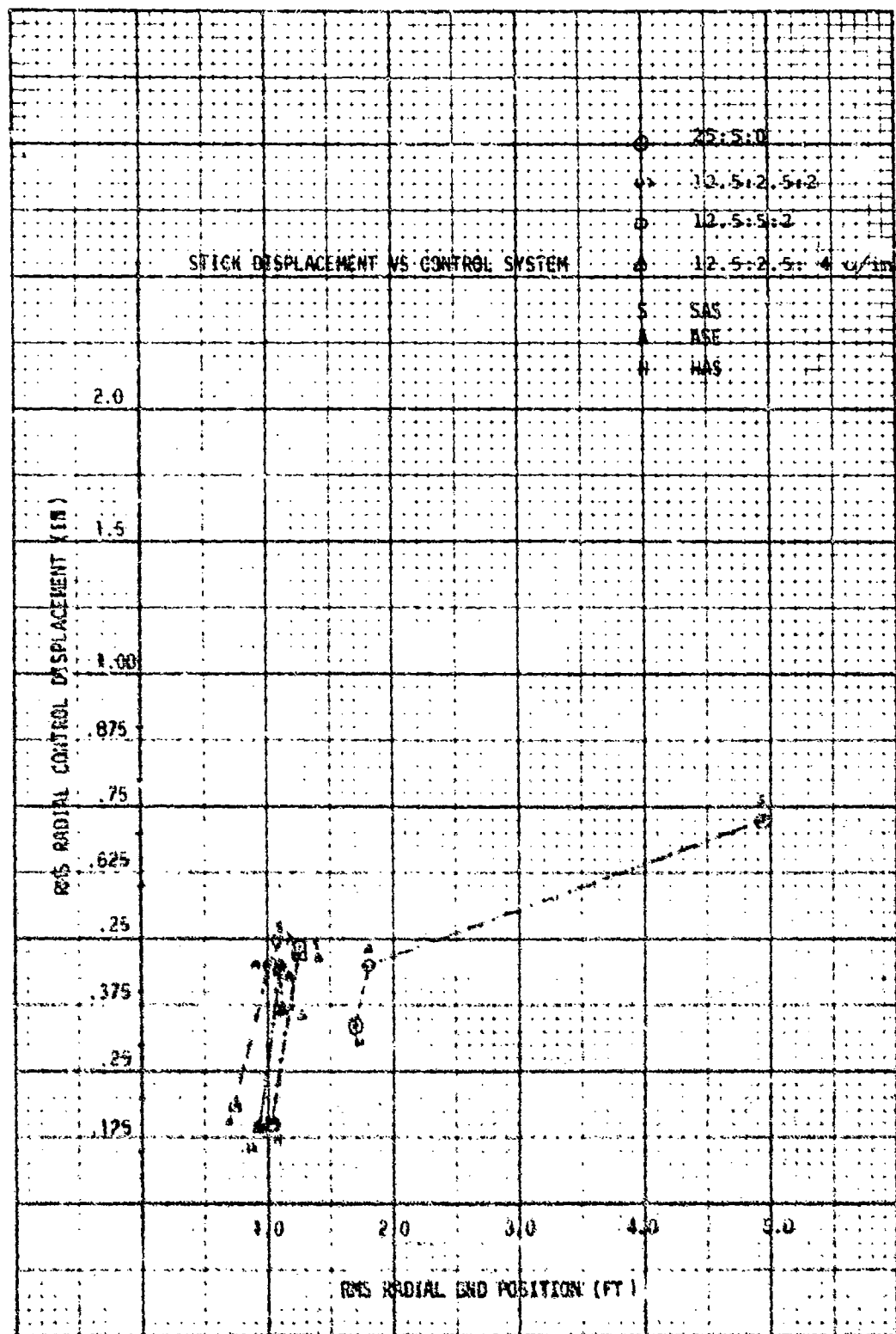Figure 13. Time required versus control system
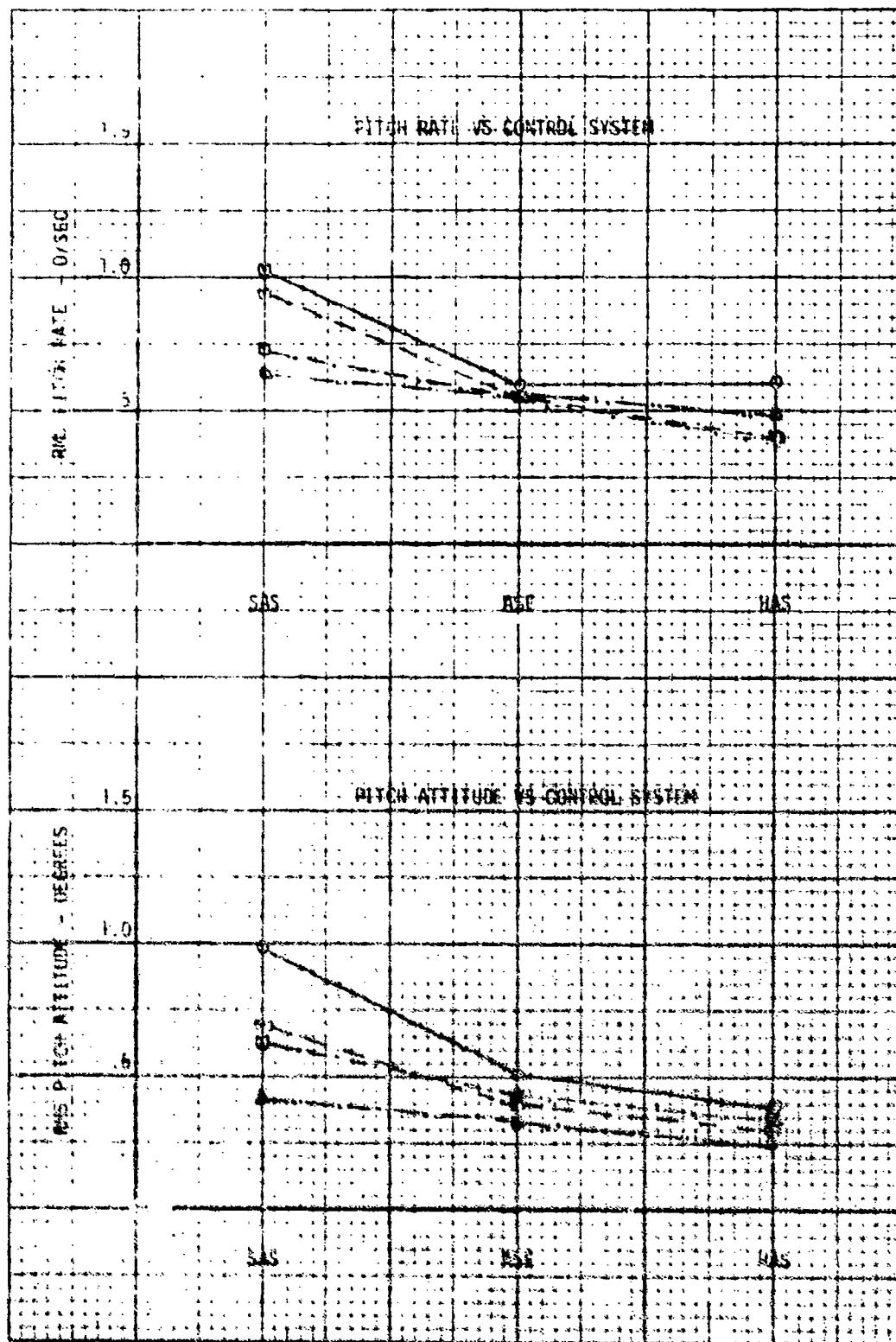
Figure 14. Stick displacement versus control system

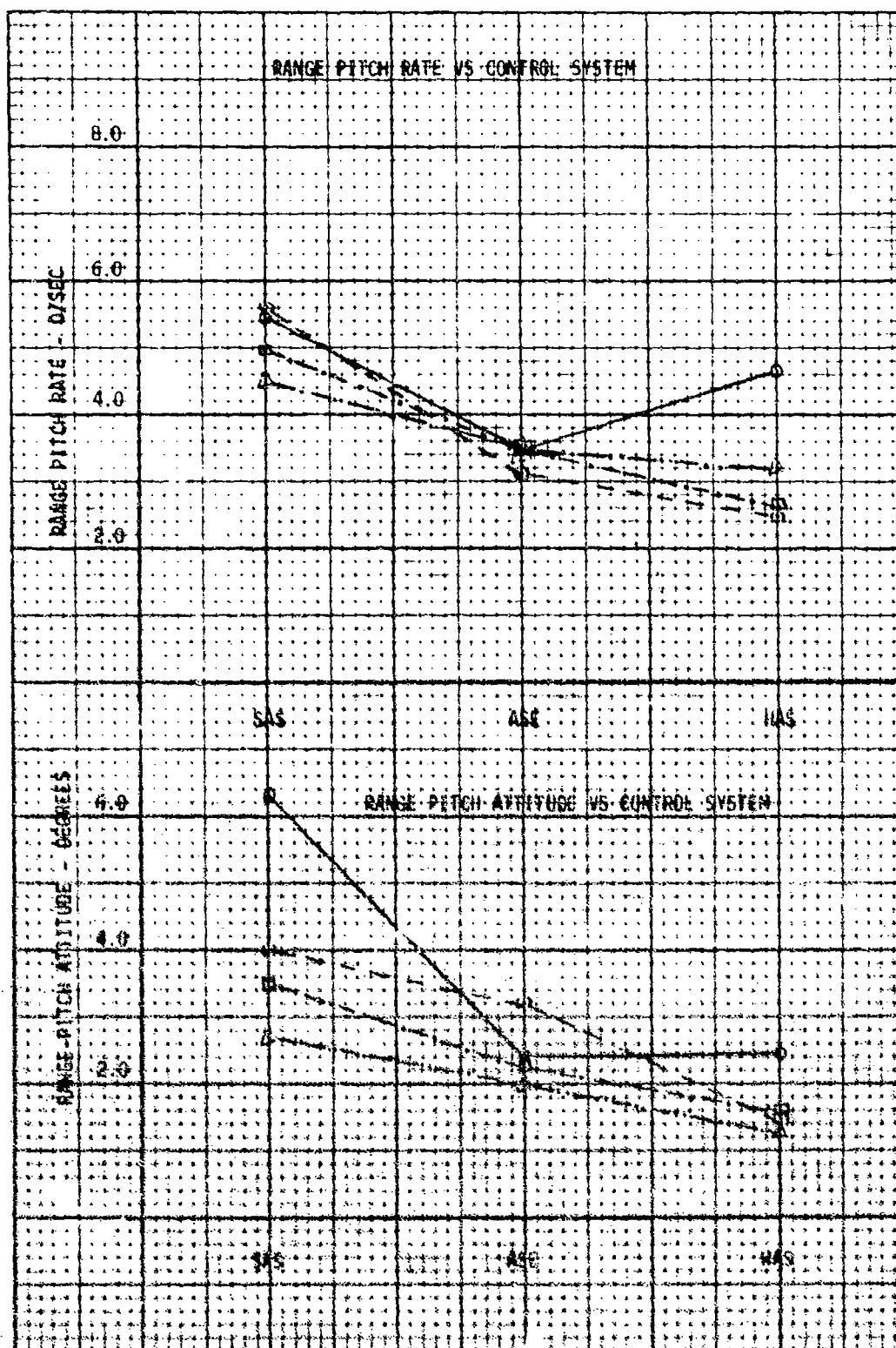22

Figure 15. Pitch rate versus control system

23

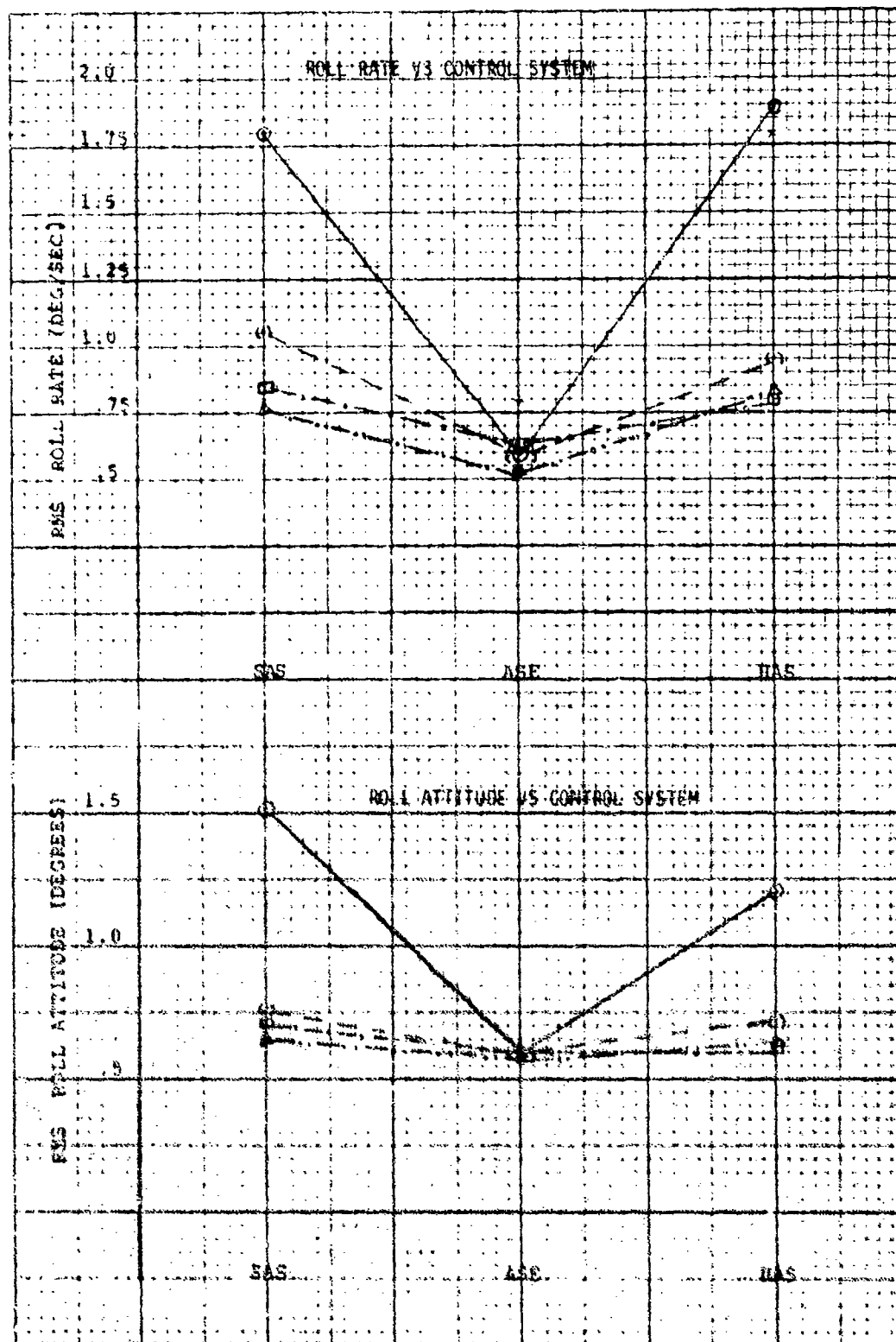Figure 16. Range pitch rate versus control system
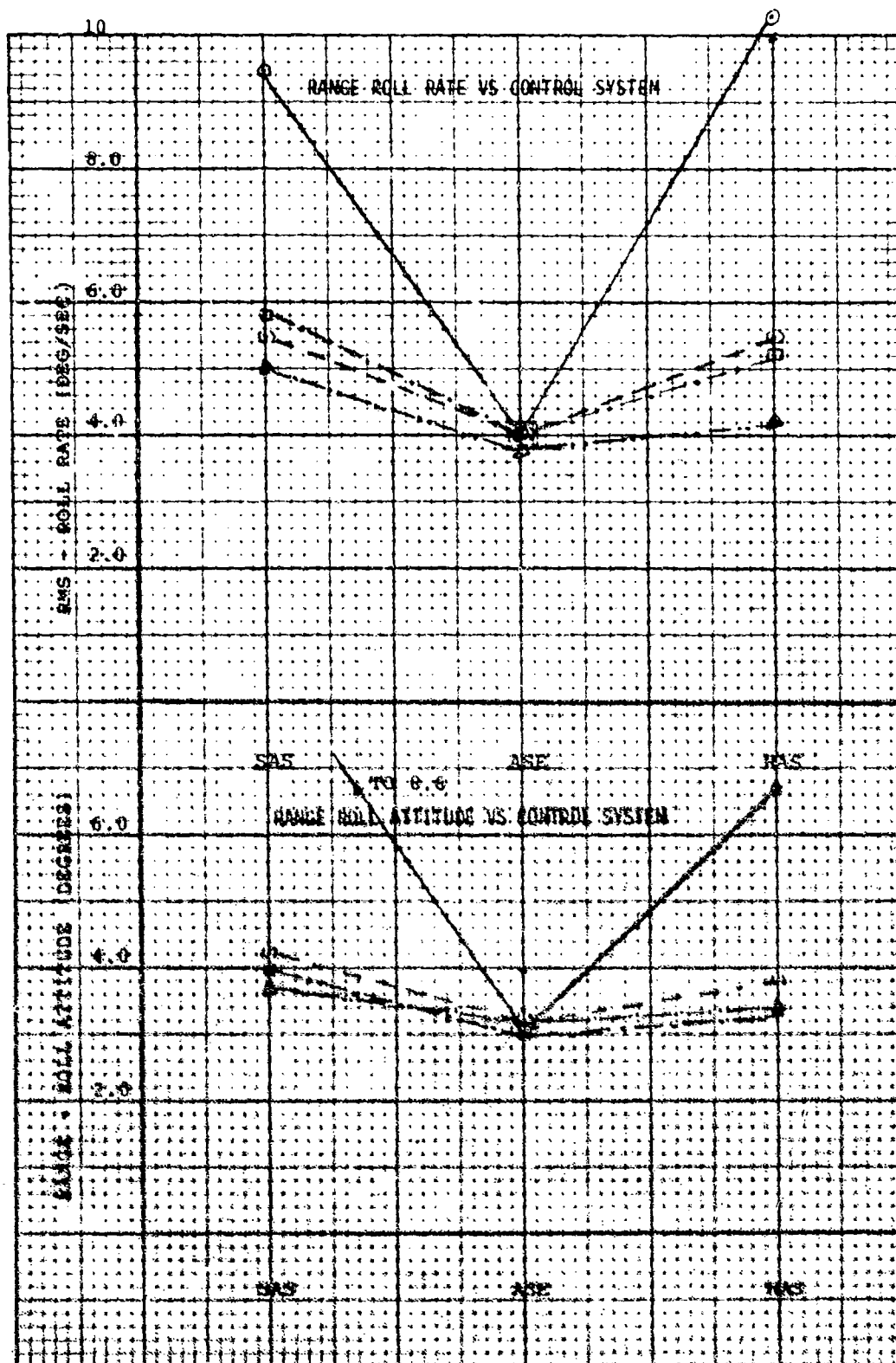
Figure 17.   Roll rate versus control system

Figure 18. Range roll rate versus control system

Because of the difficulty encountered by the pilots with the SAS, most of the training time was spent on this control system. When they felt that they had sufficient time on SAS, then the balance of the training period was conducted with the acceleration vector, velocity vector, position, and each one of the three control systems. Their first impression of the acceleration was that it was too "jerky," that is, it moved too fast and was unpredictable. With additional training, they began to become more confident in being able to use the acceleration not only to hold position, but to also stabilize and improve the handling qualities of the SAS system. The comment that acceleration was a must with the SAS system was stated repeatedly by the subject pilots.

As to their workload, once they began to understand the use of the acceleration vector, they did not seem to mind the jerkiness, although they considered themselves to be "working" harder.

In summary, all subjects agreed that they wanted a medium level ($2 ft/s^2/$ in) of the acceleration vector but were not really sure why they wanted it displayed. One comment was that with acceleration displayed, the pilot knows "where the stick is centered." Another comment was that the acceleration vector "tells him which way to go." Still another was that now he "does not have to look at attitude information."

In the comparison of pure acceleration versus attitude displayed, their general comment was the attitude derived was more predictable and less sensitive, but they felt that it was "sluggish" compared to the pure acceleration cases.

6. DISCUSSION OF RESULTS

The goal of this experiment was to simulate and determine the optimum displayed gains for the accelerations and velocity symbology as a function of three different control systems. The results of the simulation were to be incorporated in the RAVE precision hover flight test program.

The baseline used to evaluate the potential of the acceleration vector was taken from a previous study.[1] The baseline consisted of displayed ground position and velocity symbology gains of 5:1 ratio per inch of travel on the display.

Using the above as a baseline, the cells shown in Figure 8 were formed. Included in these cells were two velocity vector gains of 5 and 2.5 ft/s, and three acceleration vector gains of 3 ft/s^2, 2 ft/s^2, and 1.33 ft/s^2 per inch of travel on the display. The criteria for selecting the optimum displayed gains were based on the hover performed and subject pilot comments. The averaged results of the mean standard deviation, rms and range (peak values) for the four subject pilots are shown in bargraph form in Figures C-1 through C-10. A comparison of the performance of the three acceleration gains with the three control systems and the two velocity gains are shown in Figures 11 and 12. An additional comparison of performance is made of the attitude with the pure acceleration in Figure 13.

27

In general, the results indicate that any of the acceleration gains with either velocity combination is helpful to the pilot in reducing the radial ground position errors to less than 2.0 feet (rms) as compared to the baseline of less than 5 feet (rms). However, the radial dispersion in ground position performance for each control system with the three accelerations and the two velocities are approximately 1.1 to 1.8 feet SAS, 0.95 to 1.35 feet ASE, and 0.65 to 1.0 feet HAS (Appendix C, Figures C-14 and C-15).

The only significant dispersion in radial position with different acceleration gains can be found with the SAS system. The slight differences of performance between the ASE and HAS control systems with the different acceleration gain might be due to the display washing out the effects of the control system as well as the acceleration.

From the curves shown in Figures C-14 and C-15, and pilot comment as to the preferred acceleration gain, a selection of the appropriate cells was made. These cells were judged on minimal position errors and consistency throughout the three control systems. This choice along with the baseline cells is shown in Figures 1 and 2, following this discussion.

Included in this selection are pure acceleration gains of 2 ft/s^2 and the attitude gain of 4 degrees per second per inch of travel on the display. Both velocity gains were also selected since the differences in position error is less than 0.25 feet for the above mentioned acceleration gain.

For the above selection, some additional analysis was performed. The pilot's performance in descent to the prescribed hover altitude of 50 feet was best accomplished by the displayed attitude. The deviations about the 50-foot reference were less than 3 feet for SAS, 1 foot for ASE to almost zero for HAS (Figure 3).

Another variable that was recorded was the time required by the pilot to make the transition from approach to the hover maneuver and to minimize the position error to his liking before he initiated the data collection program. This parameter was of interest since it gave some baseline information as to flight time required in the terminal maneuvers. The time required is a function of fuel burned and as such it is an important parameter. The results of the above are shown in Figure 4. The acceleration with the low level velocity required minimum time: 26 seconds with SAS, 21 seconds with ASE, and 19 seconds with HAS. There is, however, no appreciable difference between the results stated from those of the baseline cell, but there is a significant difference between pure acceleration and attitude with HAS of approximately 10 seconds increase. One explanation for this increase can best be derived from pilot comment. The pilots felt that with the HAS system and displayed attitude "the system felt sluggish." The pilots had adopted a technique of small control inputs from approach into hover for flying the more responsive SAS and ASE systems. They apparently were using the same technique while flying the HAS, but this system is much more dampened. More control movement was required to achieve higher velocities to minimize the position errors quicker and the subjects were anticipating driving the system into instability.

28

Pilot workload was also measured by recording the rms stick position (longitudinal and lateral). In Figure 5, the results of the baseline and the previous selected cells are shown as functions of rms ground position and rms control displacement. The most obvious observation is that the acceleration vector reduces the radial position error from approximately 5 feet to less than 1.5 feet and the control displacement from 0.75 to 0.5 inches rms for SAS. For the ASE, position errors reduced from 1.8 feet to about 1 foot without any apparent stick displacement improvement. The HAS system shows improvement in radial ground position from 1.7 foot to less than 1 foot and stick displacement from 0.35 to 0.15 inches.

Finally, the aircraft attitudes and rates for pitch and roll for the selected acceleration and velocity cells, as well as the baseline, are shown in Figures 6 through 9. In general, displaced acceleration or attitude with either velocity combinations tend to reduce or dampen the aircraft oscillations. The pitch rms attitude was less than 0.4 degrees and pitch rate about 0.6 degrees per second with a negative slope as a function of more complex systems. The peak values for pitch attitude and rate were 3 and 4 degrees per second with the same general negative trend with more complex control system. The only significant improvement (30-40 percent with displayed acceleration or attitude) in aircraft pitch oscillations can be observed with the SAS control systems. The acceleration vector tends to provide the dampening required to make this system compatible to the ASE or HAS.

In the roll axis (Figures 8 and 9), the acceleration vector seems to have a more pronounced effect. There is generally greater than 50-percent reduction from the baseline roll attitudes and rates for the SAS and HAS systems and apparently no change at all with ASE. The reduction is equivalent to the level of the ASE system. This is probably due to an increase of artificial dampening provided by the acceleration vector and along with the ITED display tend to washout the effect of the different control system.

In summary, the results obtained in the TASS Simulator indicate that the acceleration vector, whether its pure or attitude derived, can be used with different control system augmentations to perform precision hover tasks of less than 1.5 feet rms. The finding also shows that the acceleration vector with the ITED display tends to washout the control system augmentations as well as reduce the pilot workload.

7. CONCLUSIONS AND RECOMMENDATIONS

a. Conclusions. Several conclusions can be made from the experiment data, the resulting data analysis, and the use of pilot comments:

(1) Displayed acceleration was required to enable pilots to satisfactorily stabilize the helicopter model when equipped with a SAS flight control system.

(2) Mean position accuracies in the order of 1 foot and less can be obtained with manual control and the acceleration vector on the display.

(3) Differences in ground position errors due to a variation of acceleration vector gains were washed out by the HAS system.

29

(4) The acceleration vector washes out aircraft flight variables of rate and attitude.

(5) Ideal or pure acceleration, velocity, and position gains of 2 ft/s^2: 2.5 ft/s: 12.5 ft/inch displayed were found to give the minimum radial ground position performance.

(6) The approach velocity to hover had to be restricted to less than 5 knots in both axis to avoid overshooting the target.

(7) The acceleration vector was a driving device in forcing the pilot to better his performance.

(8) Pilot comment was that the acceleration vector made them "work" harder.

(9) The pilot performance is reduced by a factor of two with the acceleration vector and the SAS system, yet the rms workload stick movement is identical to that of the ASE without the vector.

(10) The average time required by the pilot to minimize his errors to an acceptable level before data collection is initiated is about 20 to 25 seconds.

b. Recommendations. It is highly recommended that some of the results obtained in this study be incorporated and flown in the Research Aircraft for Visual Environment (RAVE) flight tests to include:

(1) Pure acceleration derived from the gimbal mounted accelerometers 2 ft/s^2 per inch displayed.

(2) Attitude derived acceleration 2.25 ft/s^2 per inch displayed.

(3) Low velocity and position sensitivity of 5 ft/s: 12.5 ft/inch displayed rather than the high velocity sensitivity of 2.5 ft/s since the noise of the velocity sensor will appear on the display.

(4) If possible, to disengage the AFCS and fly the aircraft with the SAS and the acceleration vector or attitude.

APPENDIX A

HELICOPTER ROOT LOCUS ANALYSIS

HELICOPTER MODEL

The linearized equations of motion for the CH-53A helicopter used in the man/machine simulation and the analysis are shown below.

Longitudinal-Vertical Axis

$$
\begin{bmatrix}
(S - X_u) & -X_w & +g \\
-Z_u & (S - Z_w) & -U_O S \\
-M_u & -M_{\dot{w}}S - M_w & S^2-(M_q + M_\alpha)s-M
\end{bmatrix}
\begin{bmatrix}
\Delta u \\
\Delta w \\
\Delta \theta
\end{bmatrix}
=
$$

$$
\begin{bmatrix}
X_{BIS} & X_{AOS} \\
Z_{BIS} & Z_{AOS} \\
M_{BIS} & M_{AOS}
\end{bmatrix}
\begin{bmatrix}
\Delta BIS \\
\Delta AOS
\end{bmatrix}
+
\begin{bmatrix}
-X_u \\
-Z_u \\
-M_u
\end{bmatrix}
\begin{bmatrix}
\Delta U_g
\end{bmatrix}
$$

Lateral-Directional Axis

$$
\begin{bmatrix}
(S - Y_v) & -Y_p S -g & -Y_r S + U_O v \\
-L'_v & (S^2-L'_p S) & -L'_r S + U_O L'_v \\
-N'_v & -N'_p S & (S^2-N'_r S + U_O N'_v)
\end{bmatrix}
\begin{bmatrix}
\Delta v \\
\Delta \phi \\
\Delta \psi
\end{bmatrix}
=
$$

$$
\begin{bmatrix}
Y_{AIS} & Y_{\theta TR} \\
L'_{AIS} & L'_{\theta TR} \\
N'_{AIS} & N'_{\theta TR}
\end{bmatrix}
\begin{bmatrix}
\Delta AIS \\
\Delta \theta
\end{bmatrix}
+
\begin{bmatrix}
-Y_v \\
-Y_v \\
-N_v
\end{bmatrix}
\begin{bmatrix}
\Delta v_g
\end{bmatrix}
$$

The dimensional derivatives for the hover condition used in the simulation and for the analysis performed are indicated below.

Longitudinal-Vertical Axis			Lateral-Directional Axis	
U_O	Ft/S	Hover		
X_u		-0.0154	Y_v	-0.0352
X_w		0.0	Y_p	-1.43
Z_u		0.0	Y_r	0.850
Z_w		-0.303	L'_v	-0.0128
M_u		0.00204	L'_p	-2.31
$M_{\dot{w}}$		0.0	L'_r	0.0946
M_w		0.00075	N'_v	0.0053
$(M_q + M_{\dot{\alpha}})$		-0.438	N'_p	0.0166
M_α		0.0	N'_r	-0.236
g		32.2	g	32.2
X_{VIS}		32.8	Y_{AIS}	33.2
X_{AOS}		0.0	$Y_{\theta TR}$	18.9
Z_{BIS}		0.0	L'_{AIS}	22.4
Z_{AOS}		-276.0	$L'_{\theta TR}$	2.18
M_{BIS}		-4.32	N'_{AIS}	0.096
M_{AOS}		0.680	$N'_{\theta TR}$	-5.12

Using the above stability derivatives and the root locus method, an analysis was performed to investigate the effect of displaying acceleration, velocity and position on longitudinal manual hover performance. The analysis also includes the effects of the ASE and SAS feedback control system since these systems provide the inner loop closures. The block diagram below shows the basic matrix set up used to solve the helicopter equations to perform the required analysis.
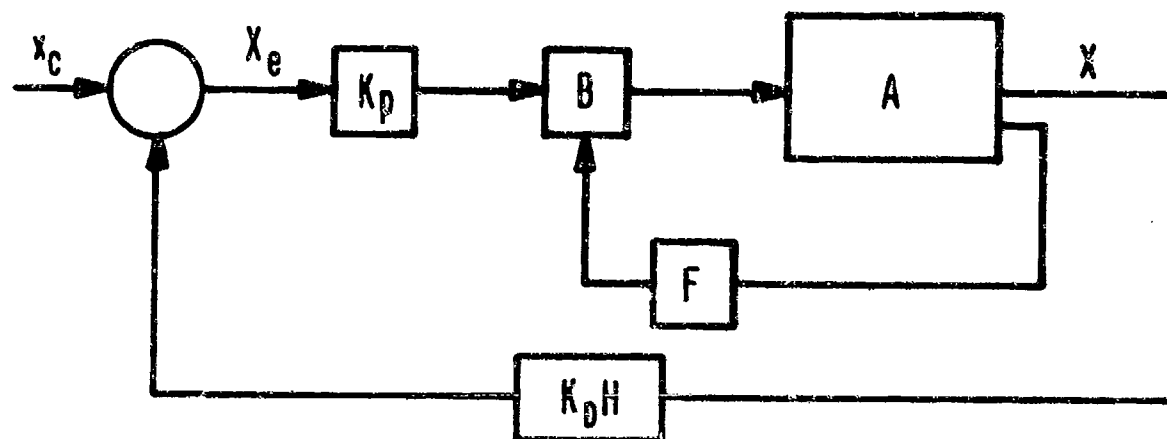
where   A = Helicopter Dynamics Matrix

B = Helicopter Control Matrix

F = Helicopter Feedback Matrix

K_D = Display Gains

H = Display Dynamics

K_p = Pilot Gain

x_c = Position Reference

X_e = Position Error

X = Position Output

The first control system to be investigated was the Automatic Stabilization Equipment (ASE). This system provides pitch rate and attitude automatically and is represented below.

$$\frac{B_{IS}}{\theta} = + (0.32S + 0.594) \tag{A-1}$$

The closed loop transfer function for θ/B_{IS} with the above equation in the inner loop closure becomes

$$\frac{\theta}{B_{IS}} = \frac{-4.33 \ (S + 0.0001) \ (S + 0.3)}{(S + 0.026) \ (S + 0.3) \ (S + 0.91 \pm j1.31)} \tag{A-2}$$

33

The dominant roots for this attitude loop closure shown in Figure A-1 is the complex pair

$$S + 0.91 \pm j1.31)$$

This pair of closed loop roots show that the aircraft has a natural frequency of $W_n = 1.59$ and damping ratio $\xi = 0.57$. With this attitude or inner loop closed, the position open loop transfer functions after solving the matrix equation for $\dfrac{X}{BIS}$ becomes

$$\frac{X}{BIS} = \frac{32.8\ (S + 0.3)\ (S + 0.22 \pm j2.07)}{S\ (S + 0.026)\ (S + 0.3)\ (S + 0.91 \pm j1.31)} \qquad \text{A-3}$$

To this open loop transfer function, displayed velocity and position were added. It should be noted that the simulation study as well as this analysis include only the manual precision hover task. The automatic precision hover was not covered. This technique should be investigated in a future study.

For the manual hover task, the displayed symbology may be viewed as a feedback device with displayed symbol gains as the feedback gains of an automatic system. The first set of symbols displaying velocity and position were determined in Reference 6 to be in the ratio of 1.0:0.2 (velocity: position) and may be expressed as

$$\frac{B_{IS}}{X} = K_x\ (S + \frac{K_x}{K_{\dot{x}}}) = 0.4\ (S + 0.2) \qquad \text{A-4}$$

The sum of velocity and position introduces a lead term or zero in the numerator of Equation 3 by direct substitution.

Since the pilot is the active controller in the manual hover task, a pilot model is required. A simplified model which assumes the pilot to operate as a pure gain, K_p is used. It is also assumed that the pilot utilizes each of the displayed symbol gains in the ratio that they appear to perform the hover task. The new open loop transfer function using Equations 3 and 4 and the pilot gain K_p now becomes

$$\frac{X}{B_{IS}} = \frac{32.8\ (0.4\ K_p)\ (S + 0.2)\ (S + 0.22 \pm j\,2.07)\ (S + 0.3)}{S\ (S + 0.026)\ (S + 0.3)\ (S + 0.91 \pm j1.31)} \qquad \text{A-5}$$

The root locus of the above transfer function with varying pilot gains K_p is shown in Figure A-2.

When acceleration, velocity, and position are displayed in the ratio of 1:.8:.16, respectively, the feedback control equation becomes

$$\frac{B_{IS}}{X} = K_x\ S^2 + \frac{K_{\dot{x}}}{K_{\ddot{x}}}\ S + \frac{K_x}{K_{\ddot{x}}}) = 0.5\ (S^2 + 0.8\ S + 0.16) \qquad \text{A-6}$$

34

Figure A-1. Closed loop roots for $\dfrac{\theta}{\delta_{IS}}$ with ASE
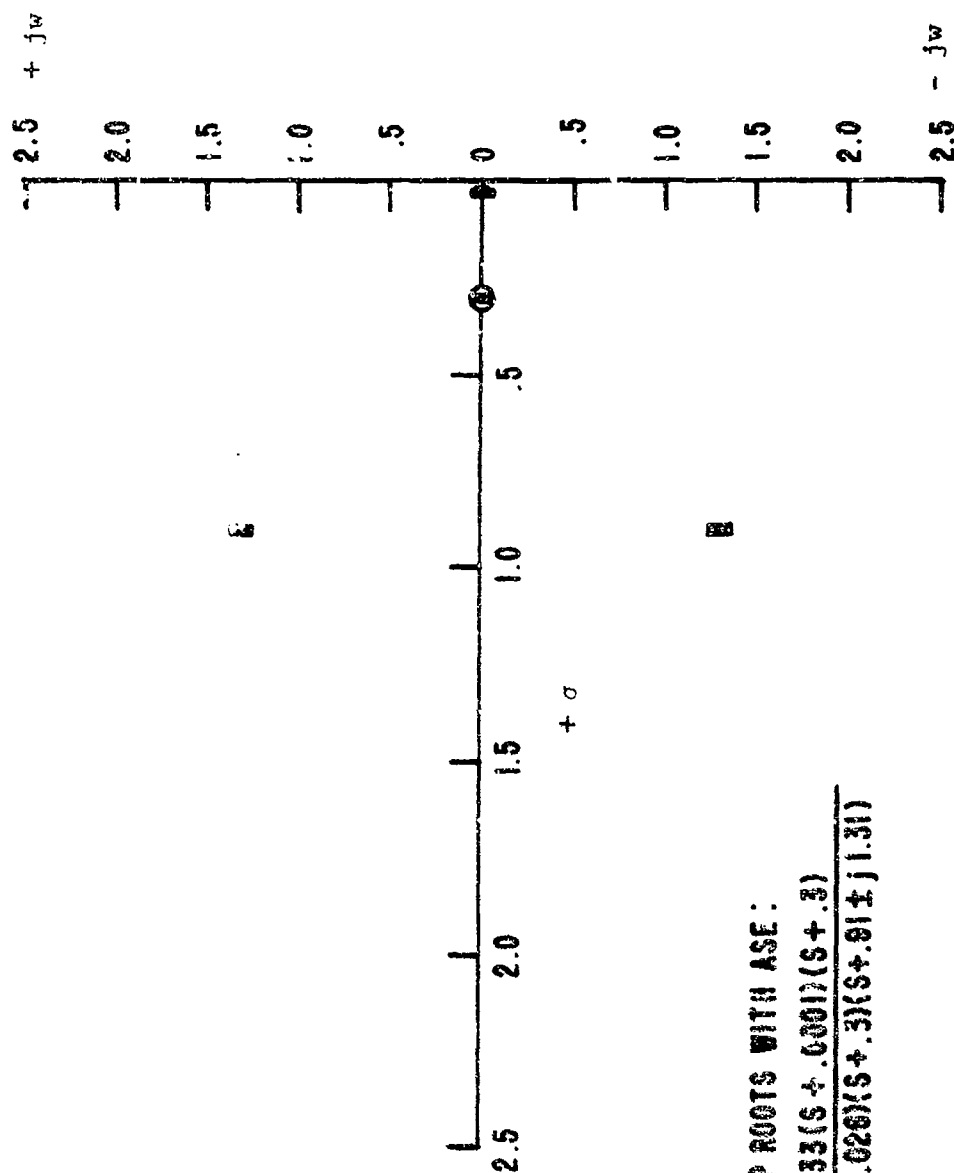
CLOSED LOOP ROOTS WITH ASE:

$$\frac{\theta}{\delta_{IS}} = \frac{-4.33(S+.0001)(S+.3)}{(S+.026)(S+.3)(S+.81 \pm j1.31)}$$

35
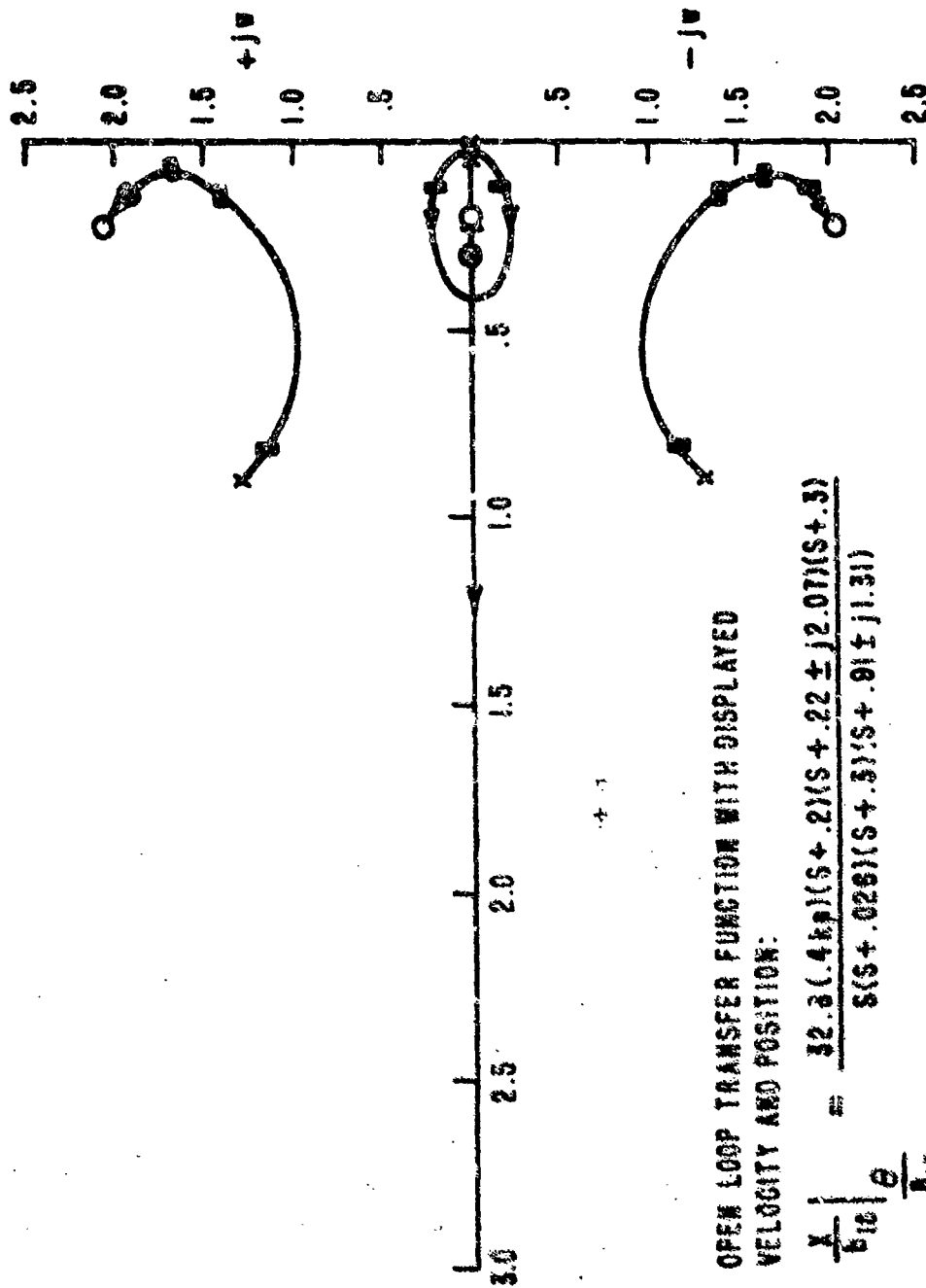
OPEN LOOP TRANSFER FUNCTION WITH DISPLAYED
VELOCITY AND POSITION:

$$\frac{X}{\theta_{IS}}\bigg|\frac{\theta}{\theta_{IS}} = \frac{32.8(.4k_p)(S+.2)(S+.22 \pm j2.07)(S+.3)}{S(S+.028)(S+.5)(S+.91 \pm j1.31)}$$

DISPLAYED VELOCITY AND POSITION:

$$\frac{\theta_{IS}}{X} = .4(S+.2)$$

Figure A-2. Root locus of $\frac{X}{\theta_{IS}}$ with displayed velocity and position

35

The vector sum of this equation introduces a double lead term in the numerator of Equation 3 by direct substitution.

The open loop transfer function using Equations 3 and 6, and the pilot K_p becomes

$$\frac{X}{B_{IS}} = \frac{32.8\ (0.5\ ^{K}p)\ (S^2 + 0.8\ S + 0.16)\ (S + 0.22 + j2.07)\ (S + 0.3)}{S\ (S + 0.026)\ (S + 0.3)\ (S + 0.91 \pm j1.31)} \quad \text{A-7}$$

The root locus of this transfer function with varying pilot gain K_p is shown on Figure A-3.

A comparison of Figures A-2 and A-3 indicate that there is no significant improvement in controlling position for low pilot gain K_p with and without acceleration. However, as the pilot increases his gain ($K_p = 0.1$), the damping of the dominant roots without the acceleration displayed (Figure A-2) tends to be reduced. This reduction in damping forces the pilot to generate additional lead from some other source to dampen the aircraft positional oscillations.

The analysis of displayed acceleration, velocity, and position was also carried out with the SAS system. The closed loop transfer function for $\frac{\theta}{B_{IS}}$ with the pitch rate in the inner loop is

$$\frac{\theta}{B_{IS}} = \frac{4.33\ (S + 0.0001)\ (S + 0.3)}{(S + 0.3)\ (S + 1.85)\ (S - 0.008 \pm j0.19)} \quad \text{A-8}$$

The closed loop roots are shown in Figure A-4. It should be stated that to generate the SAS only, the attitude loop of the ASE system was set equal to zero, thus proving a SAS system. The particular gain 0.33 $\hat{\theta}_B$ does not seem to be sufficient to make the system stable. This unstable closed loop system was solved for the manual position control of $\frac{X}{B_{IS}}$ which is

$$\frac{X}{B_{IS}} = \frac{32.8\ (S + 0.3)\ (S + 0.22 \pm J2.07)}{S\ (S + 1.85)\ (S + 0.3)\ (S - 0.008 \pm J0.19)} \quad \text{A-9}$$

To this transfer function velocity and position were added to provide a lead term or zero shown by

$$\frac{B_{IS}}{X} = K_{\dot{x}}\ (S + \frac{K_{\dot{y}}}{K_{\ddot{y}}}) = 0.4\ (S + 0.2) \quad \text{A-10}$$

as was done with the ASE case. The open loop transfer function becomes

$$\frac{X}{B_{IS}} = \frac{32.8\ (0.4\ ^{K}p)\ (S + 0.2)\ (S + 0.3)\ (S + 0.22 \pm J2.07)}{S\ (S + 1.85)\ (S + 0.3)\ (S - 0.008) \pm j0.19} \quad \text{A-11}$$

and its root locus is shown in Figure A-5.

37
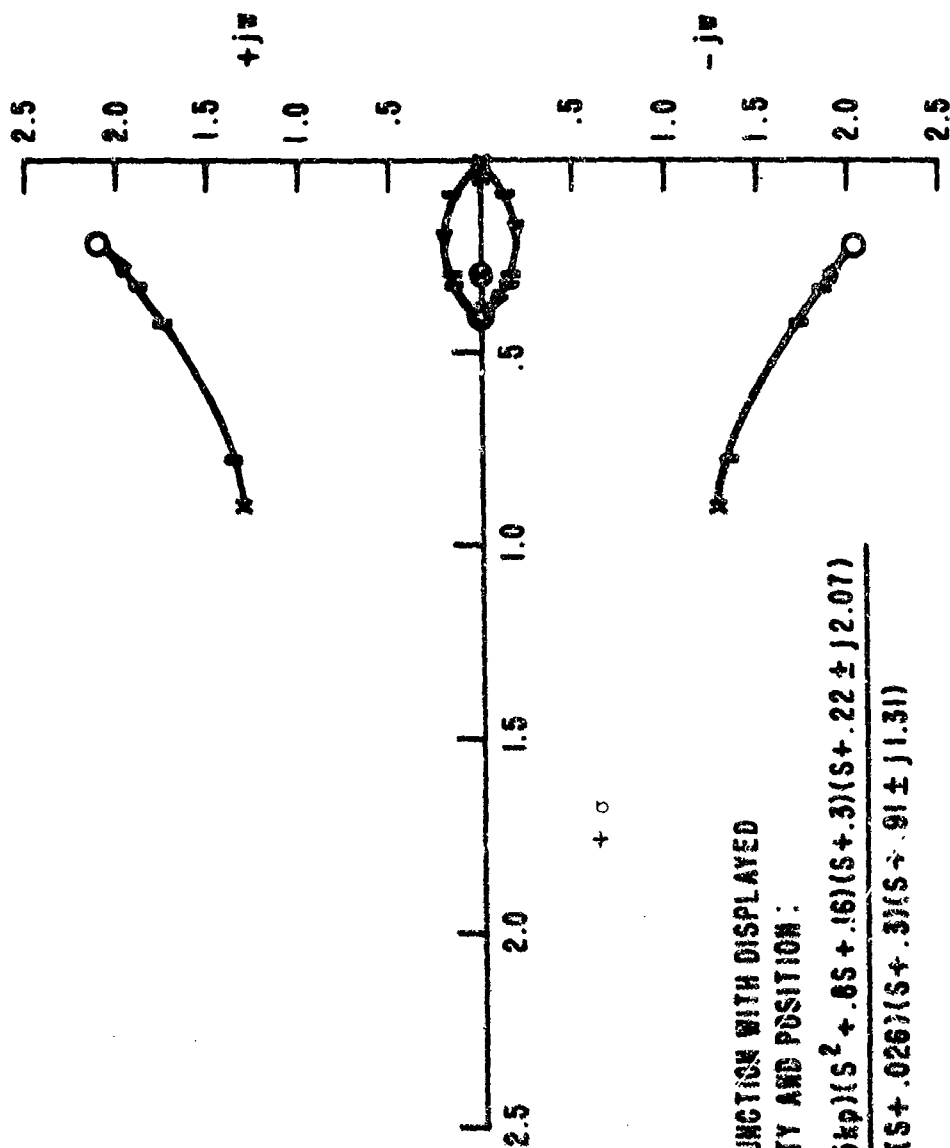
OPEN LOOP TRANSFER FUNCTION WITH DISPLAYED
ACCELERATION, VELOCITY AND POSITION:

$$\frac{K}{\theta_{1S}}\Big|\frac{\theta}{\theta_{1S}} = \frac{32.8(.5xp)(S^2+.85+.16)(S+.3)(S+.22\pm j2.07)}{S(S+.026)(S+.3)(S+.91\pm j1.31)}$$

DISPLAYED ACCELERATION, VELOCITY AND POSITION:

$$\frac{\theta_{1S}}{x} = .5(S^2+.85+.16)$$

Figure A-3. Root locus of $\dfrac{x}{\theta_{1S}}$ with displayed acceleration, velocity, and

38
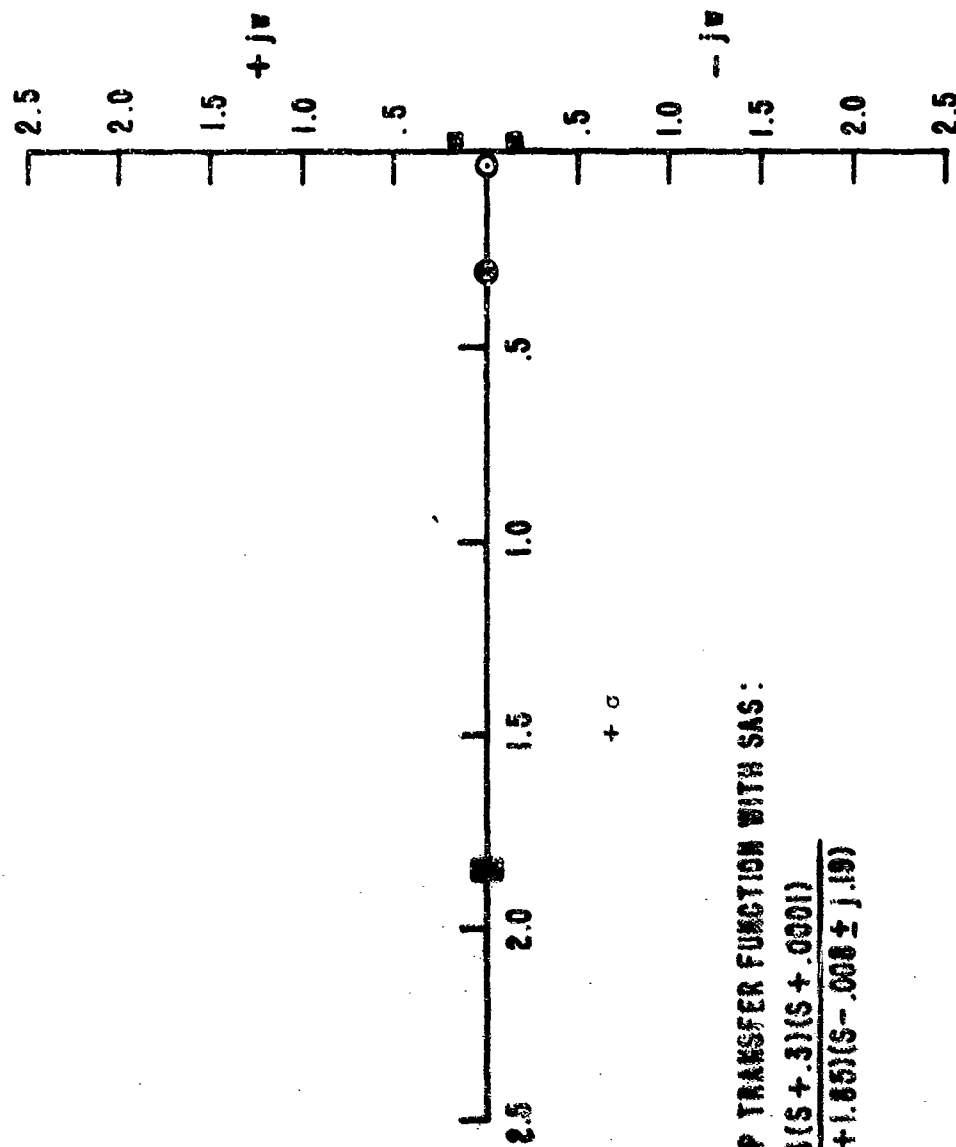
CLOSED LOOP TRANSFER FUNCTION WITH SAS:

$$\frac{\theta}{B_{IS}} = \frac{-4.33(S+.3)(S+.0001)}{S(S+1.65)(S-.008\pm j.19)}$$

Figure A-4. Closed loop roots for $\frac{\theta}{B_{IS}}$ with SAS only.

39
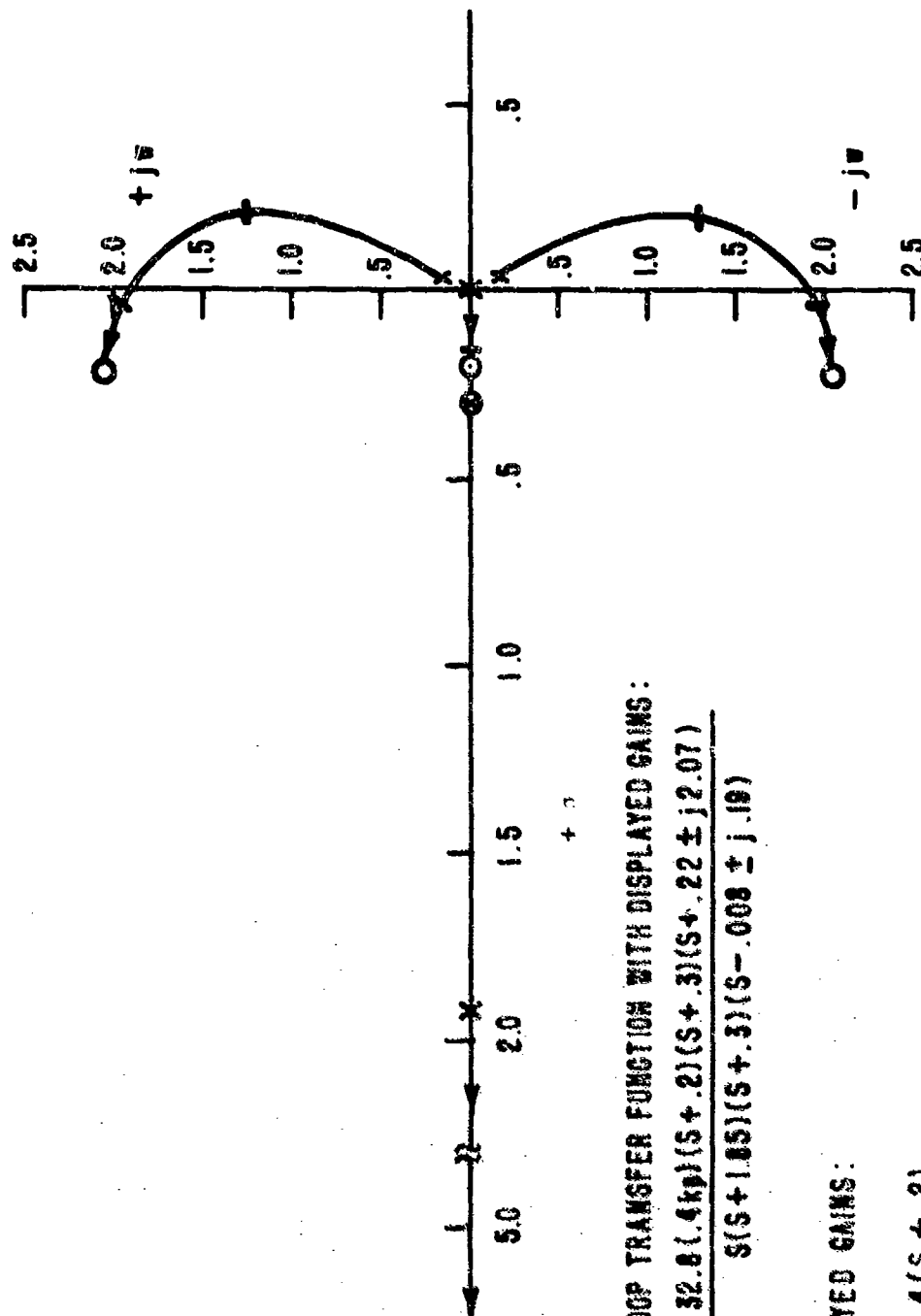
OPEN LOOP TRANSFER FUNCTION WITH DISPLAYED GAINS:

$$\frac{X}{B_{IS}} = \frac{32.8(.4k_p)(S+.2)(S+.3)(S+.22 \pm j2.07)}{S(S+1.85)(S+.3)(S-.008 \pm j.19)}$$

DISPLAYED GAINS:

$$\frac{B_{IS}}{X} = -.4(S+.2)$$

Figure A-5. Root locus of $\frac{X}{B_{IS}}$ with displayed velocity, position, and with SAS only

Acceleration, velocity, and position were also added in the same ratios as the ASE case

$$\frac{B_{IS}}{X} = 0.5 \ (S^2 + 0.8 \ S + 0.16) \qquad\qquad A-12$$

This displayed function provides a double zero or lead term to the pilot. The new transfer function with K_p as the pilot gain is

$$\frac{X}{B_{IS}} = \frac{32.8 \ (0.5 \ K_p) \ (S^2 + 0.8 \ S + 0.16) \ (S + \ .3) \ (S + 0.22 \pm j2.07)}{S \ (S + 1.85) \ (S + 0.3) \ (S - 0.008 \pm j0.19)}$$

$$A-13$$

Its root locus is shown in Figure A-6. A comparison of Figures A-5 and A-6 indicates that for low pilot gain $K_p < 1.0$, the position control with only velocity and position displayed is unstable. The addition of acceleration provides the pilot with enough lead time to make the position control task possible without instability even for pilot gains $K_p < 0.1$.

In summary, this analysis shows that displayed acceleration does increase positional stability and damping. It also shows that an unstable system can be driven into stability with less demand on pilots to provide high gain and lead compensation.

2. STABILIZATION

Three control systems were used in the experiment. The feedback as well as the forward path gain are shown below.

a. Automatic Stabilization Equipment (ASE).

(1) Pitch.

41

OPEN LOOP TRANSFER FUNCTION AND DISPLAYED GAINS:

$$\frac{X}{B_{IS}} = \frac{32.8(.4k_p)(S^2+.65+.16)(S+.16)(S+.3)(S+.22 \pm j2.07)}{S(S+1.65)(S+.3)(S-.009 \pm j.19)}$$

DISPLAYED GAINS:

$$\frac{B_{IS}}{X} = -.5(S^2+.65+.16)$$
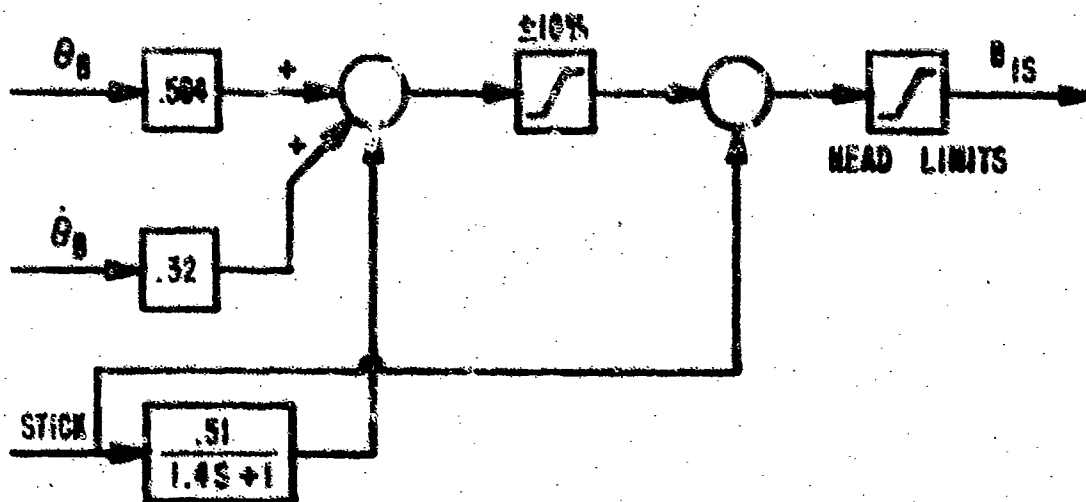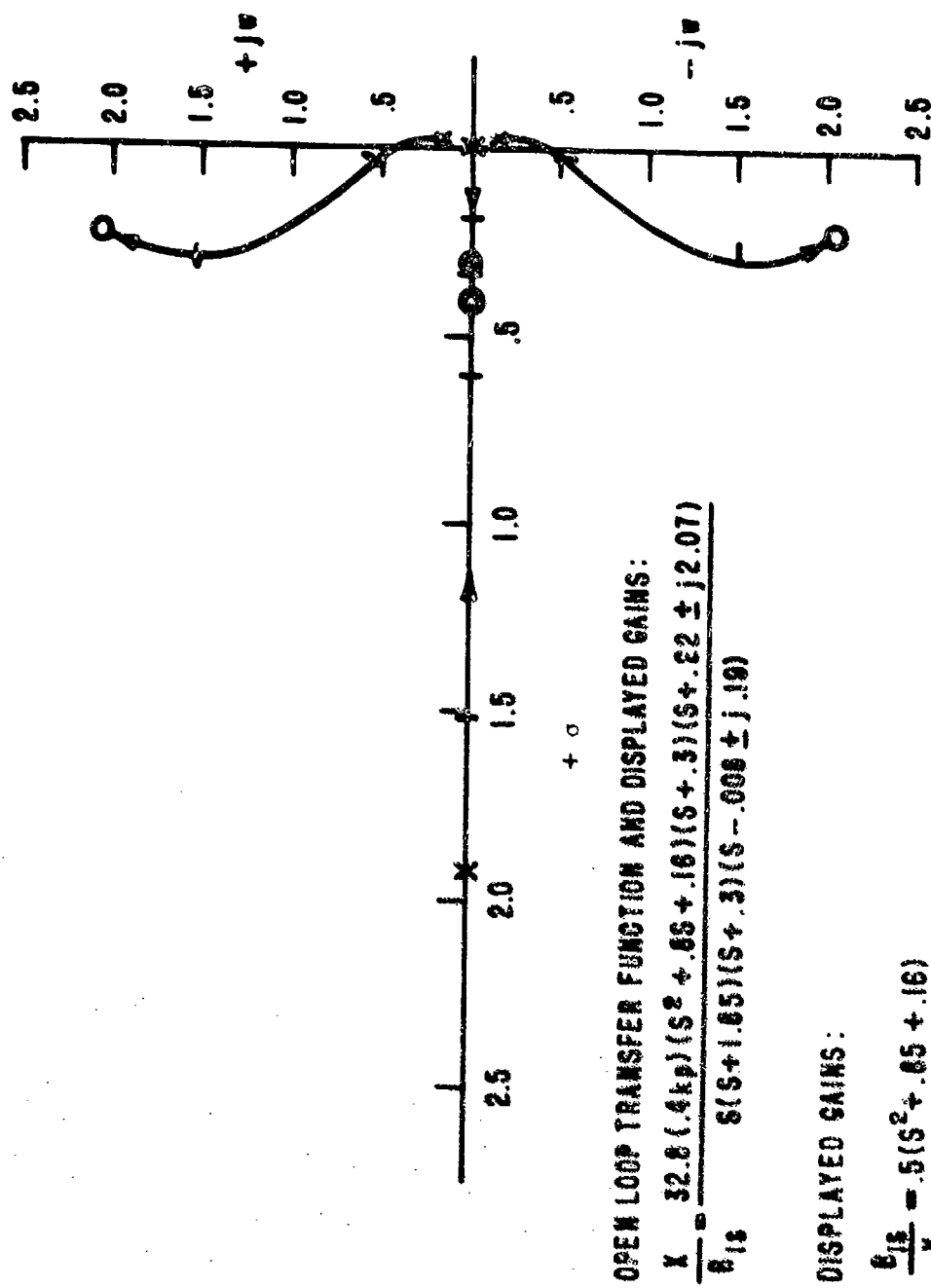
Figure A-6. Root locus of $\frac{X}{B_{IS}}$ with displayed acceleration, velocity, position, and with SAS only

42

(2) Roll.

(3) Yaw.

43

(4) Collective.

RADAR ALTITUDE SET
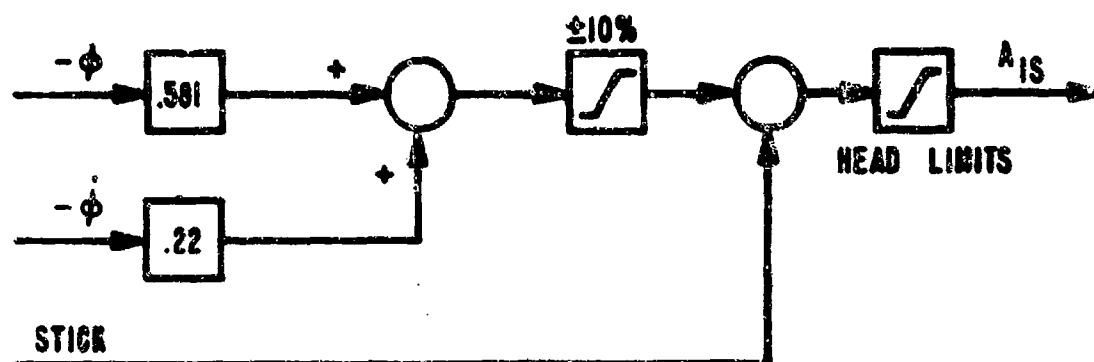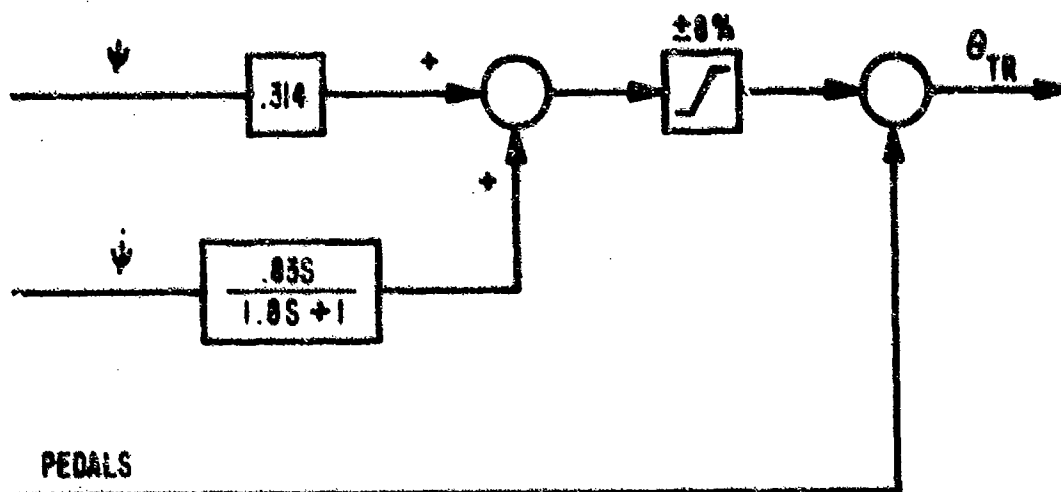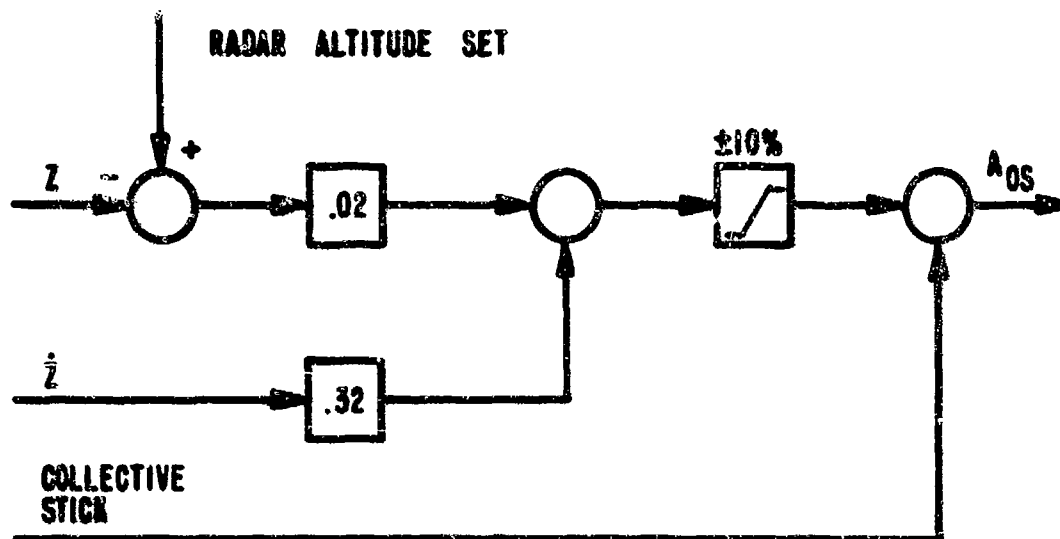
3. STABILITY AUGMENTATION SYSTEM (SAS)

   a. Pitch.

b. Roll.

c. Yaw.

45
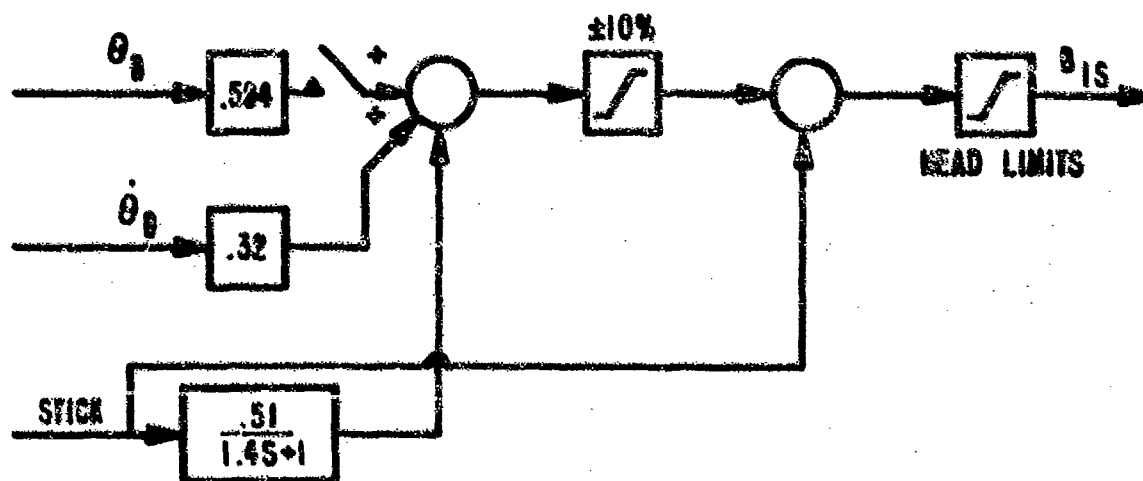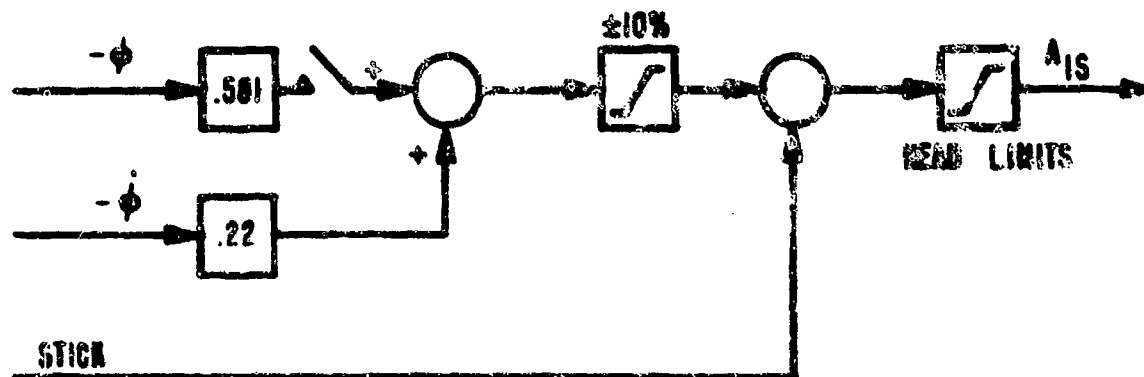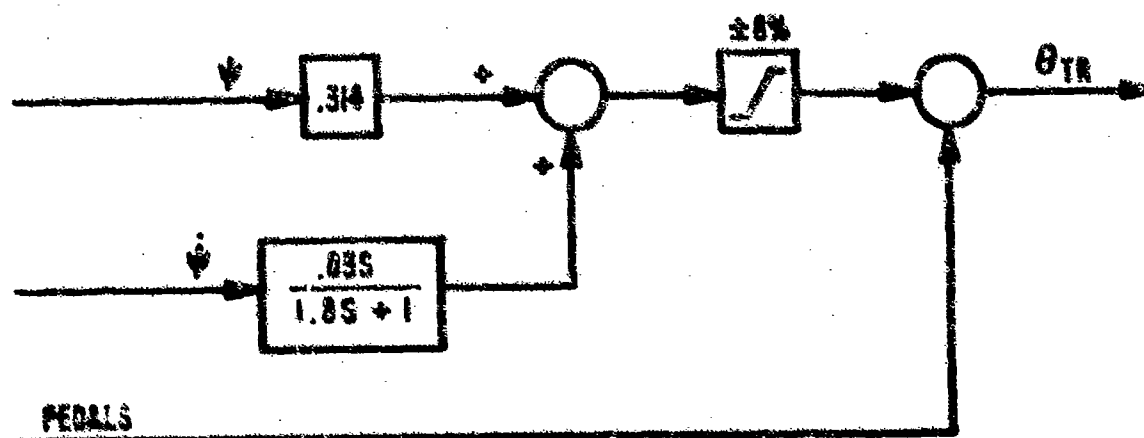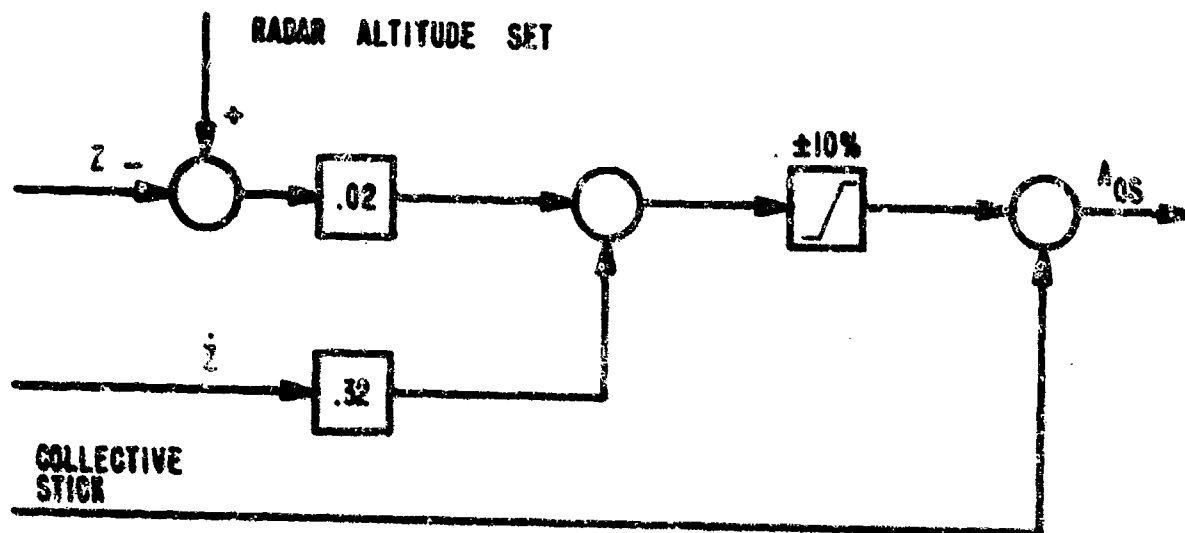
d. Collective.

4. HOVER AUGMENTATION SYSTEM (HAS)

    a. Pitch.

u_1 = 5 fps / in.

b. <u>Roll</u>.

$K_2 = 5$ fps/in

c. <u>Yaw</u>.

d. Collective.

RADAR ALTITUDE SET
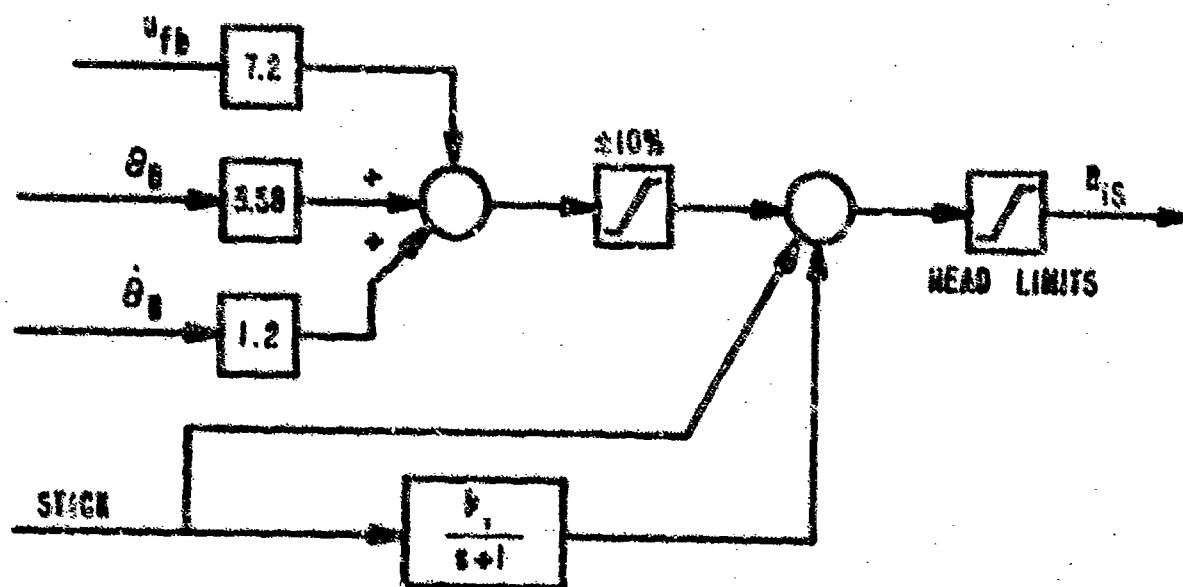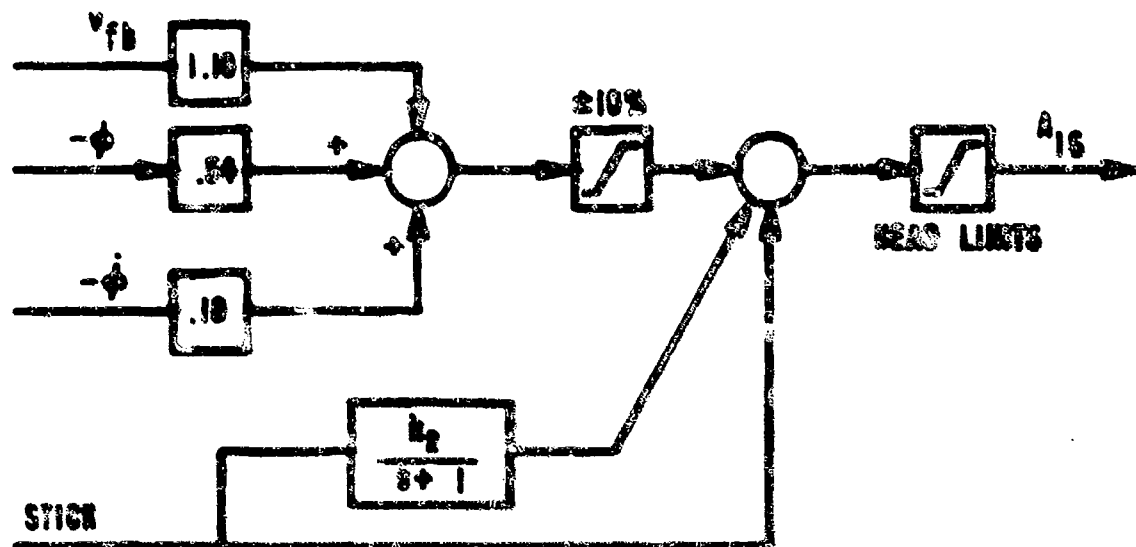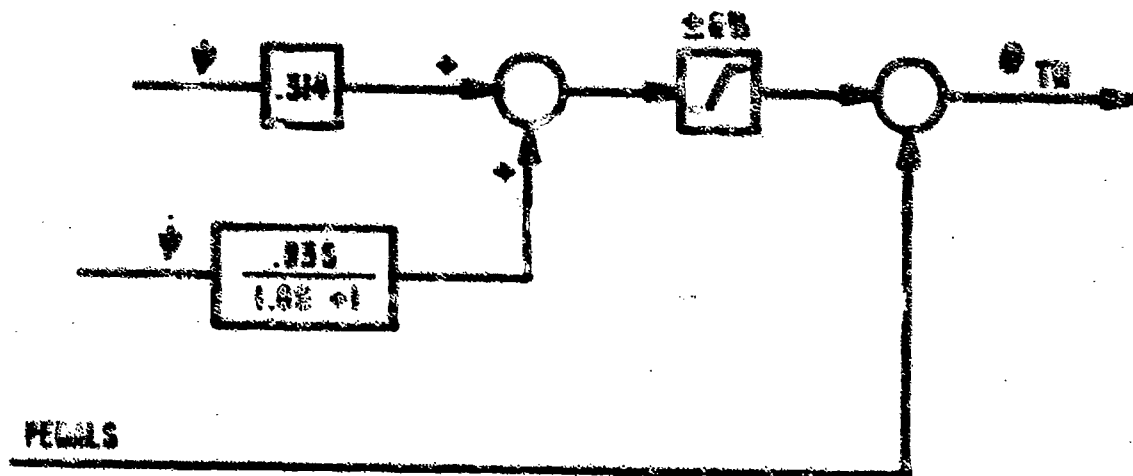
COLLECTIVE
STICK
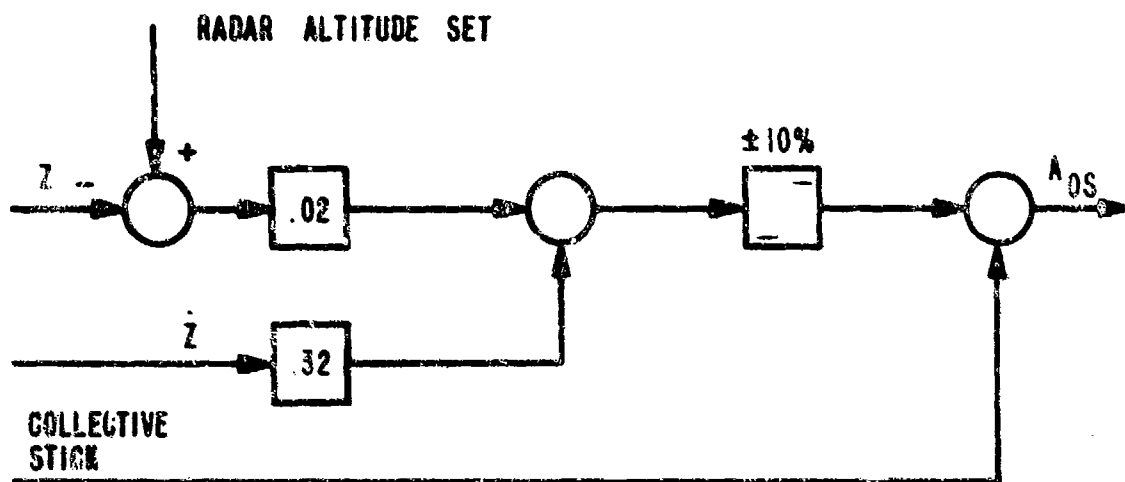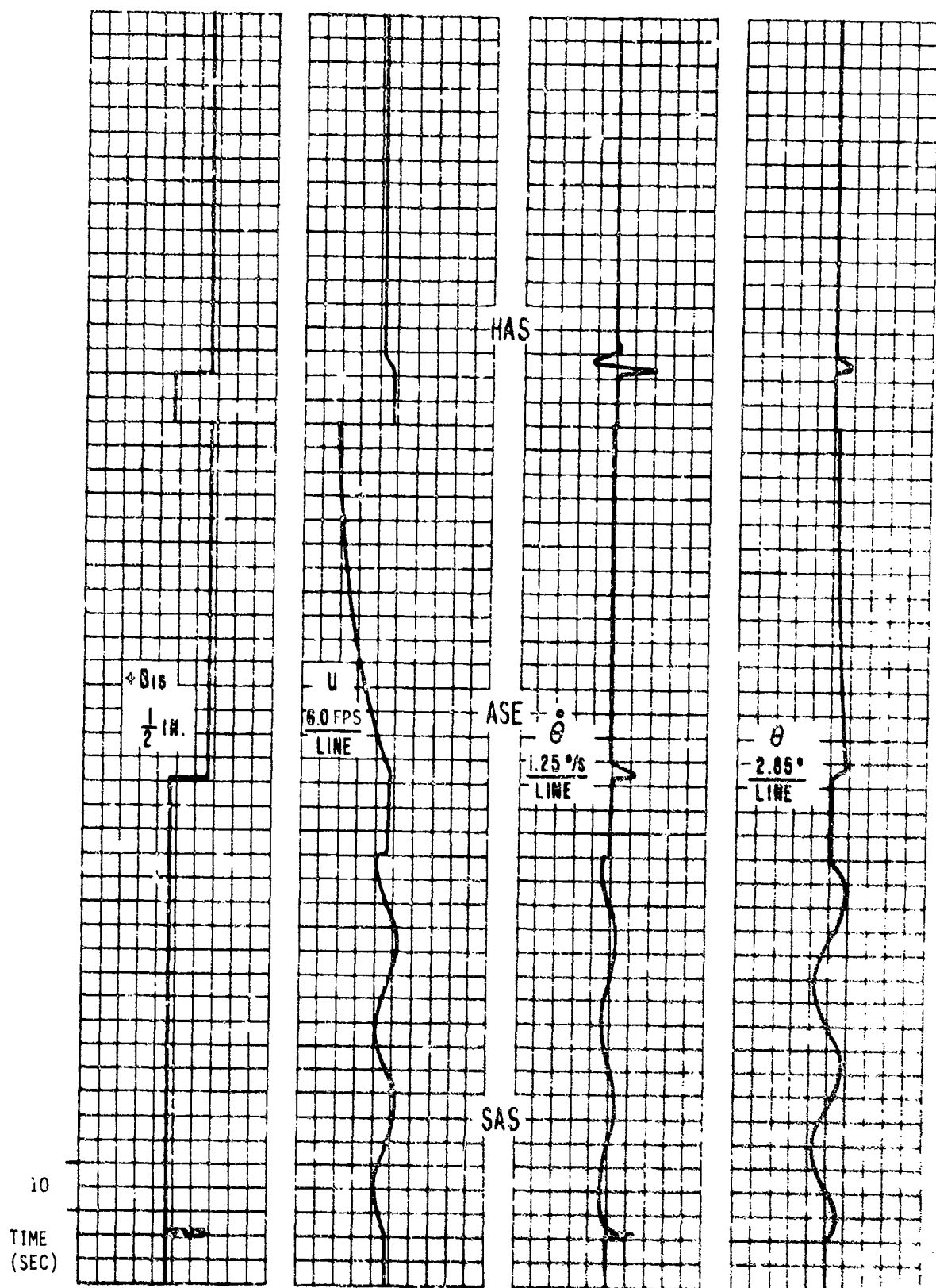
Figure A-7. CH-53A model time history response to lateral stick input

49
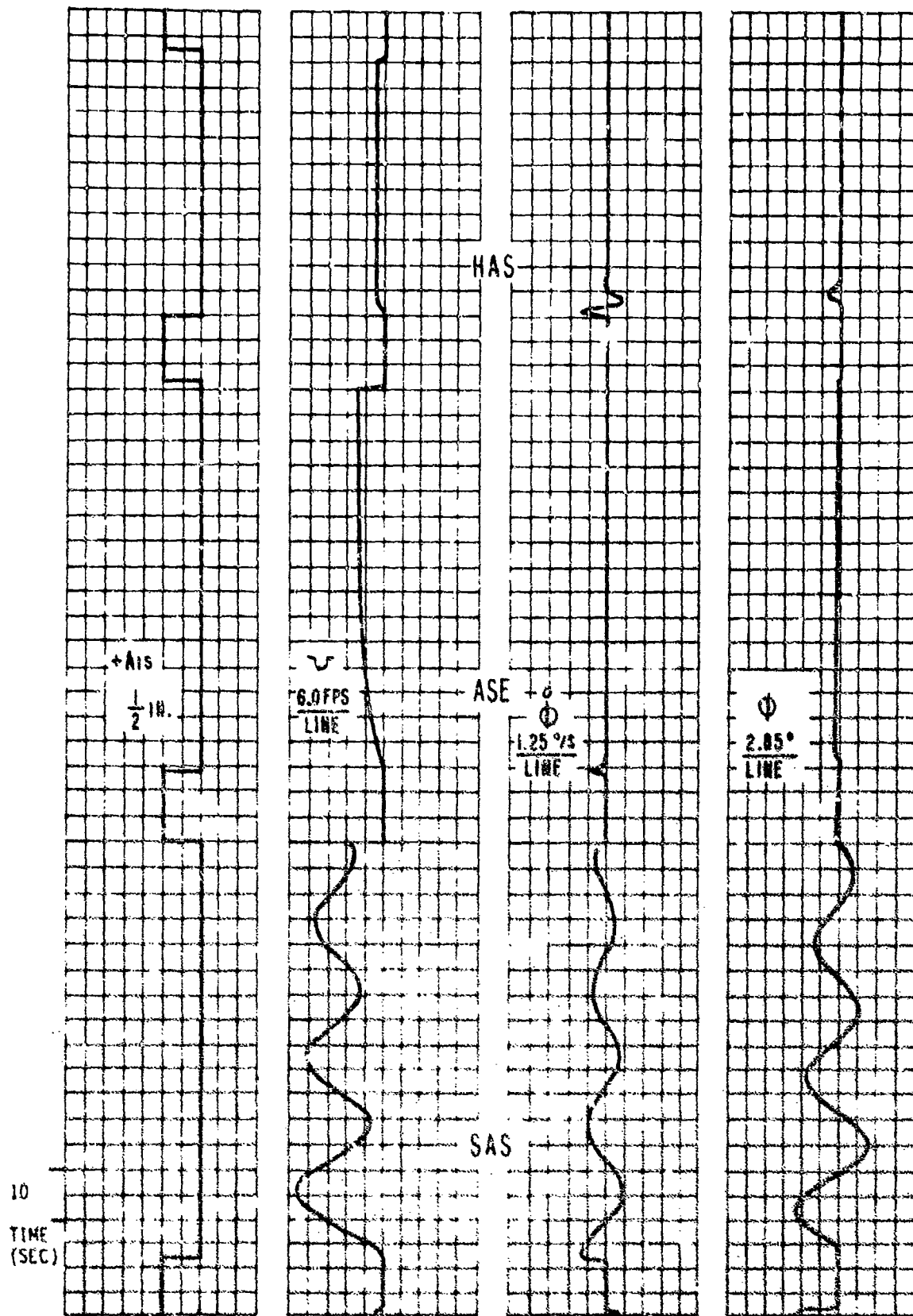
Figure 4-8. CH-53A model time history response to lateral stick input

56

APPENDIX B

WIND GUST GENERATION

A simplified diagram is presented to show the first order filter and also the analog response of the gust.
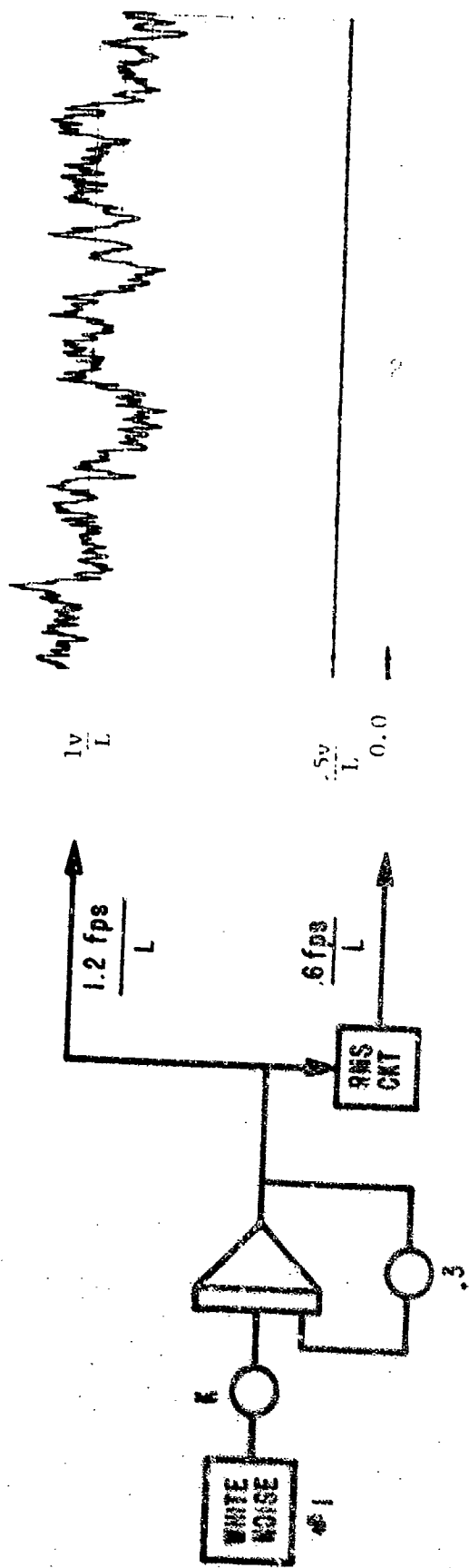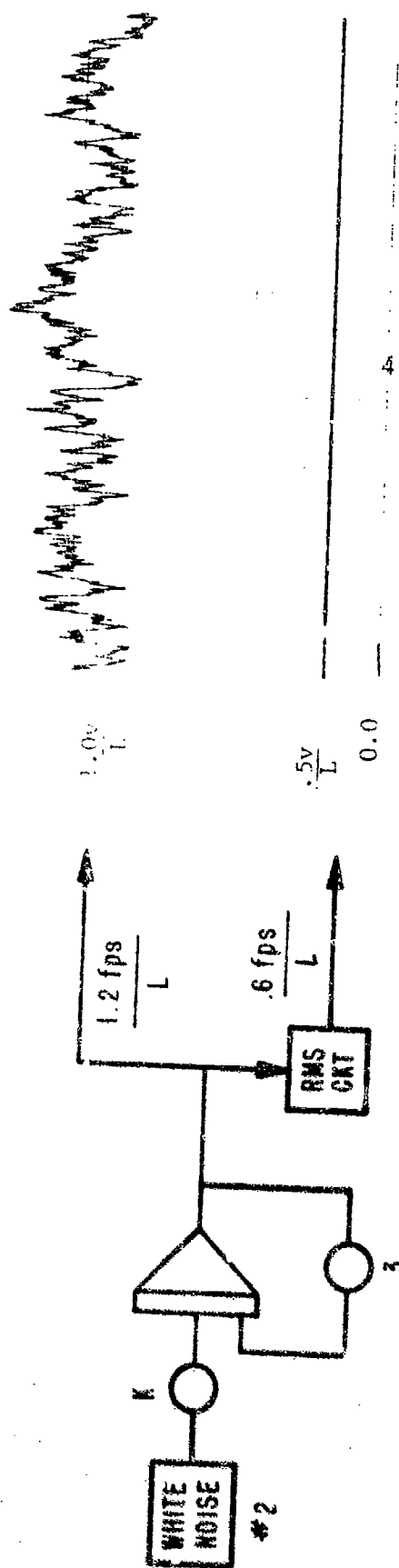
Figure B-1.   Random gust analog traces

APPENDIX C

SUMMARY OF RAW DATA

Here the raw results obtained from the four subjects are presented in Figures C-1 through C-15.

53
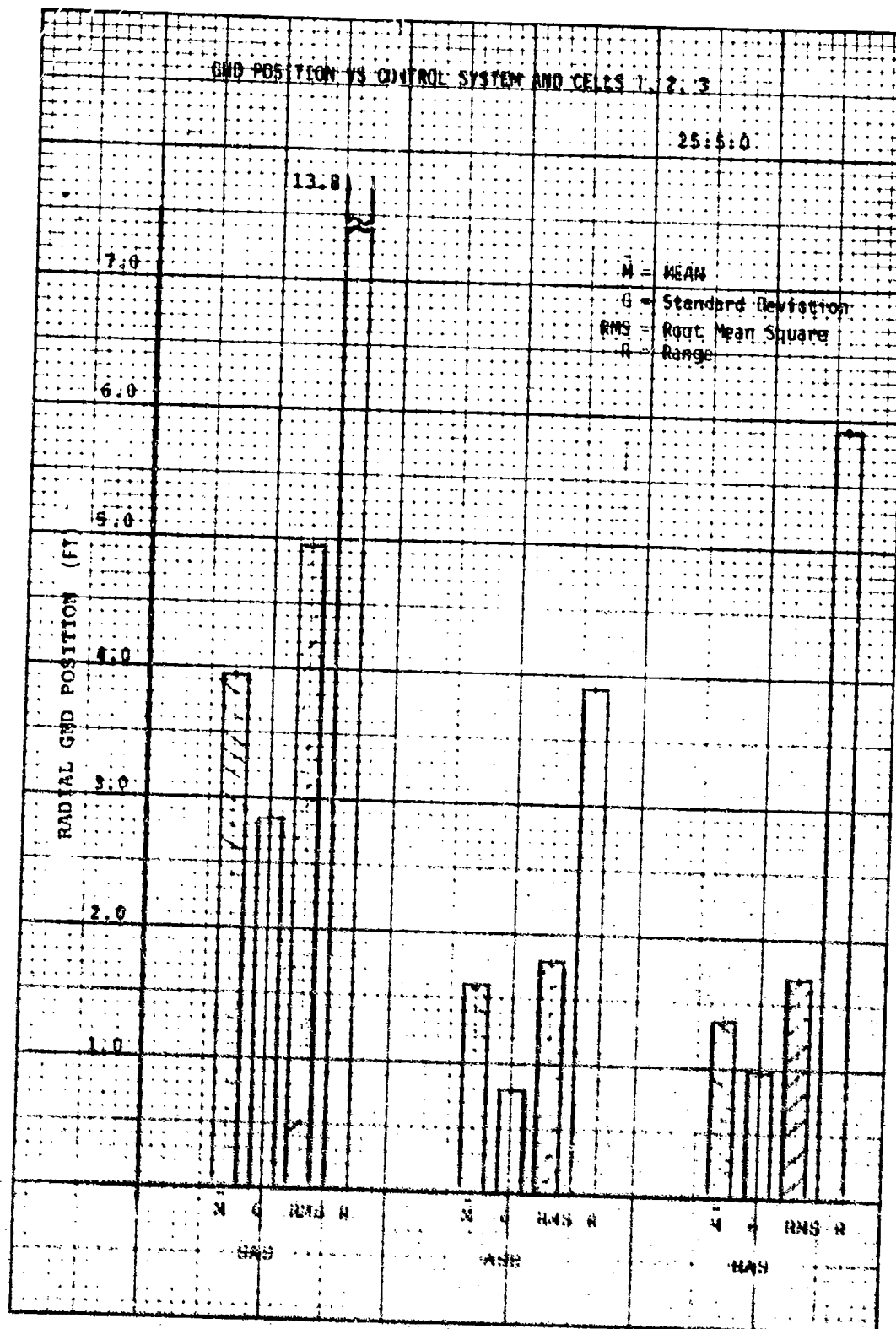
Figure C-1. Ground position versus control system and cells 1, 2, 3
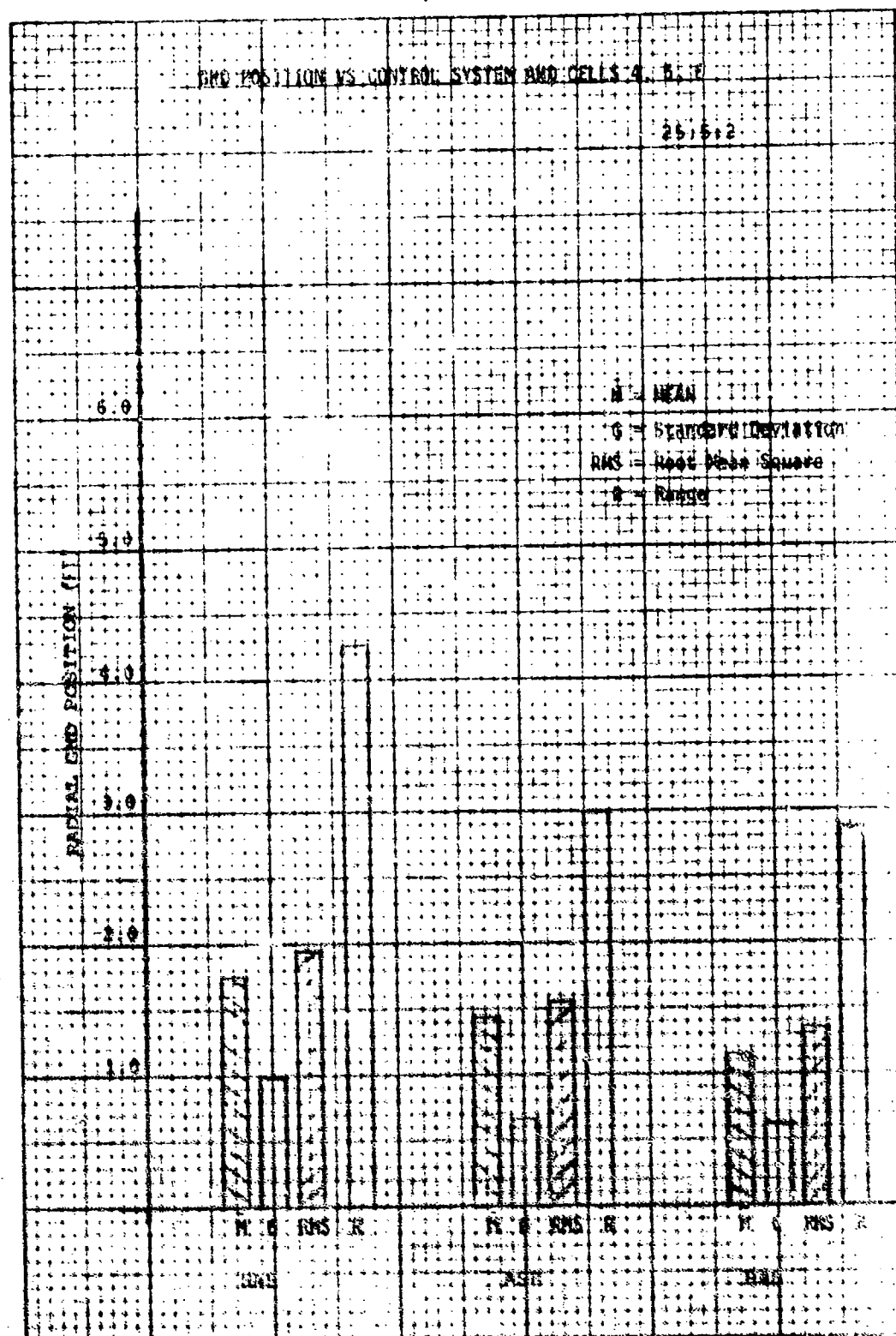
Figure C-2. Ground position versus control system and cells 4, 5, 6
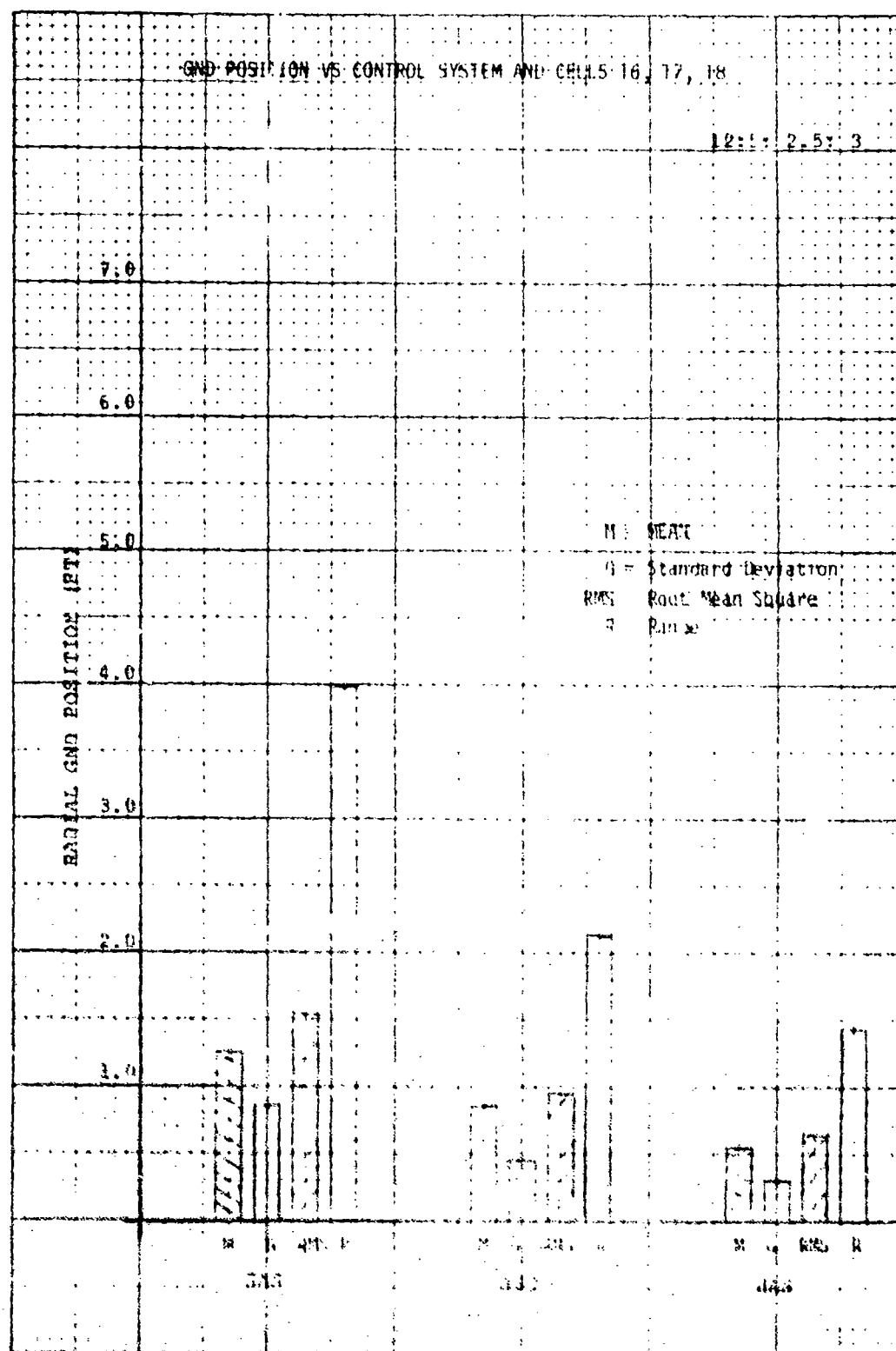
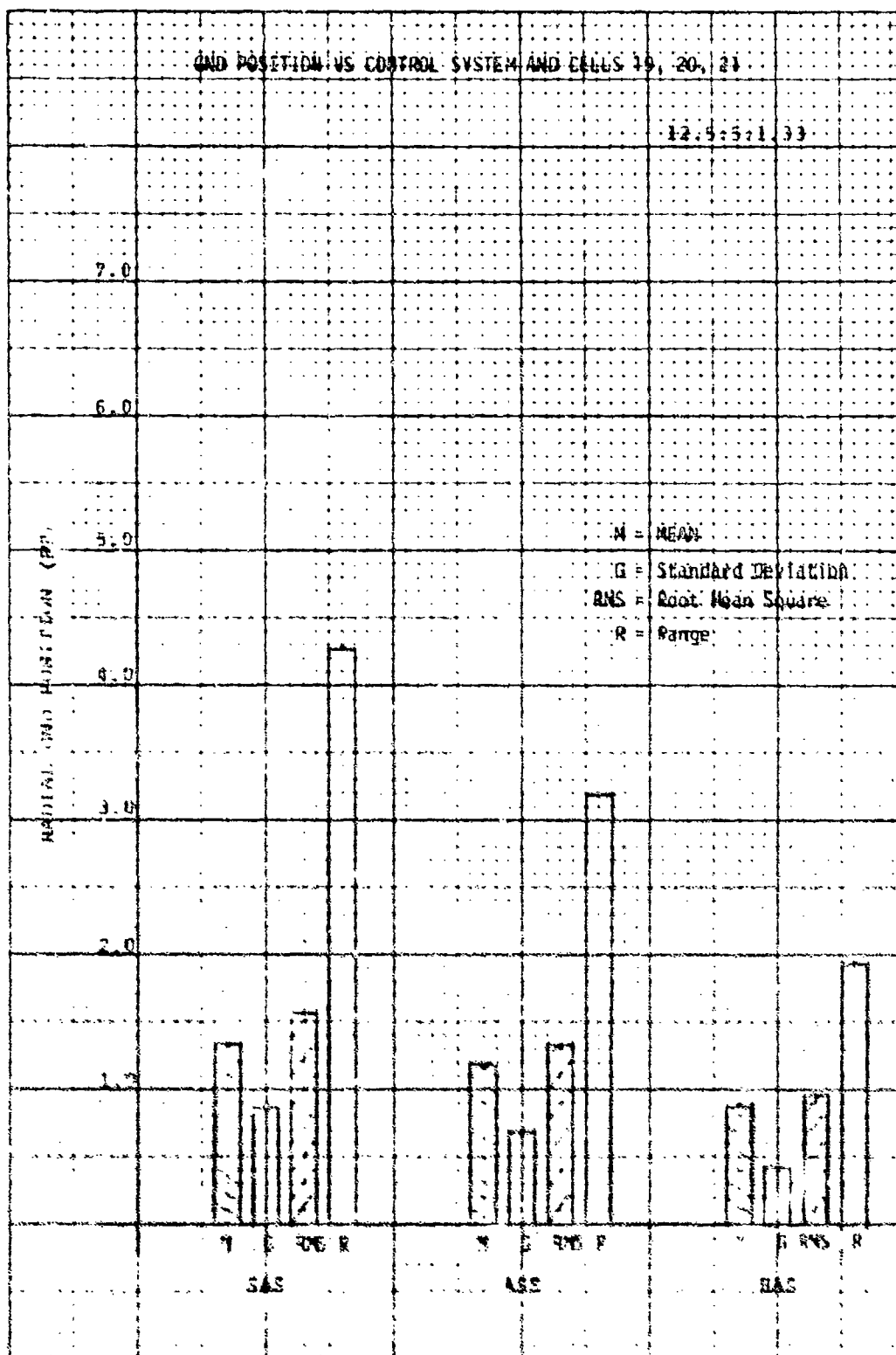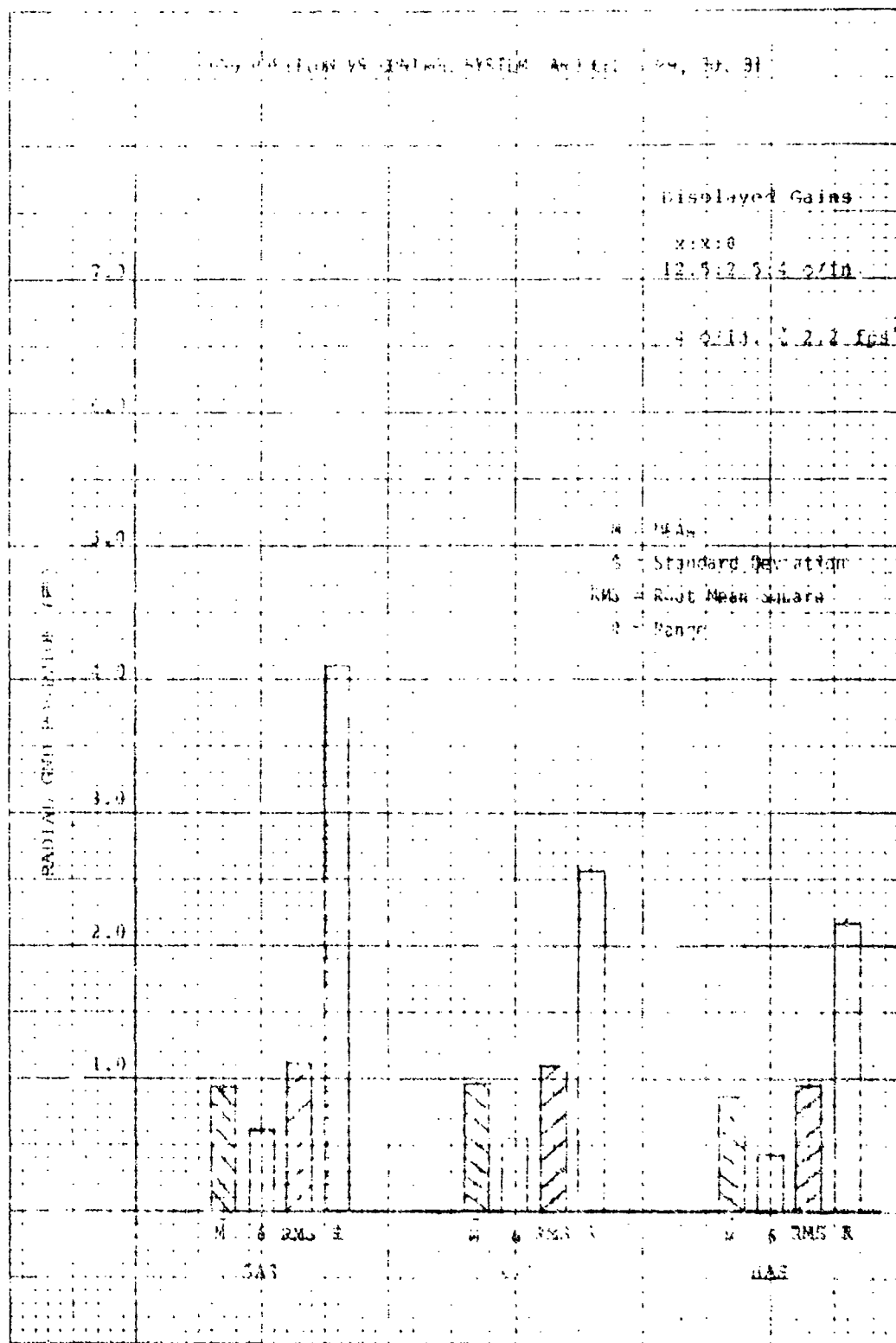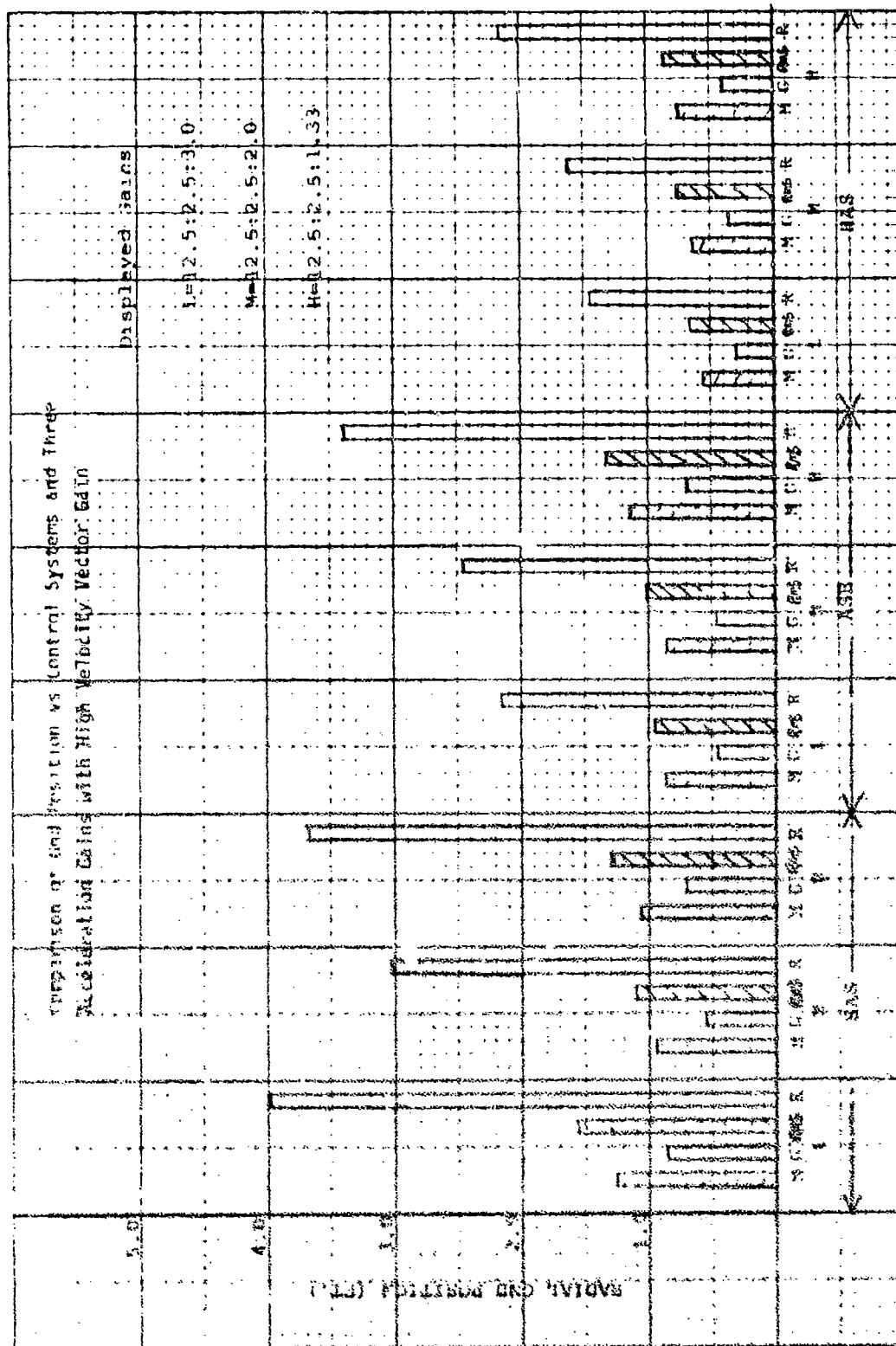Figure C-3. Ground position versus control system and cells 16, 17, 18
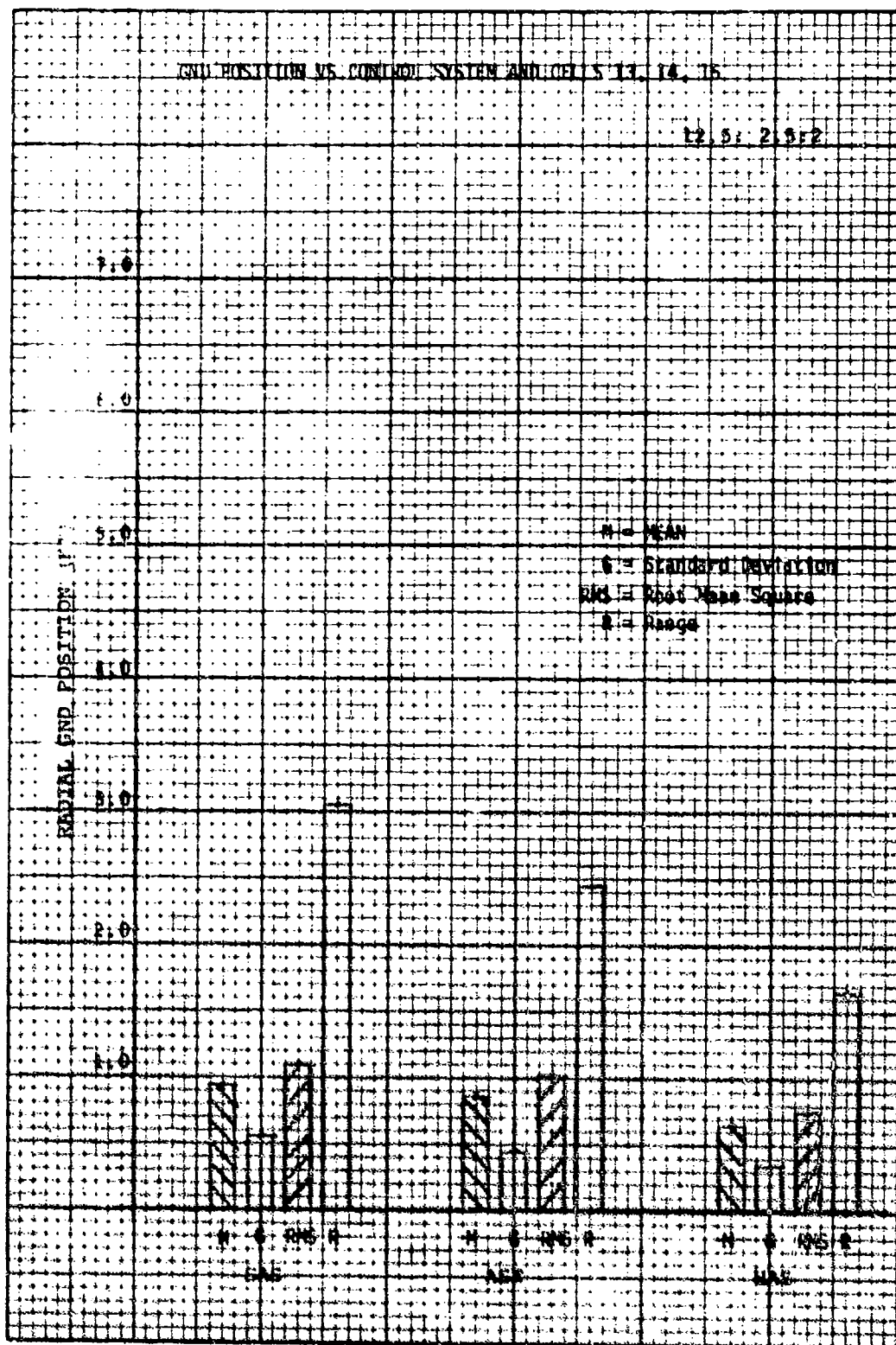
Figure C-4. Ground position versus control system and cells 13, 14, 15
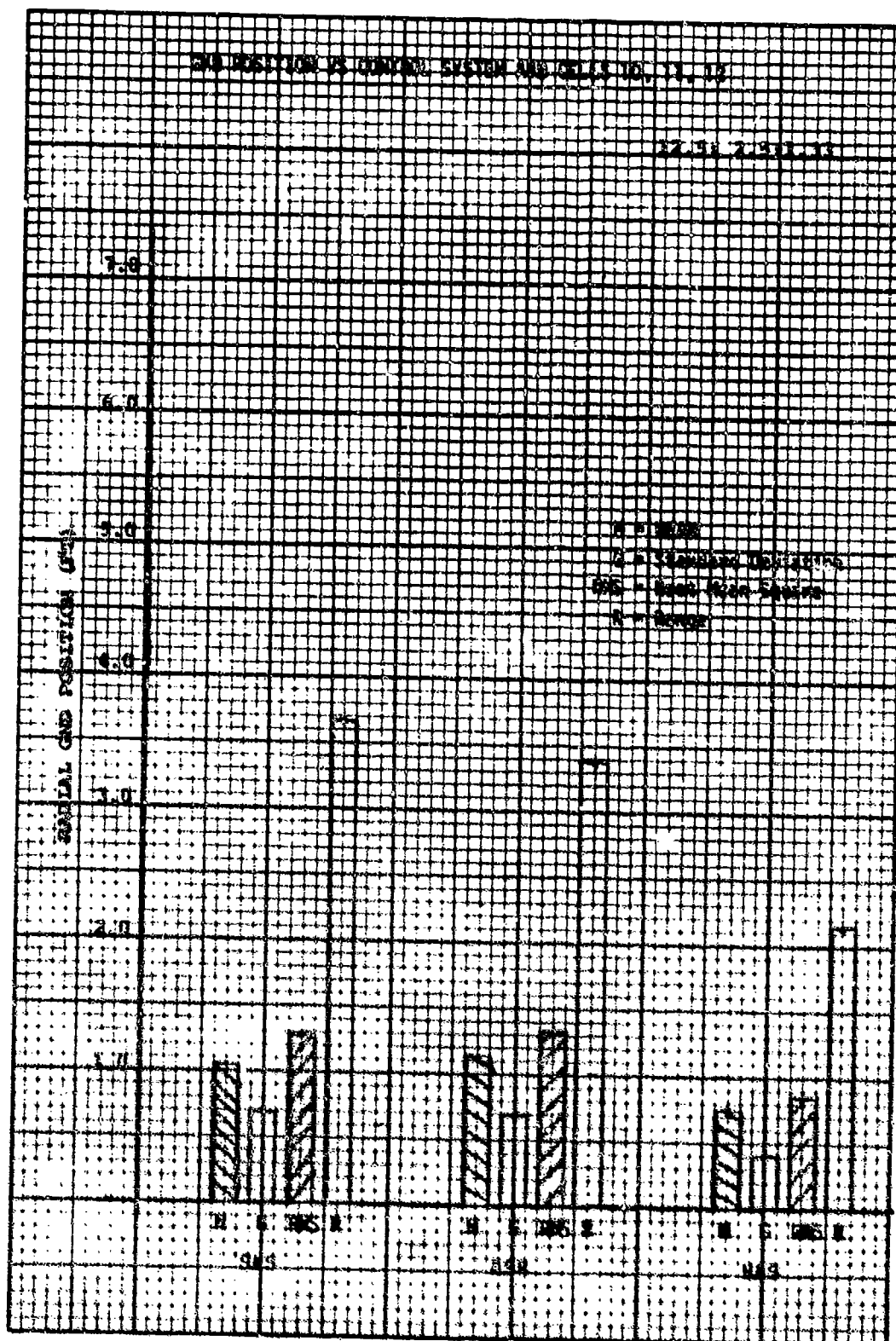
Figure C-5. Ground position versus control system and cells 10, 11, 12
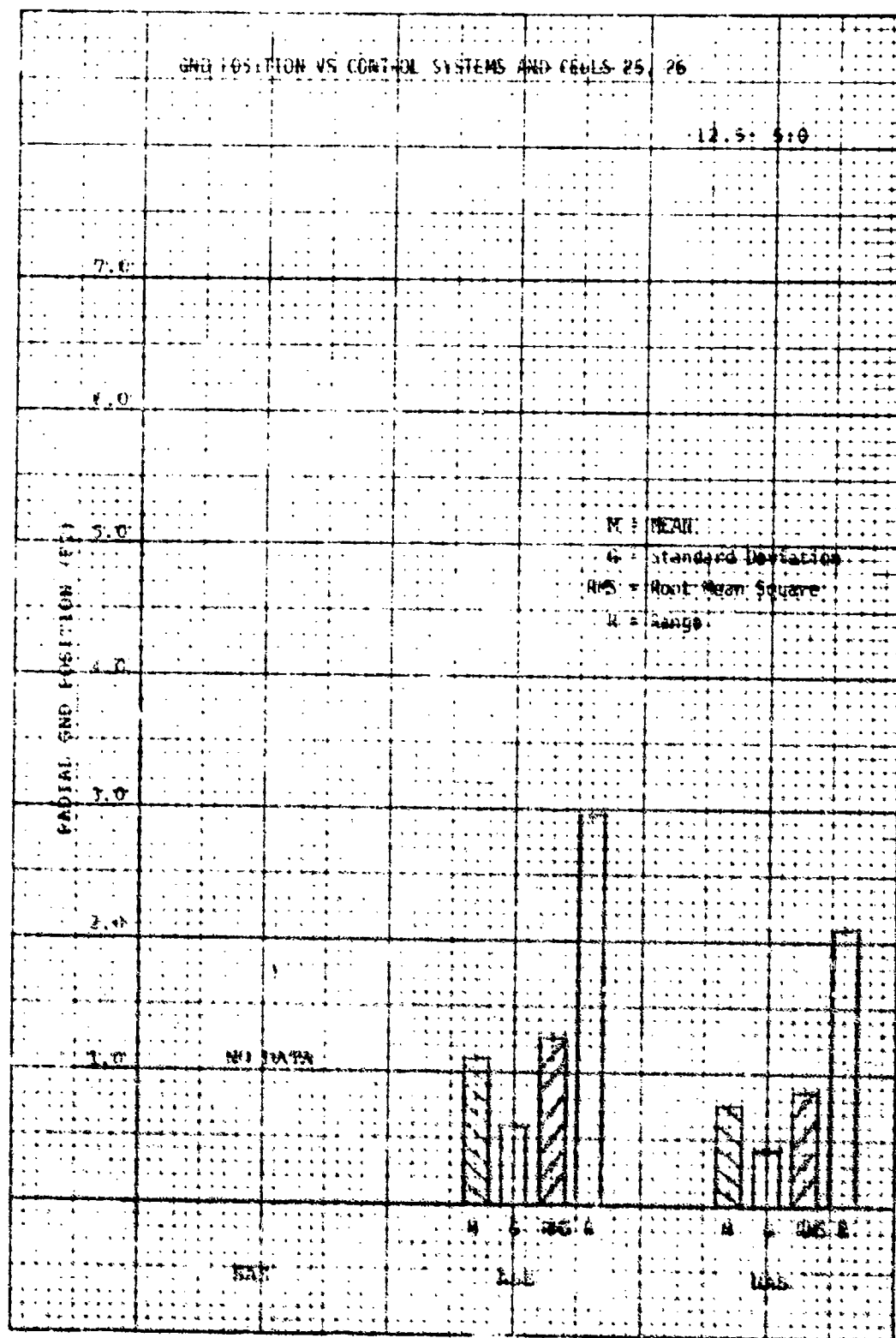
Figure C-6. Ground position versus control systems and cells 25, 26
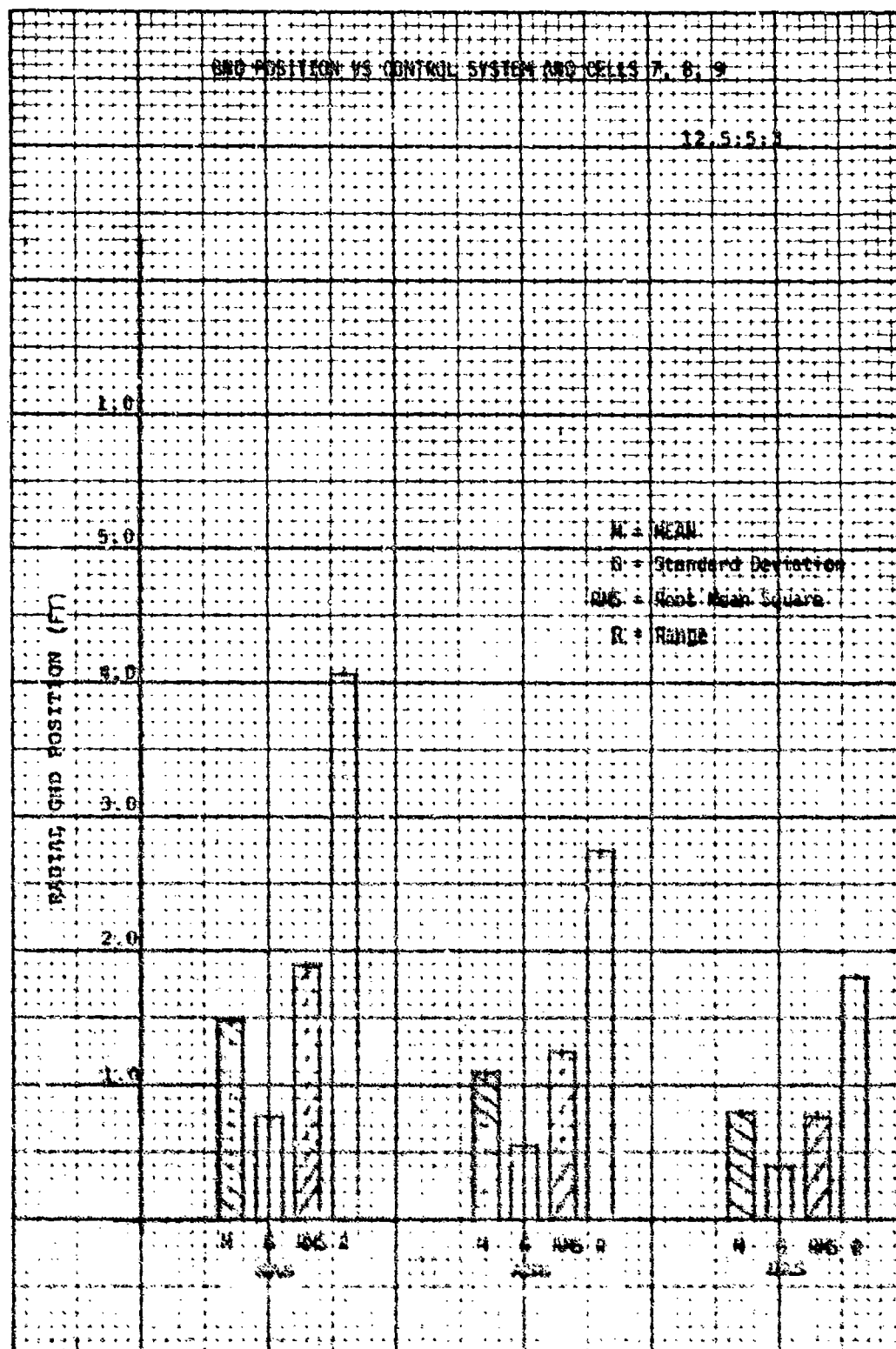
Figure C-7. Ground position versus control system and cells 7, 8, 9

Figure C-8. Command position versus control system for tests 22, 23, 24

Figure C-9. Ground position versus control system and cells 19, 20, 21

Figure C-10. Ground position versus contr... ... ...ls 29, 30, 31

Figure C-11. Comparison of ground position versus control systems and three acceleration gains with high velocity vector gain
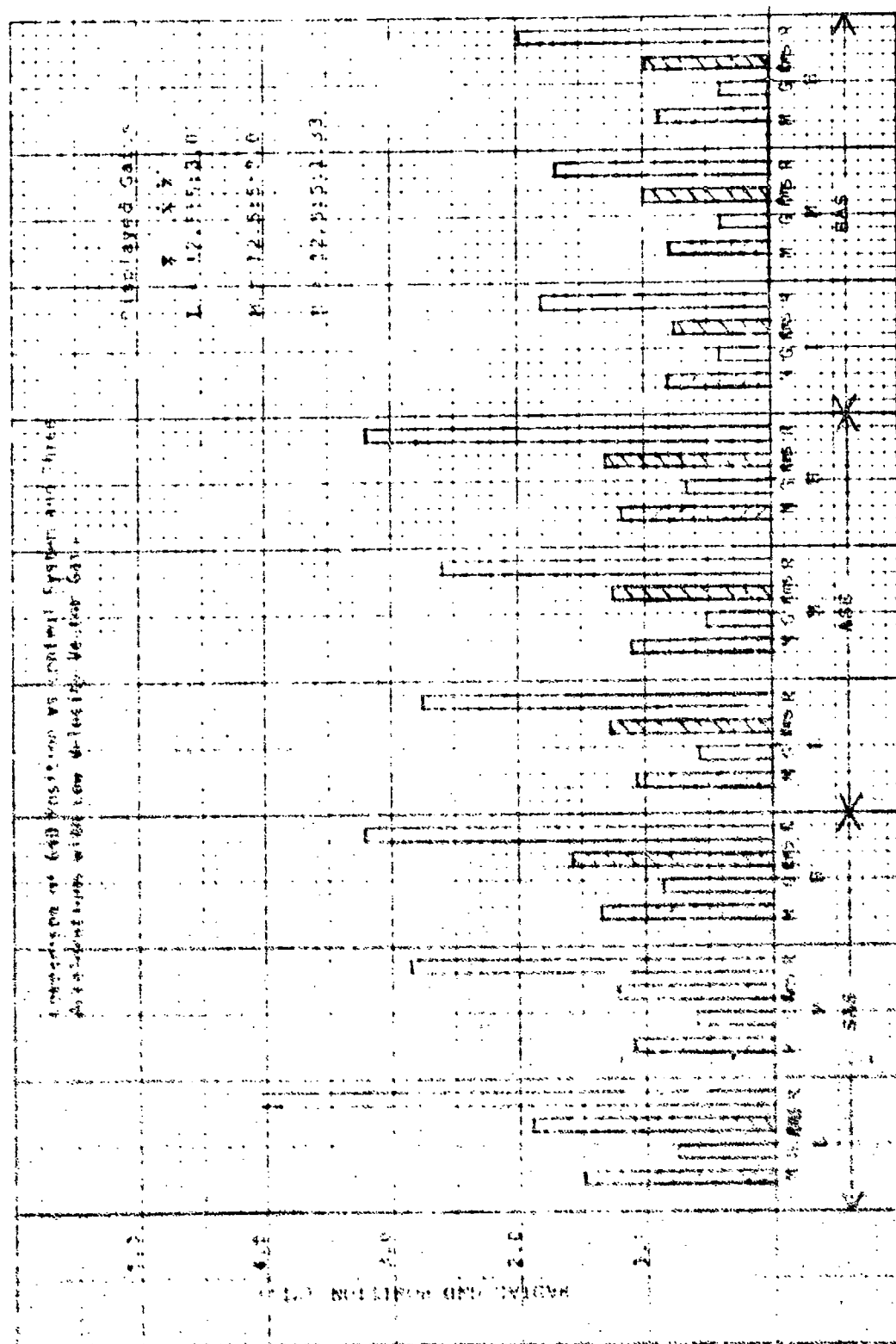
Figure C-12. Comparison of ground position versus control system and three accelerations with low velocity vector gain
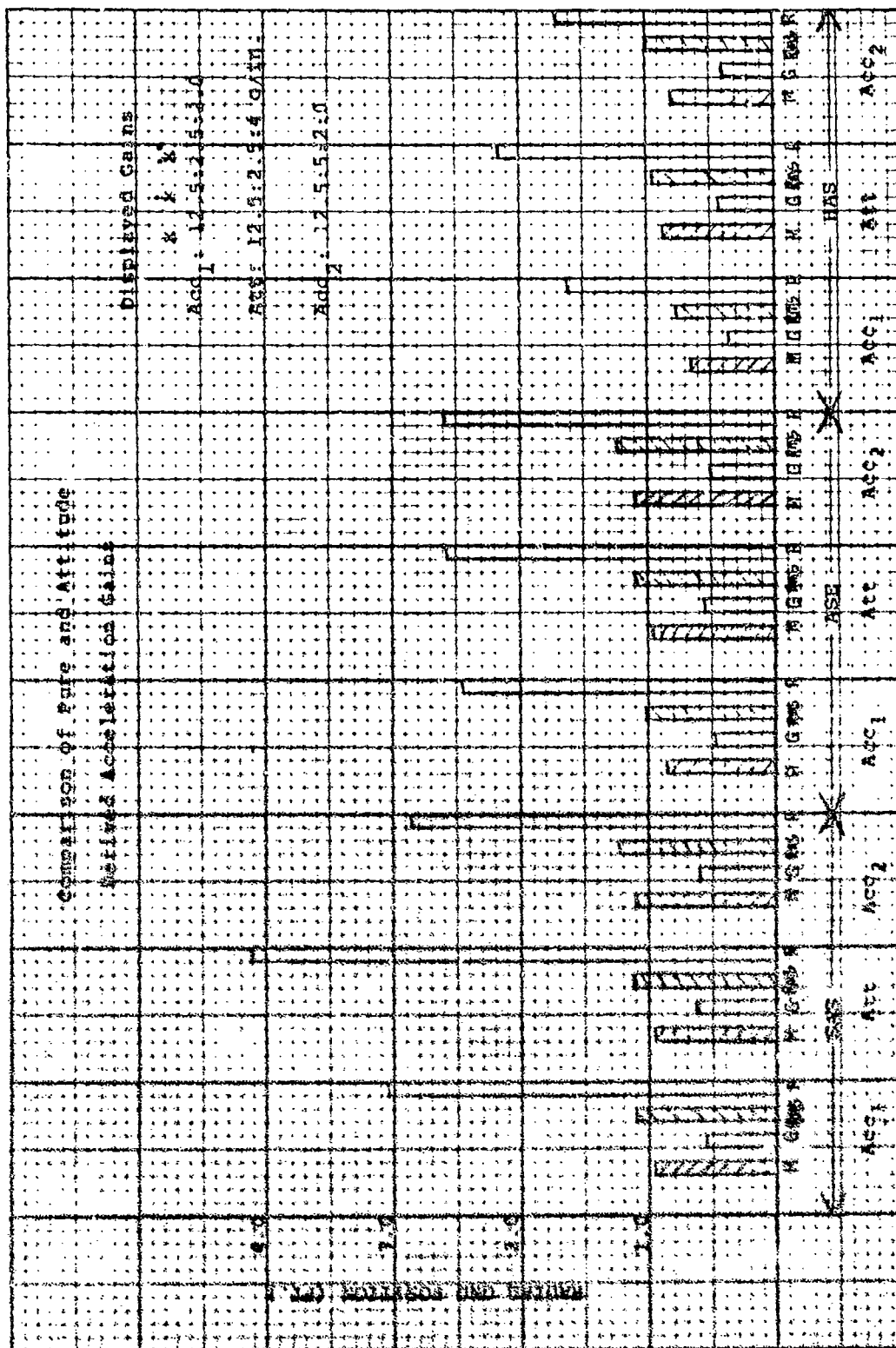
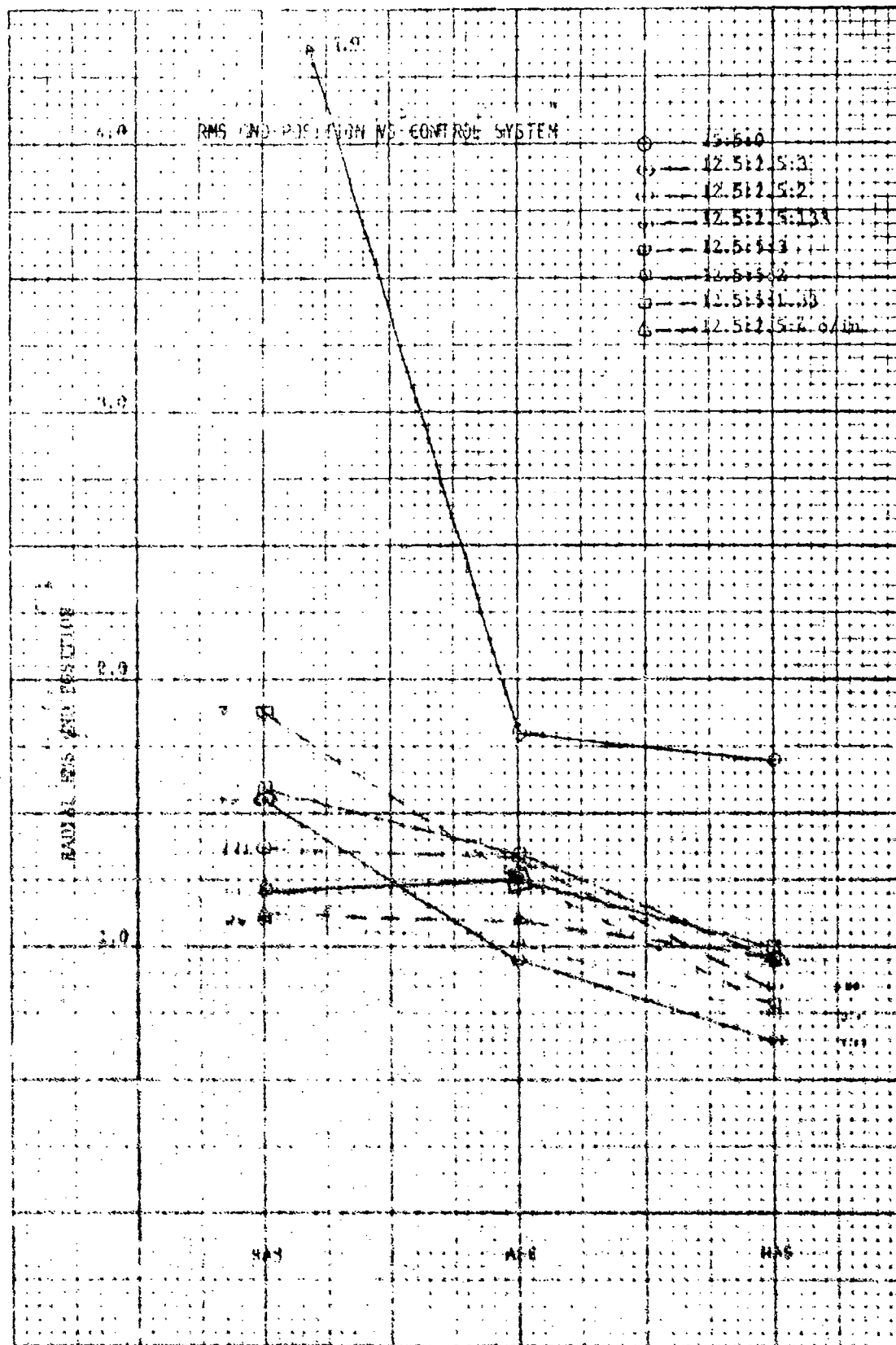Figure C-13. Comparison of pure and attitude derived acceleration gains

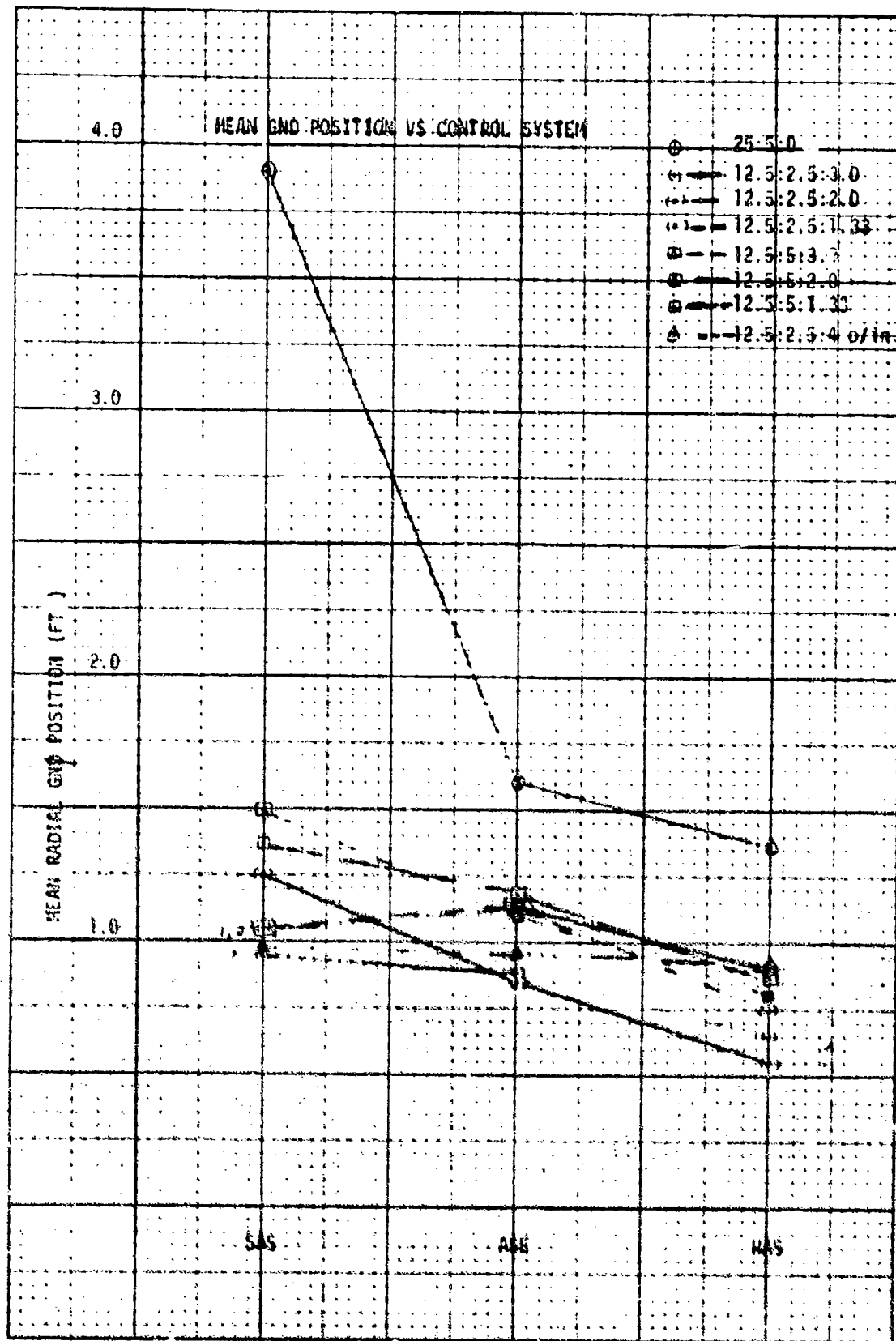Figure C-14. RMS and ground position versus control system

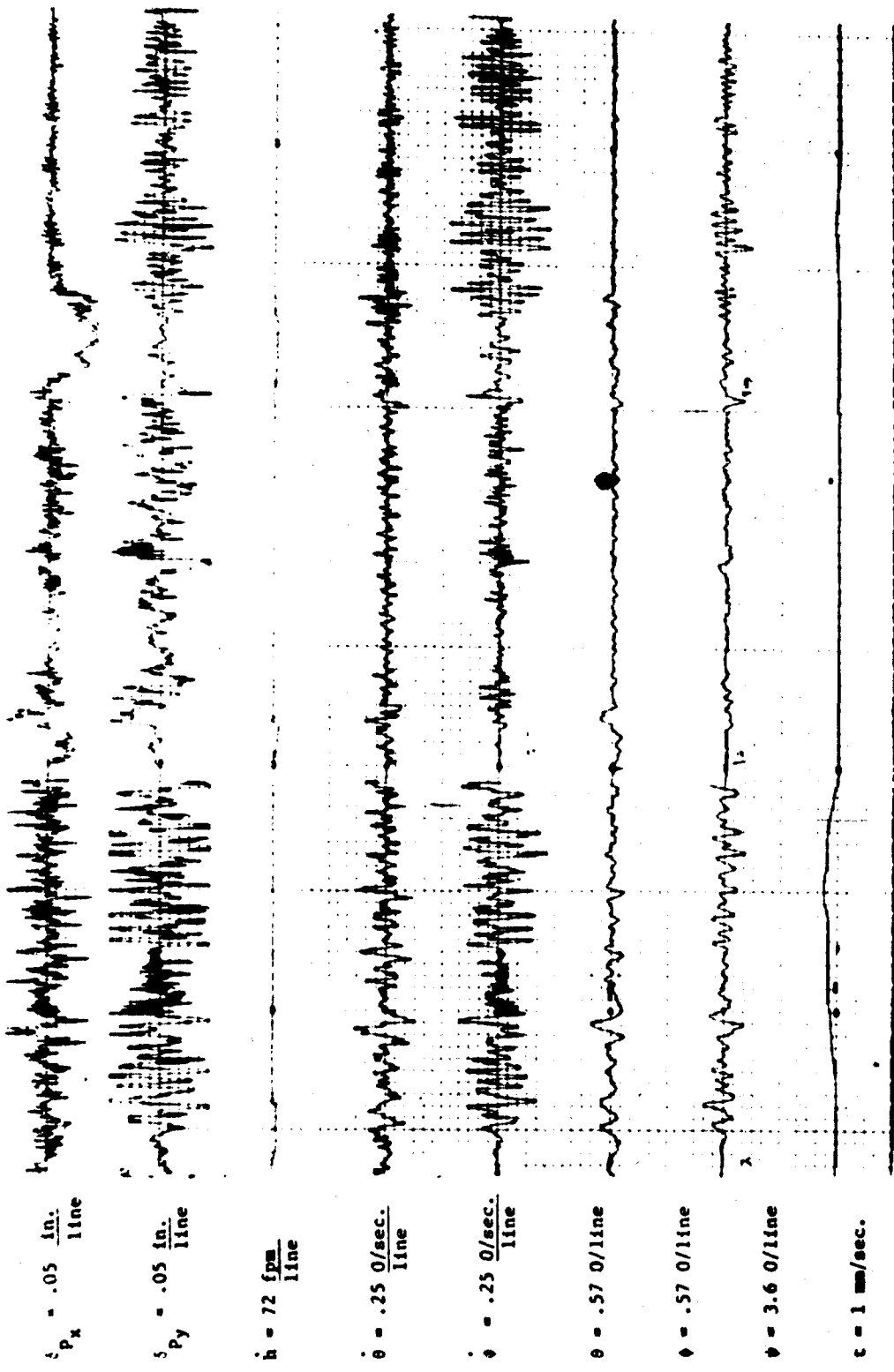Figure C-15. Mean ground position versus control system

66

APPENDIX D

SAMPLE TIME HISTORIES

See pages 69 through 72.

$^{s}P_{x} = .05 \dfrac{in.}{line}$

$^{s}P_{y} = .05 \dfrac{in.}{line}$

$\dot{h} = 72 \dfrac{fpm}{line}$

$\dot{\theta} = .25 \dfrac{0/sec.}{line}$

$\dot{\phi} = .25 \dfrac{0/sec.}{line}$

$\theta = .57 \; 0/line$

$\phi = .57 \; 0/line$

$\psi = 3.6 \; 0/line$

$t = 1 \; mm/sec.$

Displayed Gains
25 ft:5 fps:0

SAS   ASE   HAS

70

$\delta_{p_x} = \frac{.05 \text{ in.}}{\text{line}}$

$\delta_{p_y} = \frac{.05 \text{ in.}}{\text{line}}$

$h = \frac{72 \text{ fps}}{\text{line}}$

$\theta = \frac{.25 \text{ 0/sec.}}{\text{line}}$

$\dot{\psi} = \frac{.25 \text{ 0/sec.}}{\text{line}}$

$\psi = .57 \text{ 0/line}$

$\phi = .57 \text{ 0/line}$

$\dot{\phi} = 3.6 \text{ 0/line}$
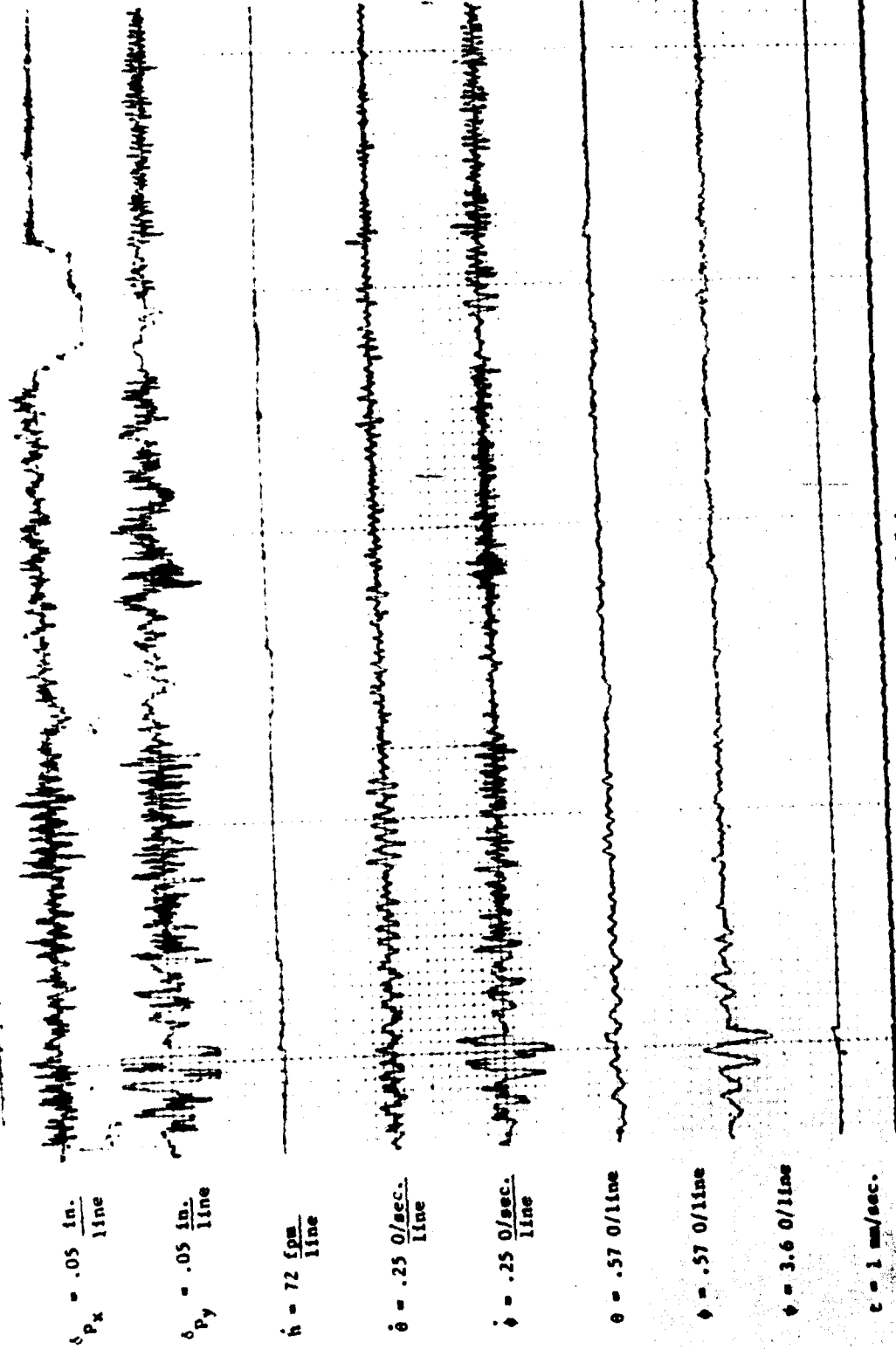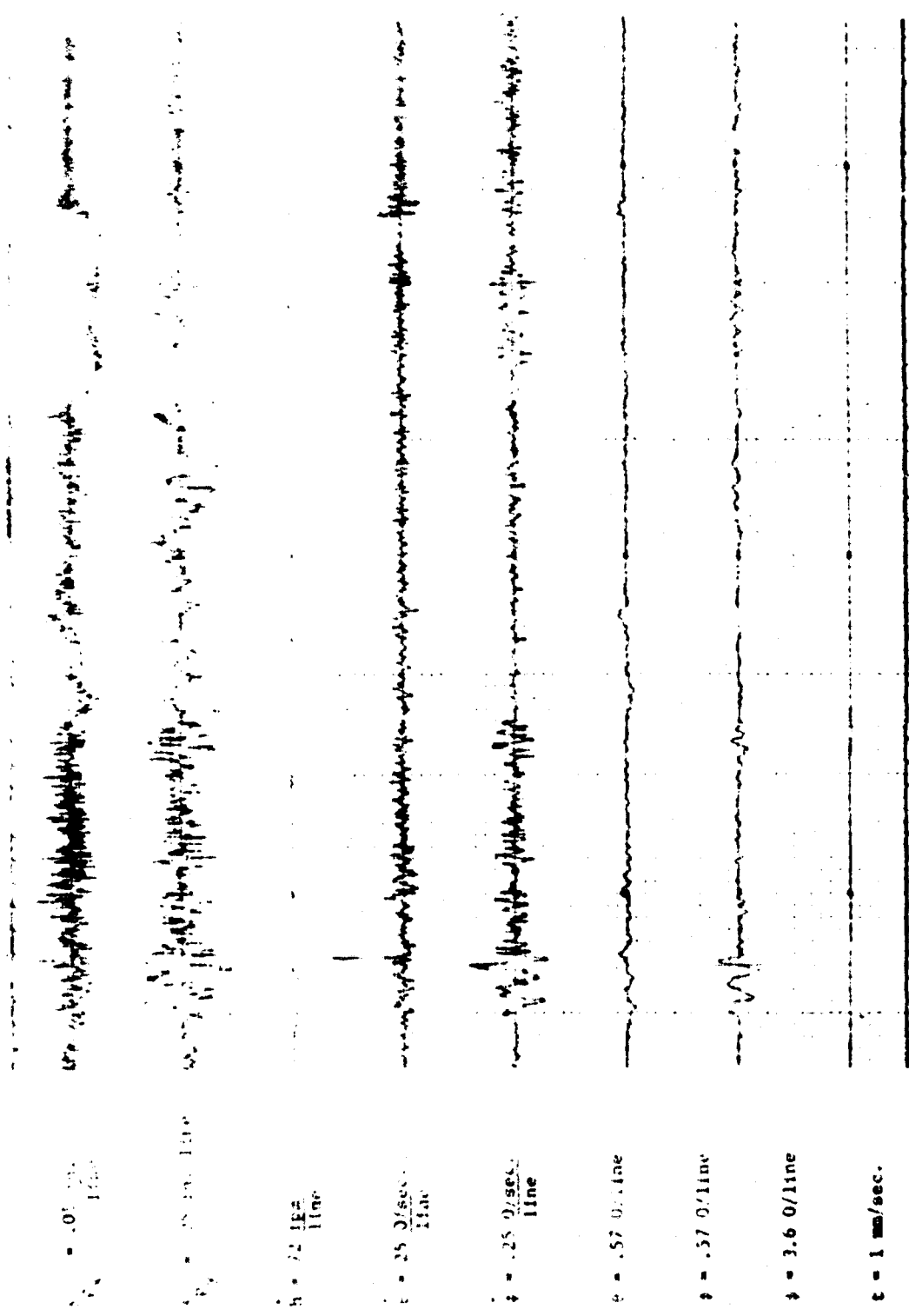
$t = 1 \text{ m/sec.}$
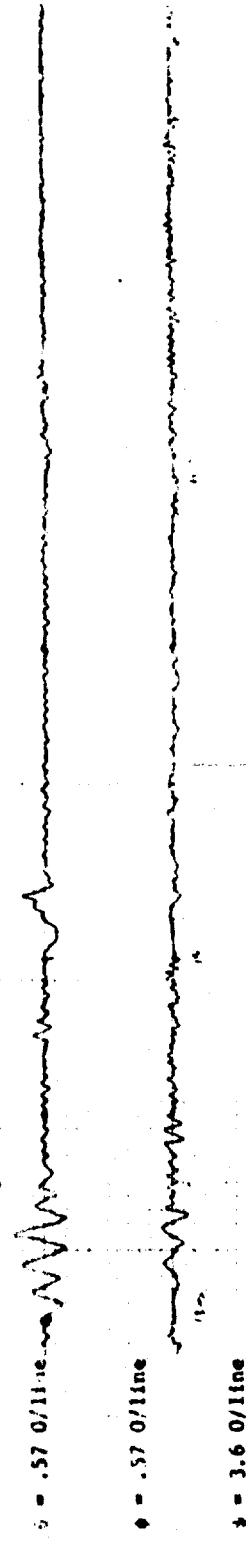
Displayed Gains
12.5 ft:2.5 fps: 2 fps^2
ASE

HAS

SAS

71

$\delta_{P_x} = .05 \frac{in.}{line}$

$\delta_{P_y} = .05 \frac{in.}{line}$

$\dot{h} = 72 \frac{fps}{line}$

$\dot{\theta} = .25 \frac{0/sec.}{line}$

$\dot{\phi} = .25 \frac{0/sec.}{line}$

$\theta = .57 \ 0/line$

$\phi = .57 \ 0/line$

$\psi = 3.6 \ 0/line$

$t = 1 \ sec/sec.$

Displayed Gains
12.5 ft:5 fps:2fps²

ASE

HAS

— 72 —

Displayed Gains
12.5 ft: 2.5: fps:4 0/in.

SAS   ASE   HAS